TECHNISCHE UNIVERSITÄT MÜNCHEN

Fakultät für Medizin

Adaptive immune responses to AQP4 in a murine model for neuromyelitis optica

Anna-Lena Vogel

Vollständiger Abdruck der von der Fakultät für Medizin der Technischen Universität München zur Erlangung des akademischen Grades eines

Doktors der Naturwissenschaften (Dr. rer. nat.)

genehmigten Dissertation.

Vorsitz:	Prof. Dr. Percy A. Knolle
Prüfer der Dissertation:	1. Prof. Dr. Thomas Korn
	2. Prof. Dr. Gabriele Multhoff
	3. Prof. Dr. Martin Kerschensteiner

Die Dissertation wurde am 31.01.2022 bei der Technischen Universität München eingereicht und durch die Fakultät für Medizin am 12.07.2022 angenommen.

Eidesstattliche Erklärung

Ich, Anna-Lena Vogel, erkläre an Eides statt, dass ich die bei der Fakultät für Medizin der TUM zur Promotionsprüfung vorgelegte Arbeit mit dem Titel:

Adaptive immune responses to AQP4 in a murine model for neuromyelitis optica

unter der Anleitung und Betreuung durch Prof. Dr. Thomas Korn ohne sonstige Hilfe erstellt und bei der Abfassung nur die gemäß § 7 Abs. 6 und 7 angegebenen Hilfsmittel benutzt habe.

(x) Ich habe keine Organisation eingeschaltet, die gegen Entgelt Betreuer*innen für die Anfertigung von Dissertationen sucht, oder die mir obliegenden Pflichten hinsichtlich der Prüfungsleistungen für mich ganz oder teilweise erledigt.

(x) Ich habe die Dissertation in dieser oder ähnlicher Form in keinem anderen Prüfungsverfahren als Prüfungsleistung vorgelegt.

( ) Teile der Dissertation wurden in _____veröffentlicht.

(x) Ich habe den angestrebten Doktorgrad noch nicht erworben und bin nicht in einem früheren Promotionsverfahren für den angestrebten Doktorgrad endgültig gescheitert.

( ) Ich habe bereits am _____ bei der Fakultät für _____ der Hochschule _____ unter Vorlage einer Dissertation mit dem Thema _____ die Zulassung zur Promotion beantragt mit dem Ergebnis _____.

(x) Ich habe keine Kenntnis über ein strafrechtliches Ermittlungsverfahren in Bezug auf wissenschaftsbezogene Straftaten gegen mich oder eine rechtskräftige strafrechtliche Verurteilung mit Wissenschaftsbezug.

Die öffentlich zugängliche Promotionsordnung sowie die Richtlinien zur Sicherung guter wissenschaftlicher Praxis und für den Umgang mit wissenschaftlichem Fehlverhalten der TUM sind mir bekannt, insbesondere habe ich die Bedeutung von § 27 PromO (Nichtigkeit der Promotion) und § 28 PromO (Entzug des Doktorgrades) zur Kenntnis genommen. Ich bin mir der Konsequenzen einer falschen Eidesstattlichen Erklärung bewusst.

Mit der Aufnahme meiner personenbezogenen Daten in die Alumni-Datei bei der TUM bin ich einverstanden.

München, 14.01.2022 _____

Unterschrift

Contents

Summary **4**

Zusammenfassung **6**

1 Introduction **8**

1.1 Immunological tolerance and autoimmunity 8

1.2 Neuromyelitis optica and aquaporin-4 11

1.3 A preclinical model for NMO 15

2 Aim of the study **18**

3 Material and Methods **19**

3.1 Material 19

3.1.1 Reagents 19

3.1.2 Plasmids 21

3.1.3 Primers 21

3.1.4 Enzymes 22

3.1.5 Kits 22

3.1.6 Cell culture media 23

3.1.7 Buffers and solutions 24

3.1.8 Antibodies 25

3.1.9 Peptides 26

3.1.10 Mice 28

3.1.11 Cell lines 29

3.1.12 Magnetic beads 29

3.1.13 Cytokines 30
3.1.14 Laboratory equipment and consumables 30
3.1.15 Software 31
3.2 Methods 32
3.2.1 Molecular biology 32
3.2.1.1 Synthesis of cDNA 32
3.2.1.2 Cloning of *Aqp4* expression vectors 33
3.2.1.3 Sequencing 34
3.2.2 Protein biochemistry 34
3.2.2.1 Expression and purification of AQP4 protein 34
3.2.2.2 Electrophoretic separation of proteins 35
3.2.2.3 Western blot and immunodetection of proteins 35
3.2.3 Cell biology 36
3.2.3.1 Cultivation of primary cells and cell lines 36
3.2.3.2 Preparation of lymphocytes 36
3.2.3.3 Flow cytometry 37
3.2.3.4 Cell sorting 38
3.2.3.5 Stimulation of T cells with antigen ex vivo 39
3.2.3.6 T-cell proliferation assay 39
3.2.4 Imaging 40
3.2.4.1 Immunohistochemistry 40
3.2.4.2 Confocal microscopy 40
3.2.5 Animal experimentation 40
3.2.5.1 Housing and breeding conditions 40
3.2.5.2 Mouse strains 41
3.2.5.3 Genotyping 41
3.2.5.4 Immunization procedures and induction of disease 43
3.2.5.5 Bone marrow chimeras 43
3.2.5.6 OCT analysis of murine retina 44
3.2.6 Statistical analysis 44

4 Results 45
4.1 Generation of mouse AQP4 full-length protein 45
4.2 T-cell and B-cell responses to AQP4 46
4.2.1 Identification of immunogenic T-cell epitopes of AQP4 46

4.2.2 Anti-AQP4 serum response in mice upon immunization with AQP4 full-length protein ... 51
4.3 Tolerance mechanism to AQP4 in AQP4-sufficient mice ... 53
4.4 Animal model for features of NMO disease ... 57
4.4.1 $Aqp4^{\Delta T}$ compound mice show clinical signs of disease upon immunization with AQP4 protein ... 57
4.4.2 Immunization with AQP4(201-220) epitope in addition with administration of anti-AQP4 antibody results in NMO-specific lesional patterns ... 61
4.5 Tetramer staining of AQP4-specific T cells ... 64

5 Discussion ... 67
5.1 AQP4(201-220) is the major immunogenic T-cell epitope of AQP4 in C57BL/6 mice ... 67
5.2 Adaptive anti-AQP4 responses are efficiently tolerized in AQP4-sufficient mice ... 69
5.3 AQP4(201-220)-specific T-cells induce an encephalomyelitic syndrome ... 72
5.4 Tetramer staining of AQP4(201-220)-specific T cells is a tool for AQP4-specific TCR repertoire analysis and cloning ... 73
5.5 Conclusion and Outlook ... 74

Bibliography ... 76

Appendix ... 86
Supplementary figures ... 86
List of figures ... 88
List of tables ... 89
Attributions ... 90
Abbreviations ... 91
Danksagung ... 94
Lebenslauf ... 95

Summary

Neuromyelitis optica (NMO) is an autoimmune disease of the central nervous system (CNS) that predominantly affects spinal cord, optic nerves and brainstem, potentially leading to paralysis and blindness. It is mediated by antibodies against the water channel protein aquaporin-4 (AQP4) that is expressed in astrocyte foot processes at the glia limitans. Binding of AQP4-IgG to astrocytic AQP4 causes complement-dependent cytotoxicity with loss of AQP4 and GFAP and secondary inflammation with granulocyte and macrophage predominance, disruption of the blood-brain-barrier and oligodendrocyte injury. The contribution of AQP4-specific T cells to the class switch recombination of pathogenic AQP4-IgG and the inflammation of the blood-brain-barrier is unclear, since immunogenic naturally processed T-cell epitopes are still unknown.

In this study *Aqp4*$^{-/-}$ mice and wild type (WT) mice were immunized with full-length murine AQP4 protein followed by recall of T-cell responses to single overlapping peptides in order to determine potential epitopes. In the non-tolerized repertoire of *Aqp4*$^{-/-}$ mice, AQP4(201-220) was identified as the major immunogenic IA^{b}-restricted epitope of AQP4. While *Aqp4*$^{-/-}$ mice raise a robust AQP4(201-220)-specific T-cell response, the natural repertoire of WT mice is devoid of AQP4(201-220)-specific T-cell clones due to deletional tolerance. To overcome tolerance and induce AQP4-specific T-cell responses in AQP4-sufficient mice, compound mice were generated by transferring the mature T-cell repertoire of *Aqp4*$^{-/-}$ mice into *Rag1*$^{-/-}$ mice. Immunization of these *Aqp4*$^{\Delta T}$ *x Rag1*$^{-/-}$ mice with AQP4(201-220) resulted in an encephalomyelitic syndrome with clinical manifestation comparable to experimental autoimmune encephalomyelitis (EAE). Similarly to the T-cell repertoire, the B-cell repertoire of WT mice is purged of AQP4-reactive clones. A robust anti-AQP4 serum response could only be mounted in *Aqp4*$^{-/-}$ mice after immunization with AQP4 protein. Transfer of these

antibodies or alternatively a murinized monoclonal anti-AQP4 antibody (rAb-53) into *Aqp4*$^{\Delta T}$ *x Rag1*$^{-/-}$ aggravated the disease course upon immunization with AQP4(201-220) and lesions were reminiscent of NMO. Thus, AQP4(201-220)-specific T cells alone induce encephalomyelitis, while NMO-specific lesional patterns in the CNS and retina only occur in the presence of both, AQP4(201-220)-specific T cells and anti-AQP4 antibodies. The failure of deletional T-cell and B-cell tolerance against AQP4 sets the stage for NMO-like autoimmune pathology in the CNS and understanding how tolerance to AQP4 is broken is key to a potential curative treatment option.

Zusammenfassung

Neuromyelitis optica (NMO) ist eine autoimmune Erkrankung des zentralen Nervensystems (ZNS), die sich vor allem im Rückenmark, den optischen Nerven und im Hirnstamm manifestiert und bei Betroffenen zu Lähmungserscheinungen und Erblinden führen kann. Von zentraler Bedeutung für die Ausbildung der Krankheit sind Antikörper gegen den Wasserkanal Aquaporin-4 (AQP4), der im ZNS vor allem in den Fortsätzen von Astrozyten exprimiert wird, die an die Basalmembran reichen und das Hirn- und Rückenmarksgewebe gegen die Gefäße hin abgrenzen. Die Bindung der Antikörper an AQP4 auf der Oberfläche von Astrozyten führt zu einer Aktivierung des Komplementsystems, das zunächst die Astrozyten selbst schädigt und zu einem Verlust der AQP4 und GFAP Expression in den Zellen führt. Anschließend tragen Immunzellen wie Granulozyten und Makrophagen zur weiteren Entzündungsreaktion bei, die eine Störung der Blut-Hirn-Schranke und Schädigung von Oligodendrozyten zur Folge hat. Inwieweit AQP4-spezifische T-Zellen zur Bildung der pathogenen anti-AQP4 Antikörper und der Entzündungsreaktion an der Blut-Hirn-Schranke beitragen ist noch unklar, da immunogene, natürlich prozessierte T-Zell-Epitope noch nicht bekannt sind.

Um potentielle T-Zell-Epitope zu bestimmen, wurden *Aqp4*$^{-/-}$ und Wildtyp Mäuse mit murinem AQP4 Protein immunisiert und anschließend die AQP4-spezifische T-Zell-Antwort auf einzelne überlappende Peptide anhand der gemessenen Proliferation bestimmt. Im T-Zell-Rezeptor Repertoire der *Aqp4*$^{-/-}$ Mäuse, das nicht durch Mechanismen einer Immuntoleranz gegen AQP4 beeinflusst ist, konnte AQP4(201-220) als das wichtigste, immunogene IA^{b}-restringierte T-Zell-Epitop von AQP4 identifiziert werden. Während *Aqp4*$^{-/-}$ Mäuse eine starke AQP4(201-220)-spezifische T-Zellantwort ausbilden, bleibt diese in Wildtyp Mäusen aus. Ihrem natürlichen Immunrepertoire fehlen AQP4-reaktive T-Zellen, da diese bereits während

ihrer Reifung im Thymus negativ selektioniert werden und somit nicht ausreifen. Um diese Immuntoleranz gegen AQP4 zu umgehen und eine AQP4-gerichtete T-Zellantwort in Mäusen zu induzieren, die das Zielantigen im ZNS exprimieren, wurde das reife, nicht-tolerierte T-Zell-Repertoire von *Aqp4*$^{-/-}$ Mäusen in *Rag1*$^{-/-}$ Mäuse übertragen, die selbst keine endogenen T-Zellen besitzen. Diese so genannten *Aqp4*$^{\Delta T}$ *x Rag1*$^{-/-}$ Mäuse zeigten nach Immunisierung mit AQP4(201-220) Anzeichen einer Enzephalomyelitis, deren klinische Symptome vergleichbar waren mit einer klassisch induzierten Experimentellen autoimmunen Enzephalomyelitis (EAE). Ähnlich wie das T-Zell-Repertoire weist auch das B-Zell-Repertoire von Wildtyp Mäusen keine Zellen mit AQP4-spezifischen Rezeptoren auf. Folglich zeigten nur *Aqp4*$^{-/-}$ Mäuse, nicht aber Wildtypen eine robuste anti-AQP4 Serumantwort nach Immunisierung mit AQP4. Der Transfer dieser anti-AQP4 Antikörper oder eines vergleichbaren murinisierten monoklonalen anti-AQP4 Antikörpers (rAb-53) in AQP4(201-220)-immunisierte *Aqp4*$^{\Delta T}$ *x Rag1*$^{-/-}$ Mäuse führte zu einer Verschlechterung des Krankheitsverlaufs aufgrund ausgeprägter Läsionen, die NMO-typische Merkmale aufwiesen. AQP4(201-220)-spezifische T-Zellen alleine verursachen eine Enzephalomyelitis, während NMO-spezifische Läsionen im ZNS und der Retina nur durch das Zusammenwirken von AQP4(201-220)-spezifischen T-Zellen und anti-AQP4 Antikörpern entstehen. Das Versagen der Immuntoleranz gegen AQP4 ist dabei die Voraussetzung für die Ausbildung einer AQP4-spezifischen adaptiven Immunantwort und ein Verständnis der zugrundeliegenden Mechanismen könnte neue Therapien zur Behandlung von NMO ermöglichen.

1 Introduction

1.1 Immunological tolerance and autoimmunity

The function of the immune system is to protect the organism against infectious microbes, toxins and cancer. When microbes overcome physical barriers and enter host tissue, the innate immune system acts as an unspecific first line of defense with cellular and biochemical defense mechanisms that are already in place even before the infection. With a set of low-affinity receptors, cells of the innate immune system recognize conserved structures on pathogens that are absent in mammalian cells and rapidly trigger an inflammatory response. The subsequent activation of the complement system as well as the secretion of cytokines then leads to the recruitment of other effector cells such as macrophages, natural killer T (NKT) cells and granulocytes, and eventually to the activation of the adaptive immune system.

In contrast to the innate immune system, cells of the adaptive immune system are characterized by high-affinity receptors to recognize pathogens in a more specific manner. Moreover, they are able to form an immunological memory that allows for a much faster and stronger immune response upon reencounter with the same microbe. Humoral adaptive immune responses are mediated by antibodies that are produced by B lymphocytes (plasma cells) whereas cell-mediated adaptive immune responses are composed of antigen-specific $CD4^+$ helper T lymphocytes and $CD8^+$ effector T lymphocytes. All lymphocytes bear a highly specific antigen receptor that is generated via random somatic rearrangements of receptor gene segments during cell maturation in primary lymphoid organs. This creates a vast diversity and specificity of antigen receptors that allow lymphocytes to successfully cope with novel antigenic challenges and to adapt to infectious agents over time. Here, B-cell receptors (BCRs) and secreted antibodies recognize conformational antigens whereas T-cell receptors

(TCRs) bind to peptide-bound major histocompatibility complexes (MHC) on cell surfaces. Since the generation of antigen receptors is based on random DNA rearrangements, there are inevitably receptor specificities that are reactive to self-antigens. In order to provide protective immunity and prevent autoimmune responses against self-antigens, immature lymphocytes need to undergo distinct selection processes and have to meet certain checkpoints during their maturation in primary lymphoid organs. To assure the expression of a functional antigen receptor and to mediate deletion or inactivation of self-reactive clones, immature lymphocytes are challenged with different self-antigens that are presented by antigen-presenting cells (APCs). Lymphocytes that bind to self-antigens with low affinity proceed in maturation (positive selection), whereas cells that strongly recognize self-antigens are eliminated from the repertoire (negative selection). In addition, binding to self-antigens with high avidity can lead to receptor editing in B cells or a change in functional capabilities with deviation into the $Foxp3^+$ regulatory T (T_{reg}) cell lineage in T cells (Wirnsberger et al., 2011). Here, the strength and duration of TCR engagement are crucial, with stronger signals leading to deletion and weaker signals leading to diversion (Hinterberger et al., 2010).

While B cells develop in the bone marrow, T-cell precursor cells circulate to the thymus where they mature along different compartments in a spatiotemporal manner. In the outer zone, the cortex, positive selection takes place, whereas tolerance induction is mediated in the inner zone, the medulla. Here, there are two cell types that are most important for presenting antigens to thymocytes during negative selection: thymic dendritic cells (thymic DCs) and medullary thymic epithelial cells (mTECs) (Sprent and Kishimoto, 2002) (Kyewski and Klein, 2006). The latter are able to not only present ubiquitously expressed antigens but rather express a large number of otherwise tissue-restricted antigens (TRAs) under the control of the autoimmune regulator gene (AIRE) (Derbinski et al., 2001). By mirroring the peripheral-self, broad tolerance to self-antigens is induced and only T cells with useful specificities that recognize foreign peptides presented on self-MHC complexes mature and enter the peripheral immune system.

This process of removing potentially harmful self-reactive lymphocytes from the repertoire in primary lymphoid organs is called central tolerance and is essential to prevent autoimmune responses. Since central tolerance mechanisms are incomplete, autoreactive T cells can escape clonal deletion or diversion and must thereupon be held in check by peripheral tolerance. Mechanisms for peripheral tolerance include anergy, clonal deletion and diversion but also suppression of self-reactive lymphocytes (Mueller, 2010) (Xing and Hogquist, 2012).

There is a distinct population of $CD4^+Foxp3^+$ T_{reg} cells that mediates suppression of autoreactive T cells that egress the thymus and seed the peripheral immune compartment despite negative selection. T_{reg} cells limit productive immune responses either by cell-cell contact, local secretion of inhibitory cytokines (IL-10 and TGF-β) or competition for growth factors (Sojka et al., 2008). Thus, they interfere with both the initial activation of B cells and T cells and their effector functions in the target tissue. Besides thymic-derived natural T_{reg} cells (nT_{reg}), also conventional $CD4^+CD25^-$ T cells can be converted into Foxp3 expressing regulatory T cells in the periphery and henceforth function as induced T_{reg} cells (iT_{reg}). This conversion requires a combination of strong TCR signaling under suboptimal co-stimulation and a cytokine milieu rich in TGF-β and IL-2 (Chen et al., 2003).

A more passive mechanism to maintain peripheral immune tolerance is the physical separation of autoreactive T cells from the site of TRA expression. Naive T cells circulate from blood to secondary lymphoid organs and through efferent lymph back to the blood and therefore are more or less excluded from nonlymphoid peripheral tissue where TRAs are mostly expressed. This restricted trafficking is guided by concentration gradients of CCR7 and binding of T-cell L-selectin (CD62L) to epitopes on epithelial cells of secondary lymphoid organs and provides immunological ignorance towards self-antigens. This effect is even more profound for certain self-antigens that are sequestered behind anatomical barriers (e.g. blood-brain-barrier, BBB) with only limited access by immune cells.

When a breach of both central and peripheral tolerance leads to the activation of autoreactive B cells and T cells, the subsequent immune response can cause tissue injury and eventually systemic or organ-specific autoimmune disease. A defect in tolerance induction is the fundamental cause but there are several factors that further promote such immunopathology. This includes infections with persistent microbes that elicit excessive immune reactions and bystander activation of self-reactive lymphocytes as well as genetic predisposition and environmental influences. Other mechanisms that can trigger autoimmune responses are microbial molecular mimicry in which foreign antigens share sequence similarities with self-antigens, leading to activation of self-reactive lymphocytes upon infection (Fujinami and Oldstone, 1985) or cross-reactivity of T cells that recognize both, microbial and self-antigens (Harkiolaki et al., 2009).

1.2 Neuromyelitis optica and aquaporin-4

Neuromyelitis optica (NMO) is an autoimmune inflammatory disease of the human CNS that predominantly affects the spinal cord, optic nerves and brainstem. Cases of optic neuritis in combination with myelitis were first reviewed by Eugène Devic in 1894 and the disease originally became known as Devic's disease. Since NMO often shows a relapsing course with a specific pattern of demyelinating lesions in the CNS, it was thought to be a clinical variant of multiple sclerosis (MS), until in 2004 a circulating IgG autoantibody was described in NMO patients that was completely absent in MS patients (Lennon et al., 2004). Approximately three-quarters of NMO patients are seropositive for this autoantibody that targets the water channel protein aquaporin-4 (AQP4) and therefore is also referred to as AQP4-IgG or NMO-IgG. Together with unique clinical features (i.e. a sequence of monophasic, longitudinal, extensive transverse myelitis and optic neuritis) as well as neuroimaging, immunological and histopathological characteristics, AQP4-IgG serostatus is now included into the diagnosis criteria for NMO. Recently, these criteria were revised and the term neuromyelitis optica spectrum disorder (NMOSD) was adopted to describe a rather heterogeneous group of diseases where neuroinflammation and demyelination cause visual and motor deficits as well as other neurological impairments (Wingerchuk et al., 2015).

Population-based studies in Europe, Asia and North America suggest the incidence rate of NMOSD ranges from 0.05 – 0.4 per 100.000 with a mean age of onset between 33 and 46 years and a pronounced preponderance of women (Pandit et al., 2015). Moreover, patients with AQP4-IgG seropositive NMOSD (hereinafter referred to as NMO) are more likely to show signs of co-existing autoimmunity and suffer from more severe clinical attacks compared to seronegative patients (Jarius et al., 2012). Although some human leukocyte antigen (HLA) genes are associated with increased risk for NMO, genetic susceptibility is complex (Matiello et al., 2010). Hence, the initial cause of tolerance breakdown and subsequent initiation of the inflammatory autoimmune response resulting in NMO is not known yet.

However, NMO is an autoimmune disease of the CNS with a highly specific adaptive immune response against the known target antigen AQP4. In contrast, other autoimmune diseases such as MS show less antigen specificity and despite extensive research over decades, the autoantigen in MS is only assumed to reside within myelin sheaths of axons. With AQP4 being a well-defined target in NMO, different animal models have been established to study disease pathogenesis mechanisms and evaluate potential drug candidates. Knowing the

autoantigen allows for the development of antigen-specific treatment options in NMO such as aquaporumab antibodies (Tradtrantip et al., 2012b) (Duan et al., 2020) and small molecule blockers of AQP4-IgG/AQP4 binding (Tradtrantip et al., 2012a) and furthermore gives the opportunity to study characteristics of autoreactive immune responses and underlying errors in tolerance induction.

Insufficient tolerance to AQP4 allows for the generation of AQP4-IgG, that not only serves as a serological biomarker but plays a central role in the pathogenesis of NMO upon entering the CNS. Here, the autoantibodies target AQP4, the most abundant water channel protein that enables water flow across cell membranes in response to osmotic gradients. AQP4 is characterized by six helical, transmembrane domains and is predominantly expressed in the foot processes of astrocytes near perivascular sites (Papadopoulos and Verkman, 2012).

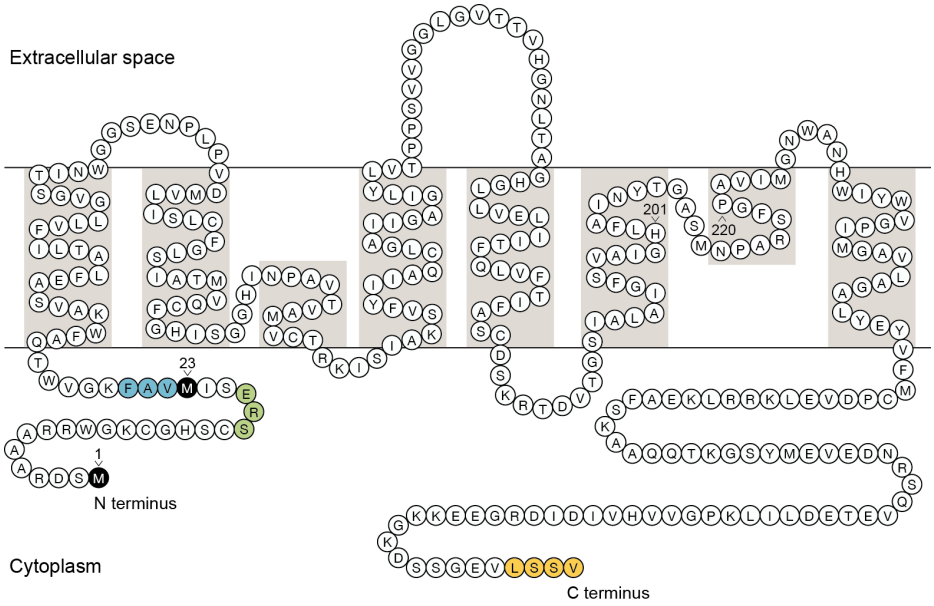

Figure 1.1: The water channel protein AQP4. Protein sequence of murine AQP4, showing translation initiation sites at Met-1 and Met-23 (black), residues that promote (blue) and prevent (green) formation of orthogonal arrays of particles and the C-terminus PDZ domain (yellow). Adapted from Papadopoulos and Verkman 2012.

Outside the CNS, AQP4 is expressed in skeletal muscle, stomach, kidney and Müller cells of the retina (Verkman, 2012). Thus, AQP4 is not sequestered behind the BBB like other CNS autoantigens (e.g. myelin oligodendrocyte glycoprotein, MOG) and antigenic "ignorance" as tolerance mechanism towards AQP4 is most likely irrelevant. There are two different isoforms produced by alternative splicing, a longer isoform (M1) with translation initiation at Met-1 and a shorter one (M23) with translation initiation at Met-23 (Figure 1.1). In membranes, AQP4 assembles in homo- or heterotetramers and, unlike other aquaporins, further aggregates

to form so-called orthogonal arrays of particles (OAPs). The appearance of OAPs depends on the isoforms involved with M23-AQP4 promoting larger clusters and M1-AQP4, which is unable to form OAPs itself, limiting their size when co-expressed with M23-AQP4 (Crane and Verkman, 2009). In context of NMO pathogenesis, OAPs are crucial for complement-dependent cytotoxicity since AQP4-IgG preferentially binds to these square supramolecular clusters rather than separated AQP4 tetramers hence facilitating complement activation by multivalent C1q binding to clustered antibodies (Crane et al., 2011).

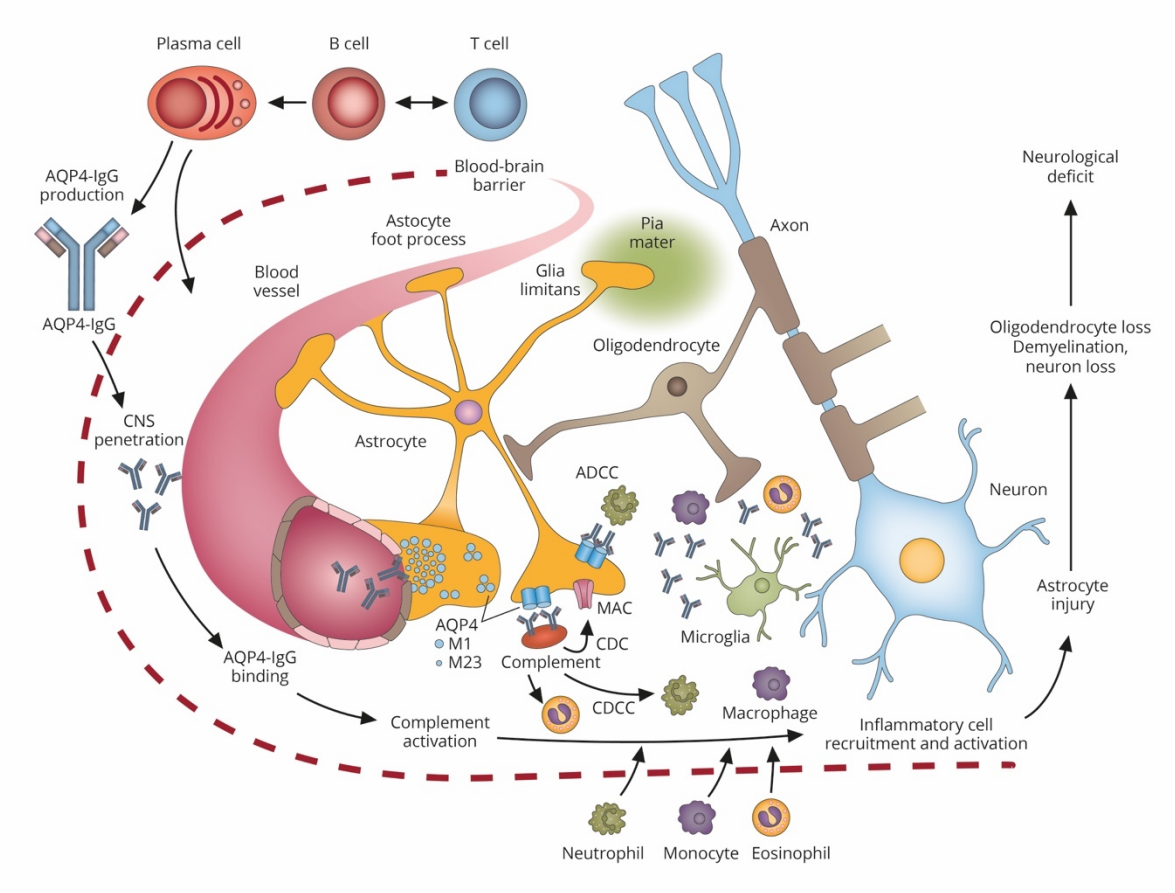

Figure 1.2: Mechanisms of NMO pathogenesis. Interaction of AQP4-specific T cells and B cells leads to the production of AQP4-IgG in the periphery. Both serum AQP4-IgG and plasma cells penetrate the CNS resulting in binding of AQP4-IgG to AQP4 expressed in foot processes of astrocytes. Antibody-dependent damage of astrocytes is mediated by complement-dependent cytotoxicity (CDC) with formation of the MAC complex, complement-dependent cellular cytotoxicity (CDCC) and antibody-dependent cellular cytotoxicity (ADCC). Here, macrophages, neutrophils and eosinophils contribute to inflammation, which eventually leads to oligodendrocyte injury, demyelination and neuronal loss. Adapted from Papadopoulos et al. 2014 and Weinshenker and Wingerchuk 2017.

This leads to complement-mediated lysis of astrocytes and recruitment of other immune cells such as granulocytes (i.e. neutrophils and eosinophils) and macrophages that further contribute to lesion formation. The absence of complement regulators including CD46

(membrane cofactor protein), CD55 (decay accelerating factor) and CD59 (protectin) in the CNS compared to their expression in close proximity to AQP4 in peripheral tissue may explain why astrocytes but not peripheral epithelial cells or parenchymal cells are a target for complement-mediated lysis in patients with high serum titers of AQP4-IgG (Saadoun and Papadopoulos, 2015).

Besides complement activation, another mechanism of anti-AQP4-induced damage is the internalization of M1-AQP4 upon antibody binding with functional consequences for other proteins such as the glutamate transporter EAAT2 that are associated with M1-AQP4 (Hinson et al., 2008) (Hinson et al., 2012). Either way, by targeting astrocytic AQP4 molecules, AQP4-IgG are necessary for the pathological processes in NMO patients. Lesions are characterized by a vasculocentric deposition of immunoglobulin and activated complement components with loss of AQP4 and glia fibrillary acidic protein (GFAP) in astrocytes, underscoring the humoral nature of the immune response against this perivascular antigen (Roemer et al., 2007) (Misu et al., 2007). However, AQP4-IgG are class-switched antibodies that need T-cell help in order to be generated (Snapper and Paul, 1987) (Toellner et al., 1998) and early lesions in NMO contain activated $CD4^+$ T cells (Pohl et al., 2013). Moreover, AQP4-specific T cells are clonally expanded in NMO patients (Matsuya et al., 2011) (Varrin-Doyer et al., 2012) and in most passive transfer studies, AQP4-IgG only unfolds its pathogenic functions in the context of T-cell mediated inflammation (Bradl et al., 2009) (Bennett et al., 2009) (Saini et al., 2013). Therefore, an underlying AQP4-specifc T-cell response must be assumed in patients with NMO, although the extent to which T cells contribute to antibody-mediated immunopathology remains to be determined. There is substantial evidence, that in NMO astrocyte damage occurs first followed by granulocyte infiltration and oligodendrocyte death leading to demyelination and ultimately neuronal cell death (Lucchinetti et al., 2002). Because the major CNS cell types are affected by necrosis in active lesions of NMO in spinal cord and optic nerve, and to a lesser extent in the brain, clinical deficits are severe and recovery is poor (Wingerchuk et al., 2007). Patients often suffer from vision loss in one or both eyes, vomiting and sensory loss as well as weakness or paralysis in arms or legs. To date there is no cure for the disease and therapy focuses on the treatment of acute clinical relapses as well as prevention of future relapses with long-term immunosuppression or B-cell depletion (Whittam et al., 2017).

1.3 A preclinical model for NMO

Ever since the discovery of AQP4-IgG as highly specific IgG1 biomarker of NMO that is also crucial for the immune response causing immunopathology against AQP4, great efforts have been made to establish an experimental animal model for this disease that reproduces its distinct features. The first models evolved around the passive transfer of AQP4-IgG from NMO patient's sera or human recombinant monoclonal anti-AQP4 antibody into rodents either by direct intracerebral injection (Saadoun et al., 2010) (Ratelade et al., 2013) or, when applied peripherally, accompanied by a T-cell mediated autoimmune response against myelin antigens in the CNS (Bradl et al., 2009) (Saini et al., 2013). To induce this T-cell driven inflammation that results in an inflammatory milieu in the CNS and allows AQP4-IgG to overcome the BBB and gain access to the CNS parenchyma, the well-established protocol for experimental autoimmune encephalomyelitis (EAE) was used.

EAE is a model for CNS inflammation and demyelination that is induced in rodents by immunization with myelin antigens emulsified in complete Freund's adjuvant (CFA) to efficiently prime myelin epitope-specific $CD4^+$ T cells and elicit a T-cell mediated autoimmune response (Zamvil and Steinman, 1990). These auto-reactive T cells are present in the normal T-cell repertoire of wild type animals and ignore their antigen due to its "sequestered" expression in the CNS under physiological conditions (Delarasse et al., 2003). Once activated, myelin-specific T cells are able to migrate across the BBB into the CNS where they get reactivated upon antigen recognition and secrete cytokines and chemokines (Kawakami et al., 2004). This leads to the recruitment of other immune cells to the site of T-cell activation and in particular infiltrating macrophages contribute to tissue damage including demyelination and axonal damage with pro-inflammatory mediators such as TNF and IL-1 (Kuchroo et al., 2002). In mice, this results in a disease with ascending paralysis starting with the tail and progressing to hind- and forelimbs. In addition to active EAE that is based on immunization, disease can also be induced by transfer of activated myelin-specific $CD4^+$ T cells from mice with EAE to naïve mice (Bettelli et al., 2003). There are different encephalitogenic myelin antigens used in current immunization regimens including myelin oligodendrocyte glycoprotein (MOG) (Linington et al., 1993), myelin basic protein (MBP) (Ben-Nun et al., 1981) and proteolipid protein (PLP) (Kuchroo et al., 1991).

When AQP4-IgG was injected into animals with preexisting EAE (i.e. an underlying CNS inflammation), clinical disease was augmented and lesions were similar to those seen in NMO

patients with infiltration of neutrophils and eosinophils, AQP4 and astrocyte loss as well as extensive perivascular deposition of human IgG and complement (Bradl et al., 2009). Other passive transfer models involved direct intracerebral injection of AQP4-IgG together with human complement into mice without preexisting EAE resulting in loss of AQP4 and GFAP immunoreactivity and axonal injury, accompanied by only little inflammation (Saadoun et al., 2010). The same characteristic lesions were seen in naïve rats upon intracerebral injection of AQP4-IgG without the need of additional administration of human complement, since human IgG efficiently activates the classical complement pathway in rats which is not the case in mice (Asavapanumas et al., 2014a). When administered intrathecally at L5-L6 (Zhang and Verkman, 2014) or via an intracranial infusion near the optic chiasm (Asavapanumas et al., 2014b) AQP4-IgG together with human complement mediated NMO-like lesions in the spinal cord and optic nerves, tissues primarily affected by NMO pathology and therefore more relevant than brain in human NMO.

In all of the above models, injection of AQP4-IgG into rodents resulted in pathology that recapitulates some of the hallmark features of human NMO like early astrocyte cytotoxicity, loss of AQP4 and GFAP in lesions, perivascular deposition of immunoglobulin and complement, disruption of the BBB, demyelination and inflammation with granulocyte and macrophage predominance. Hence, these early models were important to confirm the pathogenicity of AQP4-IgG and further demonstrate the importance of complement-dependent cytotoxicity (CDC) and antibody-dependent cellular cytotoxicity (ADCC) in NMO immunopathology. Moreover, AQP4-IgG passive transfer models have been used to test several therapeutic strategies (Papadopoulos et al., 2014).

However, these passive transfer models have several shortcomings mainly because the administration of AQP4-IgG with preexisting EAE or in combination with human complement is highly artificial and therefore completely omits early processes involved in disease development. Moreover, in NMO pathology, there is no myelin-targeted T-cell response, making it difficult to distinguish direct effects of AQP4-IgG from those resulting from the underlying T-cell response. On the other hand, heterologous models involving the transfer of AQP4-IgG and human complement have other disadvantages, that complicate data interpretation (Liu et al., 2016). Most importantly, passive transfer models of NMO are inadequate to reproduce initial events in disease onset like tolerance breakdown and collaboration of AQP4-specific B cells and T cells.

To study the role of AQP4-specific T cells in NMO immunopathology, multiple T-cell epitopes of AQP4 have been proposed in Lewis rats (Pohl et al., 2011) (Zeka et al., 2015), C57BL/6 and SJL/J mice (Kalluri et al., 2011) (Nelson et al., 2010) (Jones et al., 2015). While direct immunization of animals with these epitopes failed to induce a T-cell driven AQP4-targeted immunopathology, transfer of in vitro polarized AQP4-specific $CD3^+CD4^+$ T-helper 1 (T_H1) cells induced subclinical disease with inflammation in particular at the glia limitans in the CNS of recipient rats (Pohl et al., 2011). More recently, T cell delivery models of NMO could show that AQP4-reactive T cells both trigger and localize inflammation to AQP4-rich sites in the CNS and in combination with AQP4-IgG induce NMO-like pathology with astrocyte-destructive lesions, loss of AQP4 and deposition of complement, suggesting a key immunopathogenic role for AQP4-specific T cells in NMO (Zeka et al., 2015) (Jones et al., 2015).

Although models of NMO have advanced over time, so far there is no model that shows spontaneous AQP4 autoimmunity with immunopathology reminiscent of human NMO. Furthermore, passive transfer models and T-cell delivery models each have major shortcomings and are intrinsically biased towards humoral or cellular immunity, respectively (Duan and Verkman, 2020). However, since the autoantigen is known in NMO, this autoimmune disease is particularly well suited to study the underlying conditions that ultimately lead to antigen-specific autoimmune pathology in the CNS, and more efforts should be made to develop a more suitable experimental animal model for NMO.

2 Aim of the study

There are different experimental animal models of seropositive NMOSD to investigate disease pathogenesis and evaluate new drug candidates. Most of them are based on passive transfer to rodents of AQP4-IgG (Saadoun et al., 2010) or AQP4-sensitized T cells under pro-inflammatory conditions (Pohl et al., 2011) and therefore inevitably show a bias towards humoral or cellular immune mechanisms respectively. While the AQP4-specific B-cell response and the pattern of CNS damage resulting from AQP4-IgG-mediated immunopathology have been well characterized in these models, the roles of other inflammatory cell types and cytokines in NMO pathogenesis as well as the underlying cause of tolerance breakdown leading to the entry of AQP4-IgG into the CNS, remain largely unknown.

In particular, the extent to which AQP4-specific T cells might contribute to the course of disease in addition to providing help to B cells during class-switch recombination of anti-AQP4 antibodies to isotype IgG1 (in humans) and IgG2 (in mice) remains to be elucidated. Here, the role of T cells in breaking tolerance and causing inflammation in NMO to be targeted to the optic nerve and spinal cord is of great interest (Bradl et al., 2009).

Thus, this study was designed to generate and characterize AQP4-specific T cells in order to investigate their ability to contribute to lesion formation in the absence or presence of AQP4-specific antibodies in the CNS of mice. In this context, a new transfer model for NMO was established using compound mice that, with respect to AQP4, were equipped with a non-tolerized T-cell repertoire while exhibiting unaltered antigen expression. Furthermore, the mechanism of tolerance induction to AQP4 was investigated since a defect in both thymic tolerance and B-cell tolerance might be a prerequisite for NMO-like autoimmune pathology in the CNS.

3 Material and Methods

3.1 Material

3.1.1 Reagents

Reagents were purchased from the respective suppliers and stored in accordance with the manufacturer's specifications.

Table 3.1: Reagents used in the experiments.

Reagent	**Supplier**
2-Propanol	Sigma-Aldrich (St. Louis, USA)
Agarose	Sigma Aldrich (St. Louis, USA)
Aqua	B. Braun (Melsungen, Germany)
Baytril, 2.5%	Boehringer Ingelheim (Ingelheim am Rhein, Germany)
Betaplate Scint® scintillation fluid	PerkinElmer (Waltham, USA)
BlueJuice™ Gel Loading Buffer 10x	Life technologies (Carlsbad, USA)
Bovine serum albumin (BSA)	Sigma-Aldrich (St. Louis, USA)
BD Cytofix/Cytoperm solutions	BD Biosciences (Heidelberg, Germany)
BD Perm/Wash buffer	BD Biosciences (Heidelberg, Germany)
DH10MultiBac	Geneva Biotech (Genf, Switzerland)
DNA ladder (1kb and 100 bp)	Life Technologies (Carlsbad, USA)
DreamTaq Green PCR Master Mix (2x)	Thermo Fisher Scientific (Waltham, USA)
Dulbecco's modified Eagle medium (DMEM)	PAA (Pasching, Austria)
EDTA	Merck Millipore (Darmstadt, Germany)

Reagent	Supplier
Enrofloxacin	Bayer (Leverkusen, Germany)
Ethidium bromide solution	Sigma-Aldrich (St. Louis, USA)
Fetal calf serum (FCS)	Sigma-Aldrich (St. Louis, USA)
GolgiStop® Protein transport inhibitor	BD Biosciences (Heidelberg, Germany)
H37RA Mycobacterium tuberculosis	BD Biosciences (Heidelberg, Germany)
Ionomycin calcium salt	Sigma-Aldrich (St. Louis, USA)
Isofluran	Abbott (Chicago, USA)
LB Agar	Life Technologies (Carlsbad, USA)
LB Broth Base	Life Technologies (Carlsbad, USA)
Lipofectamine® LTX & Plus Reagent	Life Technologies (Carlsbad, USA)
MEM non-essential amino acids	Life Technologies (Carlsbad, USA)
MEM vitamin solution	Life Technologies (Carlsbad, USA)
Mouse brain cerebellum total RNA	Clontech (Mountain View, USA)
Nuclease free water	Life Technologies (Carlsbad, USA)
NuPAGE MES SDS Running Buffer (20x)	Thermo Fisher Scientific (Waltham, USA)
Octyl β-D-glucopyranoside	Sigma-Aldrich (St. Louis, USA)
Paraffin oil	Sigma-Aldrich (St. Louis, USA)
Percoll	GE Healthcare (Munich, Germany)
Penicillin/Streptomycin solution	Life Technologies (Carlsbad, USA)
Peroxidase substrate solution B	KPL (Gaithersburg, USA)
Pertussis toxin	Sigma-Aldrich (St. Louis, USA)
PharmLyse® Red blood cell lysis buffer	BD Biosciences (Heidelberg, Germany)
Phorbol 12-myristate 13-acetate (PMA)	Sigma-Aldrich (St. Louis, USA)
Phosphate-buffered saline (PBS)	PAA (Pasching, Austria)
Ponceau S solution	Sigma-Aldrich (St. Louis, USA)
RNaseZap® decontamination solution	Sigma-Aldrich (St. Louis, USA)
SeaBlue Plus2 Protein Standard	Thermo Fisher Scientific (Waltham, USA)
SOC medium	Life Technologies (Carlsbad, USA)
SuperSignal West Pico PLUS Chemiluminescent Substrate	Thermo Fisher Scientific (Waltham, USA)
TMB peroxidase substrate	KPL (Gaithersburg, USA)
Thymidine, [Methyl-^{3}H]	PerkinElmer (Waltham, USA)
Trypan blue	Life Technologies (Carlsbad, USA)
Trypsin	Thermo Fisher Scientific (Waltham, USA)

3.1.2 Plasmids

Plasmids were used as indicated in the methods section for cloning of mouse *Aqp4* and subsequent expression of the AQP4 protein in a baculovirus system for protein production in High Five cells.

Table 3.2: Plasmids used for cloning.

Vector	**Resistance**	**Supplier**
pGem-T Easy vector	Ampicillin	Promega (Madison, USA)
pcDNA3.1(+)	Ampicillin	Life Technologies (Carlsbad, USA)
pFBDM	Ampicillin	Addgene (Watertown, USA)

3.1.3 Primers

Primers were obtained from Eurofins (Brussels, Belgium) and were used for either genotyping or cloning.

Table 3.3: Primers used for cloning.

Primer		**Sequence 5' → 3'**
mAQP4_M1_pcDNA	fwd	CCCAAGCTTATGAGTGACAGAGCTGCGGC
	rev	CCGCTCGAGTCAGTGATGGTGATGGTGATGTACGG AAGACAATACCTCTCC
mAQP4_M1_Chis_bac	fwd	TGCTCTAGAATGAGTGACAGAGCTGCGGC
	rev	CCGAAGCTTTCAGTGATGGTGATGGTGATGTACGG AAGACAATACCTCTCC
mAQP4_M1_Seq	fwd	CACTTTCCAGTTGGTGTTC
	rev	GAACACCAACTGGAAAGTG

Table 3.4: Primers used for genotyping.

Primer		**Sequence 5' → 3'**
Aqp4$^{flox/flox}$	fwd	TCCTGAGATTAGAGAGAGCACTTTC
	rev	GACCCGCAGTTATCATGGGAAAC
Aqp4$^{-/-}$	fwd	ACCATAAACTGGGGTGGCTCAG
	rev^{WT}	TAGAGGATGCCGGCTCCAATG
	rev^{KO}	CCGCTGAATATGCATAAGGCAG
Foxn1^{Cre}	fwd	CATACGATTTAGGTGACACTATAG
	rev	AATCTCATTCCGTTACGCAG

3.1.4 Enzymes

Enzymes were obtained from the respective supplier and stored at -80°C.

Table 3.5: Enzymes used for cloning, genotyping or digestion of tissue.

Enzyme	Supplier
Collagenase I	Life Technologies (Carlsbad, USA)
Collagenase D	Roche (Mannheim, Germany)
DNase I	Roche (Mannheim, Germany)
Green Taq	Thermo Fisher (Waltham, USA)
HindIII	New England Biolabs (Ipswich, USA)
NotI	New England Biolabs (Ipswich, USA)
Platinum PCR SuperMix	Life Technologies (Carlsbad, USA)
Platinum PCR SuperMix High Fidelity	Life Technologies (Carlsbad, USA)
RNase inhibitor	Life Technologies (Carlsbad, USA)
T4 Ligase	New England Biolabs (Ipswich, USA)
XbaI	New England Biolabs (Ipswich, USA)
XhoI	New England Biolabs (Ipswich, USA)

3.1.5 Kits

Kits were obtained from the depicted supplier and used according to the specifications in the respective protocol.

Table 3.6: Kits used for cloning and protein biochemistry methods.

Kit	Supplier
Colloidal Blue Staining Kit	Thermo Fisher Scientific (Waltham, USA)
Foxp3 staining buffer set	eBioscience (San Diego, USA)
HiSpeed Plasmid Maxi Kit	Qiagen (Hilden, Germany)
LIVE/DEAD fixable aqua dead cell stain kit	Life Technologies (Carlsbad, USA)
NuPAGE 4-12% Bis-Tris protein gels	Thermo Fisher Scientific (Waltham, USA)
Penta His HRP Conjugate Kit	Qiagen (Hilden, Germany)
pGEM®-T Easy Vector System I	Promega (Madison, USA)
RNeasy Mini Kit	Qiagen (Hilden, Germany)
SuperScript® VILO™ cDNA Synthesis Kit	Thermo Fisher Scientific (Waltham, USA)
ViraPower™ Bsd Lentiviral Support Kit	Thermo Fisher Scientific (Waltham, USA)

Kit	Supplier
QIAprep Spin Miniprep Kit	Qiagen (Hilden, Germany)
QIAquick Gel Extraction Kit	Qiagen (Hilden, Germany)
QIAquick PCR Purification	Qiagen (Hilden, Germany)
QIAshredder	Qiagen (Hilden, Germany)

3.1.6 Cell culture media

For all primary cell cultures DMEM medium supplemented with the respective reagents was used. It is referred to as clone medium in the following. Cell lines were cultivated in either DMEM or RPMI medium supplemented with FCS and antibiotics. To wash cells during preparation of single cell suspensions from organs, DMEM medium without supplements was used. Prior to use, all supplemented media were sterile filtered through a Nalgene 0.22 µm SFCA membrane. All media were obtained from Thermo Fisher Scientific (Waltham, USA).

Table 3.7: Composition of all media used in cell culture for primary cells and cell lines.

Medium	Supplements
DMEM clone medium	10 % FCS 50 U/ml Penicillin 50 µg/ml Streptomycin 1 x MEM-NEAA non-essential amino acids 1 x MEM Vitamin Solution 0.66 mM L-Arginine 0.27 mM L-Asparagine 13.6 µM Folic Acid 50 µM β-Mercaptoethanol 0.1 mg/ml Gentamycin
DMEM-wash	–
DMEM-10	10 % FCS 50 U/ml Penicillin 50 µg/ml Streptomycin
DMEM cryomedium	20 % FCS 20 % DMSO
MEM	–
RPMI-wash	–
RPMI 1640-10	10 % FCS 50 U/ml Penicillin 50 µg/ml Streptomycin
RPMI 1640 cryomedium	20 % FCS 20 % DMSO

3.1.7 Buffers and solutions

Buffers and solutions were prepared with water purified in a Millipore filter system (pore size 0.22 µm). All chemicals met the highest purity standards and were obtained from Roth, Sigma-Aldrich, Merck and Invitrogen.

Table 3.8: Composition of buffers and solutions.

Buffer or solution	**Composition**
CNS digestion solution	2.5 mg/ml Collagenase D 1.0 mg/ml DNase I in DMEM
Complete Freund's adjuvant	17 ml Paraffin oil 3.0 ml Arlacel A 100 mg Mycobacterium tuberculosis (pestled)
FACS buffer	2 % FCS in PBS
Gel filtration buffer	25 mM Tris-HCl 250 mM NaCl 10 % Glycerol 2 mM DTT 40 mM Octyl β-D-glucopyranoside
MACS buffer	0.5 % BSA (w/v) 2 mM EDTA in PBS, pH 8.0
MR buffer	25 mM Tris-HCl 250 mM NaCl 10 % Glycerol 5 mM Imidazole 1 mM β-Mercaptoethanol 200 mM Octyl β-D-glucopyranoside
MR elution buffer	25 mM Tris-HCl 250 mM NaCl 10 % Glycerol 250 mM Imidazole 1 mM β-Mercaptoethanol 40 mM Octyl β-D-glucopyranoside
MR wash buffer	25 mM Tris-HCl 250 mM NaCl 10 % Glycerol 25 mM Imidazole 1 mM β-Mercaptoethanol 40 mM Octyl β-D-glucopyranoside
PBS-T	0.1 % Tween-20 in PBS

Buffer or solution	Composition
Percoll mix solution	90 ml PBS (10x) 264 ml aqua dest., pH adjusted to 7.2 with HCL
Percoll, 70 %	30 ml Percoll 18 ml Percoll mix solution
Percoll, 37 %	5.2 ml 70 % Percoll 4.8 ml PBS
Spleen digestion solution	1.0 mg/ml Collagenase D 20 µg/ml DNase I 2 % FCS in HEPES-buffered RPMI-1640
TAE, 50x	242 g Tris 57.1 ml Glacial acetic acid 0.5 mM EDTA add 1 l aqua dest., pH 8.0
TBS buffer	50 mM Tris-HCl 150 mM NaCl 1 mM β-Mercaptoethanol

3.1.8 Antibodies

Antibodies were purchased from different suppliers as stated in the table and were used for T-cell cultures and staining of cells for FACS analyses. HRP-conjugated antibodies were used in western blot analysis.

Table 3.9: Antibodies used for FACS and western blot analysis as well as histology and application in cell cultures.

Specificity *(clone)*	Conjugate	Application	Supplier
AQP4 *(polyclonal)*	unconjugated	Histology Western blot	Sigma-Aldrich (St. Louis, USA)
CD3 *(CD3-12)*	unconjugated	Histology	Bio-Rad (Hercules, USA)
Mac3 *(M3/84)*	unconjugated	Histology	BD Biosciences (Heidelberg, Germany)
CD25 *(PC61)*	unconjugated	Neutralizing	BioXCell (West Lebanon, USA)
rabbit IgG (H+L) *(polyclonal)*	HRP	Western blot	Thermo Fisher Scientific (Waltham, USA)
CD3 *(500A2)*	Pacific Blue	FACS	BD Biosciences (Heidelberg, Germany)
CD4 *(GK1.5)*	FITC	FACS	BD Biosciences (Heidelberg, Germany)
CD4 *(RM4-5)*	PE	FACS	BD Biosciences (Heidelberg, Germany)
CD4 *(RM4-5)*	APC	FACS	BD Biosciences (Heidelberg, Germany)
CD4 *(RM4-5)*	BV510	FACS	BioLegend (San Diego, USA)

Specificity *(clone)*	**Conjugate**	**Application**	**Supplier**
CD45R *(RA3-6B2)*	PE-Cy7	FACS	BioLegend (San Diego, USA)
CD8 *(53-6.7)*	APC	FACS	BD Biosciences (Heidelberg, Germany)
CD8 *(53-6.7)*	APC-Cy7	FACS	BioLegend (San Diego, USA)
CD8 *(53-6.7)*	PerCP	FACS	BD Biosciences (Heidelberg, Germany)
CD11b *(M1/70)*	APC	FACS	BD Biosciences (Heidelberg, Germany)
CD11b *(M1/70)*	PE-Cy7	FACS	BioLegend (San Diego, USA)
CD11c *(HL3)*	PE	FACS	BD Biosciences (Heidelberg, Germany)
CD11c *(N418)*	PE-Cy7	FACS	BioLegend (San Diego, USA)
CD19 *(1D3)*	APC	FACS	BD Biosciences (Heidelberg, Germany)
CD19 *(1D3)*	PE	FACS	BD Biosciences (Heidelberg, Germany)
CD44 *(IM7)*	FITC	FACS	BD Biosciences (Heidelberg, Germany)
CD45R *(RA3-6B2)*	Pacific Blue	FACS	BioLegend (San Diego, USA)
CD45R *(RA3-6B2)*	APC	FACS	BioLegend (San Diego, USA)
CD45R *(RA3-6B2)*	PE-Cy7	FACS	BioLegend (San Diego, USA)
F4/80 *(BM8)*	PE-Cy7	FACS	BioLegend (San Diego, USA)
GM-CSF *(MP1-22E9)*	PE	FACS	BD Biosciences
IFN-γ *(XMG1.2)*	PE-Cy7	FACS	eBioscience (San Diego, USA)
IL-10 *(JES5-16E3)*	BV421	FACS	BD Biosciences (Heidelberg, Germany)
IL-17A *(TC11-18H10)*	PerCP-Cy5.5	FACS	BD Biosciences (Heidelberg, Germany)
I-Ab *(M5/114.15.2)*	PerCP	FACS	BioLegend (San Diego, USA)
mIgA *(polyclonal)*	FITC	FACS	Bio-Rad (Hercules, Germany)
mIgE *(polyclonal)*	FITC	FACS	Bio-Rad (Hercules, Germany)
mIgG1 *(polyclonal)*	FITC	FACS	Bio-Rad (Hercules, Germany)
mIgG2b *(polyclonal)*	FITC	FACS	Bio-Rad (Hercules, Germany)
mIgG2c *(polyclonal)*	FITC	FACS	Bio-Rad (Hercules, Germany)
mIgG3 *(polyclonal)*	FITC	FACS	Bio-Rad (Hercules, Germany)
mIgG (H+L) *(polyclonal)*	AF488	FACS	Thermo Fisher Scientific (Waltham, USA)

3.1.9 Peptides

Peptides were synthesized by Auspep (Tullamarine, Australia) or Biotrend (Cologne, Germany), respectively and possess a purity of more than 92 % after HPLC.

Table 3.10: Peptides used for immunization of mice and in cell culture for recall assays.

Protein	Peptide-No	AA residues	Sequence
AQP4	P01	1-20	MSDRAAARRWGKCGHSCSRE
	P02	6-25	AARRWGKCGHSCSRESIMVA
	P03	11-30	GKCGHSCSRESIMVAFKGVW
	P04	16-35	SCSRESIMVAFKGVWTQAFW
	P05	21-40	SIMVAFKGVWTQAFWKAVSA
	P06	26-45	FKGVWTQAFWKAVSAEFLAT
	P07	31-50	TQAFWKAVSAEFLATLIFVL
	P08	36-55	KAVSAEFLATLIFVLLGVGS
	P09	41-60	EFLATLIFVLLGVGSTINWG
	P10	46-65	LIFVLLGVGSTINWGGSENP
	P11	51-70	LGVGSTINWGGSENPLPVDM
	P12	56-75	TINWGGSENPLPVDMVLISL
	P13	61-80	GSENPLPVDMVLISLCFGLS
	P14	66-85	LPVDMVLISLCFGLSIATMV
	P15	71-90	VLISLCFGLSIATMVQCFGH
	P16	76-95	CFGLSIATMVQCFGHISGGH
	P17	81-100	IATMVQCFGHISGGHINPAV
	P18	86-105	QCFGHISGGHINPAVTVAMV
	P19	91-110	ISGGHINPAVTVAMVCTRKI
	P20	96-115	INPAVTVAMVCTRKISIAKS
	P21	101-120	TVAMVCTRKISIAKSVFYII
	P22	106-125	CTRKISIAKSVFYIIAQCLG
	P23	111-130	SIAKSVFYIIAQCLGAIIGA
	P24	116-135	VFYIIAQCLGAIIGAGILYL
	P25	121-140	AQCLGAIIGAGILYLVTPPS
	P26	126-145	AIIGAGILYLVTPPSVVGGL
	P27	131-150	GILYLVTPPSVVGGLGVTTV
	P28	136-155	VTPPSVVGGLGVTTVHGNLT
	P29	141-160	VVGGLGVTTVHGNLTAGHGL
	P30	146-165	GVTTVHGNLTAGHGLLVELI
	P31	151-170	HGNLTAGHGLLVELIITFQL
	P32	156-175	AGHGLLVELIITFQLVFTIF
	P33	161-180	LVELIITFQLVFTIFASCDS
	P34	166-185	ITFQLVFTIFASCDSKRTDV
	P35	171-190	VFTIFASCDSKRTDVTGSIA
	P36	176-195	ASCDSKRTDVTGSIALAIGF
	P37	181-200	KRTDVTGSIALAIGFSVAIG
	P38	186-205	TGSIALAIGFSVAIGHLFAI
	P39	191-210	LAIGFSVAIGHLFAINYTGA
	P40	196-215	SVAIGHLFAINYTGASMNPA
	P41	201-220	HLFAINYTGASMNPARSFGP
	P42	206-225	NYTGASMNPARSFGPAVIMG
	P43	211-230	SMNPARSFGPAVIMGNWANH
	P44	216-235	RSFGPAVIMGNWANHWIYWV
	P45	221-240	AVIMGNWANHWIYWVGPIMG
	P46	226-245	NWANHWIYWVGPIMGAVLAG
	P47	231-250	WIYWVGPIMGAVLAGALYEY
	P48	236-255	GPIMGAVLAGALYEYVFCPD
	P49	241-260	AVLAGALYEYVFCPDVELKR

Protein	Peptide-No	AA residues	Sequence
	P50	246-265	ALYEYVFCPDVELKRRLKEA
	P51	251-270	VFCPDVELKRRLKEAFSKAA
	P52	256-275	VELKRRLKEAFSKAAQQTKG
	P53	261-280	RLKEAFSKAAQQTKGSYMEV
	P54	266-285	FSKAAQQTKGSYMEVEDNRS
	P55	271-290	QQTKGSYMEVEDNRSQVETE
	P56	276-295	SYMEVEDNRSQVETEDLILK
	P57	281-300	EDNRSQVETEDLILKPGVVH
	P58	286-305	QVETEDLILKPGVVHVIDID
	P59	291-310	DLILKPGVVHVIDIDRGEEK
	P60	296-315	PGVVHVIDIDRGEEKKGKDS
	P61	301-320	VIDIDRGEEKKGKDSSGEVL
	P62	304-323	IDRGEEKKGKDSSGEVLSSV
AQP4	P41-1	196-206	SVAIGHLFAIN
	P41-2	197-207	VAIGHLFAINY
	P41-3	198-208	AIGHLFAINYT
	P41-4	199-209	IGHLFAINYTG
	P41-5	200-210	GHLFAINYTGA
	P41-6	201-211	HLFAINYTGAS
	P41-7	202-212	LFAINYTGASM
	P41-8	203-213	FAINYTGASMN
	P41-9	204-214	AINYTGASMNP
	P41-10	205-215	INYTGASMNPA
	P41-11	206-216	NYTGASMNPAR
	P41-12	207-217	YTGASMNPARS
	P41-13	208-218	TGASMNPARSF
	P41-14	209-219	GASMNPARSFG
	P41-15	210-220	ASMNPARSFGP
	P41-16	211-221	SMNPARSFGPA
	P41-17	212-222	MNPARSFGPAV
	P41-18	213-223	NPARSFGPAVI
	P41-19	214-224	PARSFGPAVIM
	P41-20	215-225	ARSFGPAVIMG
MOG	–	35-55	MEVGWYRSPFSRVVHLYRNGK
PLP	–	139-151	HSLGKWLGHPDKF

3.1.10 Mice

C57BL/6 mice, *Tcrα*$^{-/-}$ mice, *Rag1*$^{-/-}$ and SJL/J mice were obtained from Jackson Laboratories (Bar Harbor, USA). *Aqp4*$^{-/-}$ mice were kindly provided by A. Verkman (University of California, USA) and have been described before (Ma et al., 1997). *Aqp4*$^{flox/flox}$ mice and *Foxn1*^{Cre} mice were a kind gift from E. Nagelhus (University of Basic Medical Sciences, Norway) and G. Holländer (Weatherall Institute of Molecular Medicine, GB), respectively and have been described before (Haj-Yasein et al., 2011) (Rossi et al., 2007).

Table 3.11: Mice used in the experiments.

Strain	MGI	Characteristics	Supplier
Aqp4$^{-/-}$	1857808	Knockout of *Aqp4*	Provided by A.Verkman
Aqp4$^{flox/flox}$	5297539	Lox p sites flanking *Aqp4*	Provided by E. Nagelhus
C57BL/6	–	Wild type mouse	Jackson (Bar Harbor, USA)
Foxn1^{Cre}	3806589	*Foxn1* driven cre expression	Provided by G. Holländer
Rag1$^{-/-}$	1857241	Knockout of *Rag1*	Jackson (Bar Harbor, USA)
SJL/J	–	Alternative model for EAE	Jackson (Bar Harbor, USA)
Tcrα$^{-/-}$	1857255	Knockout of *TCRα* chain	Jackson (Bar Harbor, USA)

3.1.11 Cell lines

Cell lines were stored in liquid nitrogen and were cultivated in the incubator at 37 °C with 5 % CO_2.

Table 3.12: Cell lines used in cell-based flow cytometric assays or for production of mouse AQP4 protein.

Cell line	Specification
LN18^{AQP4}	Human malignant glioma cell line transduced with AQP4 expressing lentivirus
LN18^{Ctrl}	Human malignant glioma cell line transduced with empty vector
SF9	Insect cell line from ovarian tissue of *Spodoptera frugiperda*
High Five	Insect cell line from ovarian tissue of *Trichoplusia ni*

3.1.12 Magnetic beads

Magnetic beads were obtained from Miltenyi Biotec and used for magnetic-activated cell sorting (MACS) according to the recommendation in the respective protocol.

Table 3.13: Magnetic beads used for purification of cell subsets.

Magnetic beads	Supplier
CD4 (L3T4) MicroBeads mouse	Miltenyi Biotec (Bergisch Gladbach, Germany)
CD4$^+$ T cell isolation Kit mouse	Miltenyi Biotec (Bergisch Gladbach, Germany)
CD11c MicroBeads mouse	Miltenyi Biotec (Bergisch Gladbach, Germany)
CD90.2 MicroBeads mouse	Miltenyi Biotec (Bergisch Gladbach, Germany)

3.1.13 Cytokines

Cytokines were purchased from R&D and were stored at -80°C.

Table 3.14: Cytokines used in cell culture.

Cytokine	Supplier
mouse recombinant IL-2	R&D (Minneapolis, USA)
mouse recombinant IL-7	R&D (Minneapolis, USA)

3.1.14 Laboratory equipment and consumables

Laboratory equipment and consumables were obtained from various suppliers and used according to the manufacturer's instructions.

Table 3.15: Equipment and consumables used for different experimental setups.

Item	Supplier
Agarose gel electrophoresis system	Bio-Rad (Hercules, USA)
Autostainer Link 48	Dako, Agilent (Santa Clara, USA)
Blood lancets	Megro (Wesel, Germany)
Cell culture plates (96-well, 24-well flat-bottom, 96-well round-bottom)	Greiner Bio-One (Frickenhausen, Germany)
Cell harvester-MicroBeta FilterMate-96	PerkinElmer (Waltham, USA)
Cell strainer	BD Biosciences (Heidelberg, Germany)
Centrifuge 5424	Eppendorf (Hamburg, Germany)
Centrifuge-Multifuge 3SR+	Thermo Fisher Scientific (Waltham, USA)
CO_2 Incubator-APT.line C 150	Binder (Tuttlingen, Germany)
Combined refrigerator-freezer	Bosch (Gerlingen, Germany)
Conical centrifuge tubes (15 ml, 50 ml)	Greiner Bio-One (Frickenhausen, Germany)
Counting chamber, Neubauer improved	Sigma-Aldrich (St. Louis, USA)
Cryogenic storage vials	Greiner Bio-One (Frickenhausen, Germany)
Cryostorage system	Taylor-Wharton (Minneapolis, USA)
CytoFLEX analyzer	Beckman Coulter (Brea, USA)
Filtermat A for counting in cell harvester	PerkinElmer (Waltham, USA)
FUSION XPRESS	Vilber (Eberhardzell, Germany)
Heracell CO_2 incubator	Thermo Fisher Scientific (Waltham, USA)
iBlot Dry Blotting System	Thermo Fisher Scientific (Waltham, USA)

Item	Supplier
Irradiation cage	Klinikum rechts der Isar (Munich, Germany)
Irradiation unit	Gulmay (Buford, USA)
Laminar flow cabinet	Kojair Tech Oy (Vilppula, Finland)
Leica confocal microscope	Leica microsystems (Wetzlar, Germany)
Mastercycler® nexus	Eppendorf (Hamburg, Germany)
MicroBeta Trilux 1450 Scintillation Counter	PerkinElmer (Waltham, USA)
Microscope VistaVision	VWR (Radnor, USA)
Microwave R-2V14	Sharp (Munich, Germany)
Nalgene rapid flow filter	Thermo Fisher Scientific (Waltham, USA)
Nanodrop NP-1000	PEQLAB (Erlangen, Germany)
Pipet Controllers Accu-jet pro	Sigma-Aldrich (St. Louis, USA)
Pipettes (P10, P200, P1000)	Eppendorf (Hamburg, Germany)
Pipette tips	Eppendorf (Hamburg, Germany)
Power Supply PowerPac Basic	Bio-Rad (Hercules, Germany)
Quadro MACS® Multistand	Miltenyi Biotech (Bergisch Gladbach, Germany)
Reaction tubes (0.2, 0.5, 1.5, 2.0 ml)	SARSTEDT (Nümbrecht, Germany)
S200 HR 16/60 column	GE Healthcare (Marlborough, USA)
Sample bag for counting	PerkinElmer (Waltham, USA)
Scalpel-Feather	Electron Microscopy Sciences (Hatfield, USA)
Spectralis OCT	Heidelberg Engineering (Heidelberg, Germany)
Sterile filter storage bottle rapid flow	Thermo Fisher Scientific (Waltham, USA)
Syringe filter units Millex-GS	Merck Millipore (Darmstadt, Germany)
Syringes and needles of different sizes	B. Braun (Melsungen, Germany)
Thermomixer comfort	Eppendorf (Hamburg, Germany)
Ultra low temperature freezer MDF-U73V	Panasonic (Osaka, Japan)
Vortexer mixer	VWR (Radnir, USA)
Waterbath	Memmert (Schwabach, Germany)

3.1.15 Software

Data were generated and analyzed using software from the following manufacturers.

Table 3.16: Software used to collect and interpret data.

Software	Supplier
Adobe CS Suite 6	Adobe Systems (San Jose, USA)

Software	Supplier
ApE plasmid editor	Open source created by M. Wayne Davis
BLAST	NCBI (Bethesda, USA)
Confocal LAS AF	Leica microsystems (Wetzlar, Germany)
CytExpert	Beckman Coulter (Brea, USA)
Eye Explorer 6.0.9.0	Heidelberg Engineering (Heidelberg, Germany)
Microsoft Office Suite	Microsoft (Redmond, USA)
FlowJo 10	Tree Star (Ashland, USA)
Papers	Digital Science & Research Solutions (London, GB)
Prism 7	GraphPad Software (San Diego, USA)

3.2 Methods

3.2.1 Molecular biology

3.2.1.1 Synthesis of cDNA

Total RNA from mouse brain and cerebellum (Clontech) was used to serve as a template for cDNA synthesis. The reaction was set up with SuperMix reaction buffer and SuperScript enzyme mix containing reverse transcriptase according to the manufacturer's specifications (Thermo Fisher Scientific). Reaction tubes were placed into a thermal cycler to provide optimal conditions (Table 3.17).

Table 3.17: Cycling program used for cDNA synthesis.

Temperature	Time (min:sec)
25°C	10:00
42°C	60:00
85°C	05:00

3.2.1.2 Cloning of *Aqp4* expression vectors

Aqp4 was cloned into different expression vectors to generate a stable AQP4 expressing cell line for FACS assays on the one hand and to establish a baculovirus-based high-scale production system for AQP4 protein on the other.

For cloning, *Aqp4* was amplified by PCR using cDNA from total mouse brain cerebellum as described before (see chapter 3.2.1.1). Primers were designed to introduce specific restriction sites as well as a 6x HIS tag at the c-terminus (Table 3.18).

Table 3.18: PCR mix to amplify *Aqp4* from cDNA.

PCR mix
24.0 µl Platinum SuperMix HF
1.00 µl Primer fwd (10 µM)
1.00 µl Primer rev (10 µM)
2.00 µl cDNA

Table 3.19: Cycling program for amplification of *Aqp4*.

Temperature	**Time** (min:sec)	
94 °C	03:00	
94 °C	00:30	|
60 °C	00:30	| 36x
72 °C	01:00	|
72 °C	10:00	
4 °C	∞	

To improve cloning efficiency PCR products were first inserted into pGem®-T Easy vector (Figure 3.1 A) via T-overhangs, and subsequently cut and introduced into the respective expression vector. XbaI/HindIII and NotI/XhoI restriction sites were used to integrate *Aqp4* into pcDNA3.1+ vector (Figure 3.1 B) or pFBDM (Figure 3.1 C), respectively. For digestion, 1 µg of plasmid was incubated with restriction enzymes in the most suitable buffer from NEB buffer system for 3 hours at 37 °C. Purification of DNA was performed using the QIAquick gel extraction kit according to the manufacturer's specifications. DNA fragments were separated by size in an 1.5 % agarose gel via electrophoresis. To ligate the *Aqp4* insert into the respective expression vector, they were incubated overnight in a molar ratio of 3:1 with T4 DNA ligase in the appropriate T4 DNA ligase buffer at 4°C.

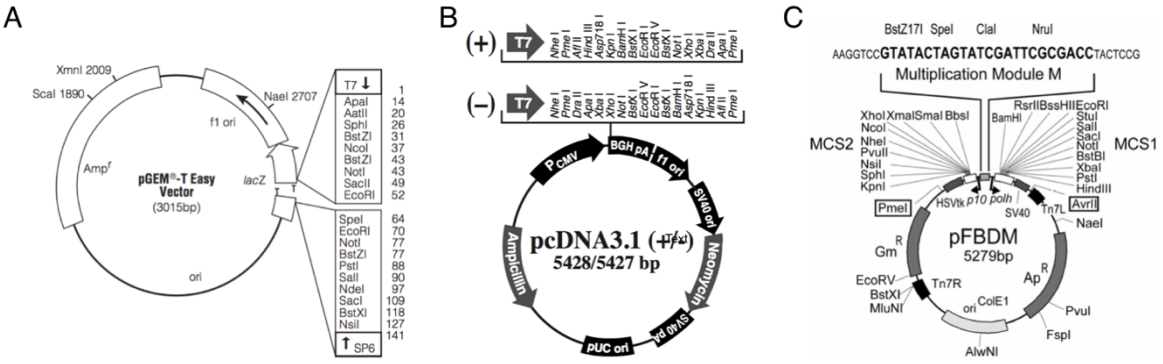

Figure 3.1: Vector maps. pGEM®-T Easy (A), pcDNA3.1(+) (B) and pFBDM (C) plasmids with information on respective size, restriction sites in the multiple cloning site and antibiotic resistance.

For transformation, DH5α cells were thawed from -80°C and directly incubated with the ligation mix for 30 min on ice. Subsequent heat shock was performed for 60 sec at 42°C and cells were plated after cooling in 600 µl of SOC medium on agar filled petri dishes containing the appropriate antibiotics. Mini and maxi preparations were executed using the QIAprep spin miniprep kit or the HiSpeed plasmid maxi kit according to the manufacturer's specifications, respectively.

3.2.1.3 Sequencing

All DNA samples were sequenced by Eurofins (Sanger sequencing). To prepare samples for sequencing, DNA was diluted to 100 ng/µl in water and primers were added. Results were evaluated using 4Peaks and ApE software to compare the sequences to those published on the NCBI database.

3.2.2 Protein biochemistry

3.2.2.1 Expression and purification of AQP4 protein

The pFBDM expression vector with the inserted mouse *Aqp4* gene was introduced into MultiBac baculoviral DNA in DH10MultiBac *Escherichia coli* cells. Bacmid DNA was prepared from selected clones and further used to transfect insect cells for protein production. Infected High Five cells were grown in 6 l spinning flasks for 48 hours before being harvested by centrifugation at 4°C and 6000 x g for 10 min. Pelleted cells were either stored at -20°C for up to 6 months or directly subjected to protein purification according to the protocol from Ho and colleagues (Ho et al., 2009).

For protein purification, cells were thawed and washed twice in TBS buffer with 1 mM β-mercaptoethanol (β-ME) before being lysed by two ultrasonication cycles of 30 sec each. Unlysed cells were removed by centrifugation at 4°C and 6000 x g for 10 min. In a next step, membranes were pelleted by ultracentrifugation at 4°C and 160 000 x g for 1 h and subsequently resuspended in 25 ml MR buffer. To keep membrane proteins in solution another 25 ml MR buffer supplemented with 400 mM *n*-octyl-β-D-glucopyranoside (β-OG) was added and stirred at 4°C for 1 h. In a second ultracentrifugation step at 4°C and 160 000 x g for 30 min insoluble material was pelleted and removed. To prepare for Ni-NTA affinity purification of AQP4 protein, supernatants were incubated with Ni-NTA beads at 4°C for 1 h in a rotator. Ni-NTA beads were then washed with MR buffer that was supplemented with 40 mM *n*-octyl-β-D-glucopyranoside and 25 mM imidazole. Ni-NTA-bound proteins were finally eluted with 250 mM imidazole. A 30 000 molecular weight cut-off amicon spin concentrator was used to concentrate AQP4 protein for subsequent gel filtration on a S200 HR 16/60 column. Peak fractions were pooled and once again concentrated. Protein concentration was determined by Nanodrop analysis. The final yield was up to 1 mg of protein per liter of cells.

3.2.2.2 Electrophoretic separation of proteins

Gel electrophoresis was used to separate proteins in cell lysates for further analysis or to verify homogeneity of protein samples. When an electrical field is applied, proteins migrate through the pores of a polyacrylamide gel with a specific rate depending on their size, charge and shape. According to the method of Laemmli (Laemmli, 1970), protein samples were incubated with 4x Laemmli protein sample buffer prior to loading onto a Bis-Tris protein gel. For size reference, a protein standard was used next to the samples. The SDS-PAGE was performed in MES running buffer at 200 V for 45 min. Separation was checked by staining all proteins using the colloidal blue staining kit according to the manufacturer's specifications.

3.2.2.3 Western blot and immunodetection of proteins

To identify specific proteins after SDS-PAGE, separated proteins were transferred from gel to a nitrocellulose membrane using the iBlot dry blotting system. The system comes with a pre-assembled dry transfer stack where the blotting membrane is on the anode side, and a pre-run gel on the cathode side so that no additional transfer buffer is needed. For western blot, the gel was placed into the stack and proteins were blotted in 7 min onto the membrane.

Successful transfer of proteins was confirmed by staining the membrane with Ponceau S solution. After stripping with 0.1 M NaOH for 1 min, the membrane was incubated in 5 % milk for at least 1 h on a shaker to prevent unspecific binding of antibodies in the subsequent immunodetection of specific proteins. Antigen-specific primary antibodies were diluted according to the manufacturer's recommendations (anti-AQP4 1 : 1000) in 5 % milk and incubated with the membrane over night at 4°C. After washing the membrane 1x 10 min and 3x 5 min with PBS-T on a shaker, the secondary antibody was added in a dilution of 1 : 3000 in PBS-T. All secondary antibodies were conjugated with the enzyme horseradish peroxidase (HRP) that catalyzes the reduction of peroxides. After washing the membrane again with PBS-T, a luminol-based substrate was used that provided a chemiluminescent signal in the presence of HRP and peroxide. This signal was then visualized using the FUSION XPRESS.

3.2.3 Cell biology

3.2.3.1 Cultivation of primary cells and cell lines

All cell lines were cultivated in the appropriate medium supplemented with 10 % FCS and antibiotics (penicillin and streptomycin) at 37°C and 5 % CO_2. Cells were examined daily under the microscope to guarantee perfect growing conditions. LN18 cells were split 1 : 4 every two days in RPMI 1640-10 medium.
Primary cells from mice were cultivated in DMEM clone medium supplemented with 10 % FCS, 50 µM β-ME, 1 mM sodium pyruvate, nonessential amino acids, L-glutamine and 50 U penicillin / 50 µg streptomycin per milliliter.

3.2.3.2 Preparation of lymphocytes

To isolate lymphocytes from mice, animals were sacrificed by isoflurane inhalation followed by cervical dislocation. When cells were harvested from CNS, mice were perfused with 10 ml PBS before dissection of the respective tissue. For single cell suspension, spleen and lymph nodes were grated through a nylon mesh with 70 µm pores (cell strainer, BD). Lysis of red blood cells was performed with 2 ml of lysis buffer (PharmLyse, BD) for 2 min. After washing thoroughly with DMEM-wash medium, cells were resuspended in clone medium and stored on ice until further processing. Cell count was determined using a Neubauer-improved

hemocytometer. Only viable cells were counted, dead cells were excluded by staining with trypan blue.

For generation of bone marrow chimeras (BMCs), cells were isolated from femurs and humeruses by breaking the joints and flushing out the bone marrow with DMEM-wash medium using a 14-gauge needle. Red blood cells were lysed as described before and cells were washed and resuspended in clone medium.

To obtain lymphocytes from CNS, brain and spinal cord were cut into small pieces and subsequently incubated in a digestion solution containing collagenase and DNase for 45 min at 37°C. The tissue was grated through a nylon mesh with 70 µm pores and washed with DMEM-wash medium. To separate lymphocytes from debris and dead cells, cells were resuspended in a 70 % percoll solution and overlaid with a 37 % percoll solution. Gradient centrifugation was performed for 20 min at 1800 rpm without break. After sucking off the top myelin layer, lymphocytes and microglia were harvested from the interphase using a 10 ml pipette. Cells were washed, resuspended in clone medium and stored on ice.

3.2.3.3 Flow cytometry

Flow cytometry or fluorescence-activated cell sorting (FACS) is a method to characterize cells regarding their size, granularity and marker protein expression. It uses a focused laser beam that hits only one cell at a time out of a single cell suspension in a laminar flow. Light is scattered in all angles which is detected by photomultipliers, providing information on cell size and cell granularity. To further characterize cells and therefore distinguish different cell types in a single cell suspension, cells are tagged beforehand with fluorochrome-conjugated antibodies. When the laser beam hits the labeled cells, light is absorbed and then emitted in a band of wavelengths that is specific for each fluorochrome marker. By using different markers, cells can be analyzed for the expression of different proteins at the same time.

For flow cytometry analysis up to 2×10^6 cells were first incubated with antibodies that block Fc receptors on the cell surface to prevent unspecific binding of fluorochrome-labeled antibodies. In case of staining only surface proteins in the membranes of cells, labeled antibodies were then added in a dilution of 1 : 100 in FACS buffer and incubated for 30 min at 4°C in the dark. To exclude dead cells, a dye that reacts mostly with free amines in the cell interior (LIVE/DEAD fixable aqua cell stain kit, Life technologies) was included in every staining panel. Staining was performed in round-bottom 96-well plates in a total volume of

100 µl and cells were analyzed using a CytoFLEX analyzer (Beckman Coulter). CytExpert and FlowJo software were used to visualize data.

For intracellular staining of cytokines, T cells first needed to be stimulated in an antigen-unspecific manner while simultaneously being prevented from releasing cytokines. Therefore, cells were incubated with phorbol-12-myristate-13-acetate (PMA), ionomycin and monensin (GolgiStop, BD) for 3 hours in clone medium prior to fixation and staining.

In order to stain antigen-specific T cells, cells were incubated with the respective soluble PE-labeled pMHC-class II tetramer in a total volume of 200 µl FACS buffer for 1 hour at 25°C in a water bath. To avoid settling down of the cells, the solution needed to be vortexed repeatedly. After washing with FACS buffer, cells were either applied to PE-bead enrichment by magnetic-activated cell sorting (MACS) or directly stained for surface markers with respective antibodies as described before.

To detect conformational anti-AQP4 or anti-MOG antibodies in the collected sera of immunized mice, a flow cytometric assay was used. It takes advantage of a LN18 cell line transduced with either AQP4 or MOG expressing lentivirus to provide a strong protein expression on the cell surface (Kalluri et al., 2010). Sera were diluted 1 : 50 in RPMI-1640 medium prior to incubation with 30 000 $LN18^{AQP4}$ or $LN18^{MOG}$ cells in a round-bottom 96-well plate. As control, every serum was also tested on $LN18^{CTRL}$ cells, that were transduced with empty vector. The plate was incubated on ice for 25 min before the cells were washed with FACS buffer. To stain murine antibodies, AlexaFluor488-labeled goat anti-mouse IgG H+L antibodies were added to the cells in a dilution of 1 : 100 followed by another incubation on ice for 25 min. Cells were washed again with FACS buffer before the samples were analyzed.

3.2.3.4 Cell sorting

There are two ways to isolate specific cell types from a heterogeneous single cell suspension: fluorescence-activated cell sorting (FACS) and magnetic-activated cell sorting (MACS). In FACS, the cell stream that passes the laser beam as described before is now broken into small droplets. Whenever a cell that matches the sorting criteria is detected, voltage is applied to charge the droplets. Subsequently, by passing an electric field, charged droplets are deflected and cells can be collected separately, whereas uncharched droplets are not affected and end up in the waste tank.

During MACS, cells are labeled with antibodies conjugated to magnetic particles. By applying the mixture of labeled and unlabeled cells onto a column that is placed in a magnetic field,

labeled cells stick in the column whereas all other cells pass through. When the column is subsequently removed from the magnetic field, labeled cells can be eluted. All magnetic beads were purchased from Miltenyi Biotec and were used to purify $CD4^+$ T cells and $CD11^+$ dendritic cells from single cell suspensions of lymph node (LN) and spleen according to the manufacturer's protocol.

3.2.3.5 Stimulation of T cells with antigen ex vivo

Splenocytes and draining LN cells from AQP4- or AQP4(201-220)-immunized mice were isolated on day 12 after immunization as described before. To find the immunogenic T-cell epitopes, a so-called peptide scan was performed where the cells were incubated with single 20-mer peptides spanning the whole sequence of AQP4. For fine-mapping of distinct epitopes, 11-mer peptides overlapping by 10 amino acids were used. In both cases, 350 000 cells were cultivated in round-bottom 96-well plates with a final concentration of 10 µg/ml peptide in clone medium for 72 hours. Proliferation was measured by incorporation of ^{3}[H]-thymidine as described in further detail in Chapter 3.2.3.6.
In one experiment, $CD4^+$ T cells, isolated from single cell suspension of spleen and draining LNs from AQP4-immunized *Aqp4*$^{-/-}$ mice, were incubated with splenocytes from wild type or *Aqp4*$^{-/-}$ mice together with AQP4 peptides or AQP4 full-length protein. The splenocytes functioned as APCs and had been irradiated with 30 Gy beforehand to prevent proliferation and therefore ensure proliferative counts could be assigned to $CD4^+$ T cells in the culture.

3.2.3.6 T-cell proliferation assay

To quantify the recall proliferative response of T cells to AQP4 in vitro, proliferation assays were performed. Splenocytes and draining LN cells from AQP4-immunized mice were challenged with either AQP4 protein or single AQP4 peptides for 72 hours in triplicate cultures. Cultivated cells were pulsed with 1 µCi of ^{3}[H]-thymidine for the last 16 hours before they were harvested on glass fiber filters. Analysis of incorporated ^{3}[H]-thymidine was performed in a β-counter (MicroBeta Trilux 1450).

3.2.4 Imaging

3.2.4.1 Immunohistochemistry

Mice were sacrificed by isoflurane inhalation followed by an intracranial perfusion with first PBS and then 4 % w/v paraformaldehyde (PFA) solved in PBS. Brains, spinal cords, optic nerves, kidneys and spleens were removed and additionally fixed in 4 % PFA overnight. Tissues were embedded and cut into 5 µm thick sections that were stained for hematoxylin and eosin (H&E) and Luxol-fast blue/periodic acid-Schiff. Immunohistochemistry was performed in the lab of Tanja Kuhlmann in Münster by using a biotin-streptavidin peroxidase-based technique (K5001, Dako) in combination with an automated immunostainer (Autostainer Link 48, Dako). Prior to incubation with the primary antibodies anti-Mac3 (1 : 100), anti-CD3 (1 : 50) and anti-AQP4 (1 : 4000), sections were pretreated in a steamer using treatment solutions with pH 6.0 or 9.0. DAB was used as a chromogen and sections were counterstained with hematoxylin.
To quantify the perivascular loss of immunoreactivity, at least five different areas of three consecutive brain sections per mouse were analyzed using Image J. The size of areas showing AQP4 loss and the corresponding vessel lumen were measured by hand in a blinded manner. Individual ratios were calculated, any ratio > 1 indicates perivascular AQP4 loss.

3.2.4.2 Confocal microscopy

With confocal microscopy it is possible to increase optical resolution and contrast to focus on single layers of a thicker section by using a spatial pinhole to block out-of-focus light. In addition, a confocal microscope uses a smaller beam of light to only illuminate a certain depth of the section compared to a conventional microscope, where light travels as far into the specimen as possible. Stained tissues of mice were analyzed using a Leica confocal microscope and Leica Application Suite AF (Leica microsystems).

3.2.5 Animal experimentation

3.2.5.1 Housing and breeding conditions

Mice were housed in individually ventilated cages under specific pathogen free (SPF) conditions at a temperature of 20 – 22°C, humidity of 40 – 50 % and a 12/12-hour light/dark

cycle in the animal facility of the Technical University of Munich (Zentrum für Präklinische Forschung, ZPF). Food and water were provided *ad libitum* and cages were equipped with bedding, plastic nest boxes and enrichments such as pieces of wood or cotton wood pads for entertainment. Breeding was usually set up as harem mating with two 8 weeks old females and one at least 6 weeks old male. Pups were weaned with 3 – 4 weeks old. For genotyping, mice were tagged via ear punches and biopsies were taken from the tail tip. All experimental protocols were approved by the standing committee for experimentation with laboratory animals of the Bavarian state authorities and carried out in accordance with the corresponding guidelines (AZ: ROB-55.2-2532.Vet_02-13-29, ROB-55.2-2532.Vet_02-17-69, ROB-55.2-2532.Vet_02-17-234, ROB-55.2-2532.Vet_02-14-95, ROB-55.2-2532.Vet_03-18-53).

3.2.5.2 Mouse strains

C57BL/6 mice and *Aqp4*$^{-/-}$ mice were used side-by-side to identify T-cell epitopes within the AQP4 amino-acid sequence. Since the knockout is global, *Aqp4*$^{-/-}$ mice lack expression of AQP4 in any tissue including the thymus. Hence, there is no deletional tolerance to AQP4 in *Aqp4*$^{-/-}$ mice.

To characterize NMO disease phenotype in mice, so-called compound mice were generated by transferring the mature T-cell compartment from unmanipulated *Aqp4*$^{-/-}$ mice into *Rag1*$^{-/-}$ or *Tcrα*$^{-/-}$ mice. Therefore CD4^{+} T cells were isolated using CD4 untouched beads (Miltenyi Biotec) and 14×10^{6} cells were transferred intraperitoneally (i.p.). Both mouse lines were chosen as recipients due to their lack of endogenous T cells. While *Tcrα*$^{-/-}$ mice still have an unaltered endogenous B-cell repertoire, *Rag1*$^{-/-}$ mice lack both, mature T cells and B cells.

In *Aqp4*$^{flox/flox}$ mice the *Aqp4* gene is modified by the insertion of two loxp sites, one upstream of exon 1 and the other downstream of exon 3, to generate a conditional knockout. Crossing these mice with *Foxn1*^{Cre} mice results in a conditional *Aqp4* ablation in medullary thymic epithelial cells (mTECs). All mice were bred on C57BL/6 background, apart from SJL/J mice that were used once to perform a peptide scan on a different genetic background.

3.2.5.3 Genotyping

For genotyping, mouse tail biopsies were digested in 180 µl lysis buffer with 50 mM NaOH for 30 min at 100°C in the heating block. To prepare the extracted DNA for the following analysis via PCR, 180 µl of neutralization buffer with 0.3 M NaOAc were added and the mixture was

vortexed thoroughly. Genotyping reactions were set up with 1 µl of DNA in a mix with DreamTaq PCR Master Mix containing DNA polymerase, $MgCl_2$ and dNTPs. To determine genotypes, locus specific primers were added with 10 µM each to the PCR reaction tubes before starting the amplification process in the thermal cycler. Cycling programs were chosen depending on primer pairs and size of the expected PCR product (Table 3.20, 3.21 and 3.22).

Table 3.20: Cycling program for *Aqp4*$^{-/-}$.

Temperature	**Time** (min:sec)	
94 °C	02:00	
94 °C	00:30	|
60 °C	00:30	| 35x
72 °C	00:40	|
72 °C	05:00	
4 °C	∞	

Table 3.21: Cycling program for *Aqp4*$^{flox/flox}$.

Temperature	**Time** (min:sec)	
94 °C	05:00	
94 °C	00:30	|
62 °C	00:30	| 32x
72 °C	00:45	|
72 °C	05:00	
4 °C	∞	

Table 3.22: Cycling program for *Foxn1-cre*.

Temperature	**Time** (min:sec)	
94 °C	05:00	
94 °C	00:45	|
56 °C	00:45	| 35x
72 °C	01:00	|
72 °C	05:00	
4 °C	∞	

In case mice were bought from Jackson laboratories, genotyping was performed according to the information available on their website. To visualize genotyping results, PCR products alongside with a 100 bp ladder were applied on a 1.5 % TAE-agarose-gel for gel electrophoresis.

3.2.5.4 Immunization procedures and induction of disease

For induction of disease, mice were immunized subcutaneously (s.c.) at the base of tail with 200 µl of an emulsion containing either 200 µg of peptide or 100 µg of protein antigen and 250 µg *Mycobacterium tuberculosis* in mineral oil (complete Freund's adjuvant, CFA). In addition, mice received 200 ng pertussis toxin intravenously (i.v.) on the days 0 and 2 after immunization. The emulsion was made by using two luer lock syringes connected by a three-way stopcock to mix the aqueous antigen solution with CFA until a viscous liquid suspension was formed.

In some experiments, serum transfer was performed i.v. on days 6 and 12 after immunization using either 100 µl of naïve or immune serum. The latter was harvested from AQP4-immunized *Aqp4*$^{-/-}$ mice and showed high titers of anti-AQP4 antibodies. Alternatively, mice received 20 µg of a monoclonal antibody recognizing mouse AQP4 (rAb-53) or a control antibody (IC-05), both also given by i.v. injection. rAb-53 is a human-mouse chimeric recombinant antibody that was kindly provided by J. Bennett. The antibody was generated by replacing the human IgG1 Fc region of an AQP4-specific antibody clone derived from an NMO patient with a mouse IgG2a Fc region (Bennett et al., 2009). IC-05 is a divalent human IgG1 antibody of unknown specificity derived from a chronic meningitis patient (Herwerth et al., 2016).

In another experiment, mice were depleted of regulatory T (T_{reg}) cells prior to EAE induction. Therefore, mice were injected i.p. 5 days and 3 days before immunization with 500 µg of a monoclonal antibody to CD25 (clone PC61).

Mice were monitored daily for signs of disease using the following criteria for scoring: **0** no disease, **1** tail paralysis, **2** hind limb weakness, **3** hind limb paralysis, **4** front and hind limb paralysis, **5** moribund.

3.2.5.5 Bone marrow chimeras

For the generation of bone marrow chimeras, recipient mice were lethally irradiated. To deliver a dose of 7 Gy in two 3.5 Gy doses 3 hours apart, mice were placed in groups of up to 10 into an antiseptically cleaned irradiation cage. From the day of irradiation until

reconstitution of the hematopoietic system was confirmed by analyzing peripheral blood, mice were maintained on antibiotic-water (0.1 mg/ml Enrofloxacin).
To prepare bone marrow, femurs, tibiae and humeri of *Aqp4*$^{-/-}$ or wild type donor mice were dissected by removing skin and muscles as well as breaking arms and shoulder joints. Bone marrow was flushed out and passed through a 70 µm cell strainer followed by depletion of CD90.2 expressing T cells by MACS. A total of 5×10^6 bone marrow cells was injected i.v. into recipients 1 day after irradiation.

3.2.5.6 OCT analysis of murine retina

OCT examination of murine retina was performed using a common spectral domain OCT with TruTrack eye tracking technology (Spectralis, Heidelberg Engineering). To adopt the machine for mice, a 78-diopter lens was placed directly in front of the OCT. Mice were anesthetized by i.p. injection of medetomidine (0.5 mg/kg), midazolam (5 mg/kg) and fentanyl (0.05 mg/kg) and subsequently treated with eye drops containing 2 % atropine. A 100-diopter contact lens was placed on the eyes using contact gel and mice were placed on a self-manufactured platform in front of the OCT for analysis. The retina was analyzed using a volume scan centered on the optic nerve head consisting of 12 vertical B-scans (each with 768 A scans). A scanning angle of 15° x 15° was used. Both eyes were measured and all scans had to meet high quality criteria to be further analyzed. Scans were first automatically segmented into the different layers of the retina by using the Eye Explorer software. Segmentation was then checked manually and corrected if necessary in a blinded manner. For longitudinal measurements, the so-called “follow-up” software modus was used to ensure analysis of the exact same place.

3.2.6 Statistical analysis

Statistical analysis of cell numbers, MFIs and OCT data were performed with the unpaired Student’s t-test when two populations were compared and a normal distribution could be assumed. $p < 0.05$ was considered significant. For multiple comparisons, one-way ANOVA followed by specific post-tests as indicated in the figure legends were used. Clinical scores of EAE between groups were analyzed using a Mann-Whitney U test for nonparametric values.

4 Results

4.1 Generation of mouse AQP4 full-length protein

In order to study AQP4-directed immune responses in mice, establishing a reliable source of full-length AQP4 protein was a prerequisite. AQP4 is a transmembrane protein with six transmembrane domains that assembles in cell membranes as tetramers. Therefore, I used insect cells and a baculovirus system for the expression and subsequent purification of AQP4 (Ho et al., 2009). First, the full-length mouse M1 isoform of *Aqp4* was amplified from cDNA of mouse brain cerebellum total RNA with primers designed to introduce XbaI/HindIII restriction sites as well as a C-terminal 6x HIS tag. To facilitate further cloning, the *Aqp4* gene was then cloned into the pGEM®-T Easy vector before it was cut and integrated into the pFBDM expression vector. The latter was introduced into MultiBac baculoviral DNA in DH10MultiBac cells to prepare Bacmid DNA for virus production in SF9 cells. Protein production was performed in transfected High Five cells. For purification of AQP4 protein, cells were first lysed by ultrasonication and subsequently centrifuged two times at high speeds in an ultracentrifuge, first to pellet membranes and second to remove insoluble material after cell membranes were resuspended in buffer containing *n*-octyl-β-D-glucopyranoside (β-OG). The AQP4 protein was subsequently purified by Ni-NTA affinity chromatography, using the 6x HIS tag on the C-terminus of the protein. Eluted protein was then concentrated with cut-off amicon spin concentrators to prepare for the following gel filtration, which finally provided two peaks of protein (Figure 4.1 A). To check for purity and compare AQP4 protein levels in Ni-NTA elution fractions and the pooled fractions of gel filtration peaks 1 and 2, coomassie staining as well as western blot analysis were performed (Figure 4.1 B). Here, the biggest portion of AQP4 protein was detected in the pooled fractions of gel filtration peak 2. Distinct

bands with the sizes of 28 kDa and 45 kDa were visible in the western blot for detection of AQP4 as well as HIS6, suggesting high amounts of AQP4 monomer and dimer, respectively.

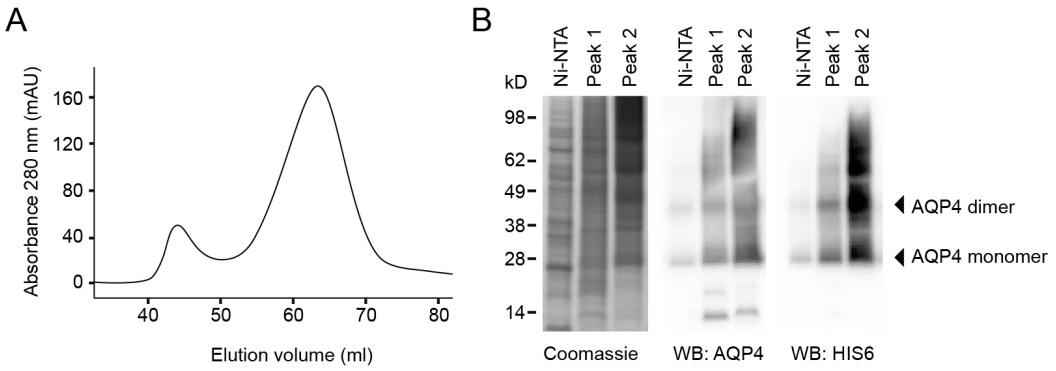

Figure 4.1: Expression and purification of mouse AQP4 protein. The full-length mouse AQP4 isoform M1 was produced in High Five cells using the baculovirus-insect cell expression system. **(A)** Purification of the protein by several ultracentrifugation steps, Ni-NTA affinity chromatography, and subsequent gel filtration on a S200 HR 16/60 column. N-Octyl-β-D-glucopyranoside was used as detergent to provide solubility of the protein throughout the process. **(B)** Side-by-side analysis of the Ni-NTA elution fraction and the pooled fractions of gel filtration peaks 1 and 2 using coomassie staining and western blot analysis for detection of AQP4 and HIS6. Data are representative of six independent experiments **(A, B)**.

To prepare for administration in mice as well as application in cell culture assays, pooled fractions of gel filtration peak 2 were concentrated with cut-off amicon spin concentrators to reach a total protein concentration of 2 mg/ml. In fact, higher protein concentrations would have been desirable to minimize the proportion of detergent but could not be achieved due to precipitation of the protein.

4.2 T-cell and B-cell responses to AQP4

4.2.1 Identification of immunogenic T-cell epitopes of AQP4

To better understand the role of T cells in the pathogenesis of NMO, particularly regarding class switch recombination of pathogenic AQP4-specific antibodies and inflammation of the BBB, it is essential to know the immunogenic naturally processed T-cell epitopes of AQP4. Previously AQP4(22-36) was reported as an IA^b-restricted T-cell epitope (Kalluri et al., 2011). However, AQP4(22-36)-specific T cells failed to respond to full-length AQP4 protein and did not induce any immunopathology in the CNS of animals upon immunization with the antigen. Therefore AQP4(22-36) is most likely no naturally processed epitope.

In order to assess the entire AQP4 protein for encephalitogenic epitopes, I used full-length mouse AQP4 protein emulsified in CFA to immunize not only C57BL/6 wild type (WT) but also *Aqp4*$^{-/-}$ mice (Manley et al., 2000), in which the naturally occurring T-cell repertoire is not tolerized against AQP4. T-cell responses to AQP4 were examined by recall assays of spleen and draining LN cells with AQP4 20-mer peptides spanning the entire mouse sequence of AQP4 and overlapping by 15 amino acids each (Table 3.10). To quantify T-cell proliferation to single AQP4 peptides, incorporation of ^{3}[H]-thymidine was measured in a β-counter. These so-called peptide scans revealed a strong proliferative response to AQP4 in *Aqp4*$^{-/-}$ mice with an immunogenic epitope in the region of AQP4(201-220) (Figure 4.2 B). In contrast, T cells from WT mice showed only weak proliferation to AQP4 without pointing to an epitope (Figure 4.2 A). This suggests that the major immunogenic epitope AQP4(201-220) is tolerized in AQP4 sufficient WT mice. To further analyze the proliferative response to the epitope AQP4(201-220) in *Aqp4*$^{-/-}$ mice, the corresponding AQP4 peptide 41 (p41) as well as the irrelevant peptide 12 (p12) were titrated in a recall assay with splenocytes and draining LN cells from AQP4-immunized *Aqp4*$^{-/-}$ mice. The counts showed that T cells proliferate to peptide 41 in a dose-dependent manner, peaking at a peptide concentration of 30 µg/ml (Figure 4.2 C). To test whether AQP4(201-220) is not only an immunogenic but also a naturally processed epitope and therefore potentially relevant in anti-AQP4-directed adaptive immune responses, *Aqp4*$^{-/-}$ and WT mice were immunized with the epitope AQP4(201-220) (p41) to subsequently asses T-cell proliferation in response to titrated full-length AQP4 protein (Figure 4.2 D). Since AQP4 is a transmembrane protein with limited solubility, only low concentrations of protein could be used in these recall cultures. However, T cells from AQP4(201-220)-immunized *Aqp4*$^{-/-}$ mice showed a profound proliferative response to the protein. This suggests that processing of the full-length protein by APCs resulted in epitopes similar or identical to AQP4(201-220). Hence, the major immunogenic epitope of AQP4, AQP4(201-220), is most likely a naturally occurring epitope. In accordance with the results from previous peptide scans, T cells from WT mice did not proliferate in response to the AQP4 protein upon immunization with AQP4(201-220) peptide.

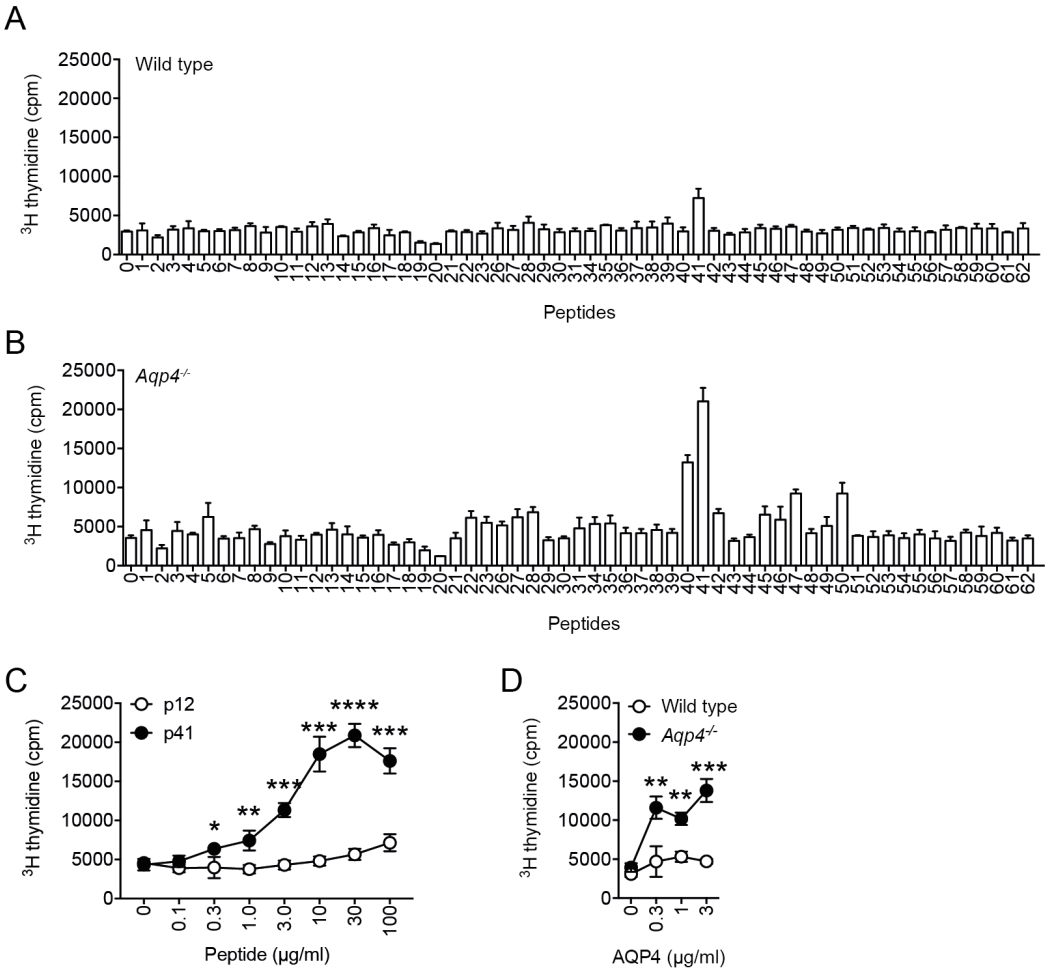

Figure 4.2: AQP4(201-220) is the immunodominant IA^b-restricted epitope of AQP4. C57BL/6 WT and *Aqp4*$^{-/-}$ mice were immunized s.c. with full-length mouse AQP4 protein **(A, B, and C)** or AQP4(201-220) peptide **(D)** emulsified in CFA. Splenocytes and draining LN cells were tested for cell proliferation in response to single AQP4 peptides or full-length AQP4 protein. **(A, B)** Splenocytes and LN cells from AQP4-immunized WT and *Aqp4*$^{-/-}$ mice were harvested at day 10 for ex vivo stimulation with single 20-mer peptides spanning the whole sequence of AQP4. **(C)** Stimulation of splenocytes and LN cells of an AQP4-immunized *Aqp4*$^{-/-}$ mouse with a titration of peptide 41 and peptide 12. **(D)** Draining LN cells from AQP4(201-220)-immunized WT and *Aqp4*$^{-/-}$ mice were tested for their proliferative recall response to titration of full-length AQP4 protein. Proliferation was measured by ^{3}[H]-thymidine incorporation. Mean values of triplicate cultures ± SD are shown. *$p < 0.05$, **$p < 0.01$, ***$p < 0.001$, ****$p < 0.0001$ (Student's t-test). Data are representative of five independent experiments **(A-D)**.

In order to narrow down the core epitope within the region of AQP4(201-220), once again *Aqp4*$^{-/-}$ mice were immunized with AQP4 full-length protein emulsified in CFA. This time, splenocytes and draining LN cells were interrogated for their response to single 11-mer peptides spanning the region of AQP4(196-225). The recall assay revealed that AQP4(205-215) is the core epitope of AQP4 (Figure 4.3 A). T-cell proliferation in response to this core epitope occurred in a dose-dependent manner which could be shown by titration of AQP4(205-215) (p41-10) in comparison to the irrelevant AQP4 peptide 28 (p28) (Figure 4.3 B).

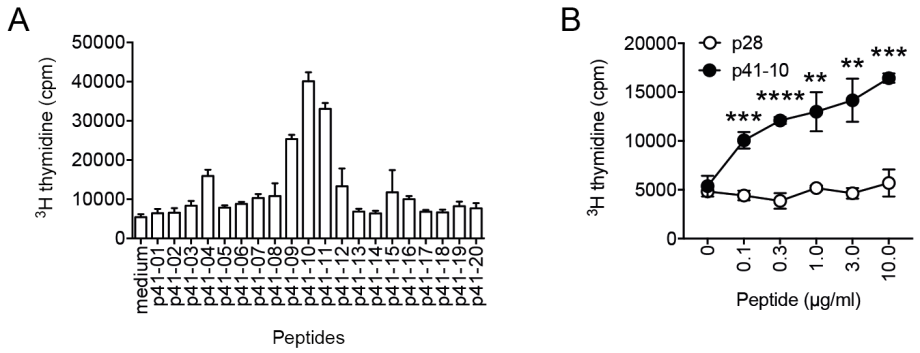

Figure 4.3: Fine mapping of the immunodominant epitope AQP4(201-220). (A, B) *Aqp4*$^{-/-}$ mice were immunized s.c. with AQP4 full-length protein emulsified in CFA to test splenocytes and draining LN cells on day 12 after immunization for their proliferative recall response to AQP4 peptides. **(A)** Fine mapping the immunodominant epitope of AQP4 by using 11-mer peptides spanning AQP4 (196-225) for ex vivo stimulation of cells. **(B)** Titration of peptide 41-10 and peptide 28 as insignificant control peptide in recall stimulation cultures. Proliferation was measured by ^{3}[H]-thymidine incorporation. Mean values of triplicate cultures ± SD are shown. $^{**}p < 0.01$, $^{***}p < 0.001$, $^{****}p < 0.0001$ (Student's t-test). Data are representative of five independent experiments **(A, B)**.

Next, I addressed the question whether there was a difference in the ability of APCs from C57BL/6 WT and *Aqp4*$^{-/-}$ mice to present AQP4 peptides to T cells. Therefore, AQP4-deficient *Aqp4*$^{-/-}$ mice were immunized with full-length AQP4 protein emulsified in CFA. On day 12 after immunization, CD4^{+} T cells were isolated from single cell suspensions of spleen and draining LNs by MACS. At the same time, splenocytes from naïve WT and *Aqp4*$^{-/-}$ mice were irradiated with 30 Gy to disable proliferation and serve as APCs in the following recall cultures. 30 000 CD4^{+} T cells were cultivated with 300 000 APCs from WT or *Aqp4*$^{-/-}$ mice in the presence of either 3 µg/ml of AQP4 peptide 12 and 41 or 1 µg/ml full-length AQP4 protein (Figure 4.4 A). T-cell proliferation was measured by incorporation of ^{3}[H]-thymidine. The counts from the proliferation assay suggested that there was no difference in the ability of presenting AQP4 antigens to T cells between APCs from WT and *Aqp4*$^{-/-}$ mice. This finding was confirmed by the additional analysis of recall cultures, where AQP4(201-220) (p41) was titrated (Figure 4.4 B).

Taken together, AQP4(201-220) is the major immunogenic epitope of AQP4 in the context of IA^{b} and appears to be efficiently tolerized in AQP4-sufficient mice. This tolerance is most likely also the reason why WT animals did not show any signs of disease upon immunization with the epitope. To check whether tolerance towards AQP4 is altered in mice with a different genetic background, SJL/J mice were chosen to be analyzed for T-cell reactivity against AQP4. These mice are widely used for sarcoma studies but are also susceptible to EAE upon

immunization with the myelin protein antigen proteolipid protein (PLP) (Zamvil and Steinman, 1990).

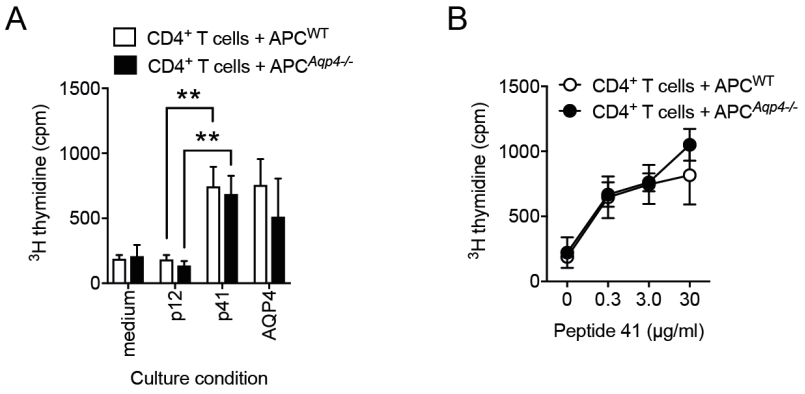

Figure 4.4: Ability of WT and *Aqp4*$^{-/-}$ APCs to present processed AQP4 full-length protein and single AQP4 peptides to CD4$^+$ T cells. *Aqp4*$^{-/-}$ mice were immunized s.c. with AQP4 full-length protein emulsified in CFA **(A, B)**. Draining LN cells and splenocytes were harvested on day 12 after immunization and CD4$^+$ T cells were isolated using the MACS untouched T cell isolation kit according to the manufacturer's instructions. Splenocytes of naïve *Aqp4*$^{-/-}$ and WT mice were irradiated with 30 Gy and then used as APCs in the stimulation cultures with a ratio of 10 : 1. **(A)** Stimulation of *Aqp4*$^{-/-}$ CD4$^+$ T cells with the immunodominant peptide 41 and the irrelevant control peptide 12 as well as AQP4 protein presented by APCs from *Aqp4*$^{-/-}$ or WT mice. **(B)** Titration of peptide 41 in stimulation cultures with *Aqp4*$^{-/-}$ CD4$^+$ T cells and APCs from WT versus *Aqp4*$^{-/-}$ mice. Proliferation was measured by ^{3}[H]-thymidine incorporation. Mean values of triplicate cultures ± SD are shown. **$p < 0.01$ (Student's t-test). Data are representative of two independent experiments **(A, B)**.

SJL/J mice are overall immunocompetent but show a higher frequency of autoreactive T cells for distinct autoantigens in the naïve T-cell repertoire. This was shown for PLP(139-151)-reactive T cells (Anderson et al., 2000) and could also be true for AQP4-specific T cells. To investigate whether tolerance to AQP4 is altered in favor of autoreactive T cells being released from the thymus, SJL/J mice were immunized with full-length AQP4 protein. In order to control for the immunization protocol, I also immunized some SJL/J mice with PLP(139-151) peptide emulsified in CFA. All mice received 200 ng of pertussis toxin on days 0 and 2. Being monitored daily for signs of disease for 40 days post-immunization, only mice immunized with PLP(139-151) showed signs of encephalomyelitis as of day 10 (Figure 4.5 A). To take a closer look at AQP4-reactive T cells in SJL/J mice, a peptide scan was performed where splenocytes and draining LN cells from AQP4-immunized mice were stimulated ex vivo with AQP4 20-mer peptides as shown before. The proliferative response of SJL/J T cells in response to overlapping AQP4 peptides was weak and did not point to a specific epitope within the AQP4 sequence (Figure 4.5 B). Hence, similar to C57BL/6 WT mice, AQP4 might be tightly tolerized in SJL/J mice resulting in the absence of AQP4-reactive T-cell clones in the peripheral T-cell repertoire.

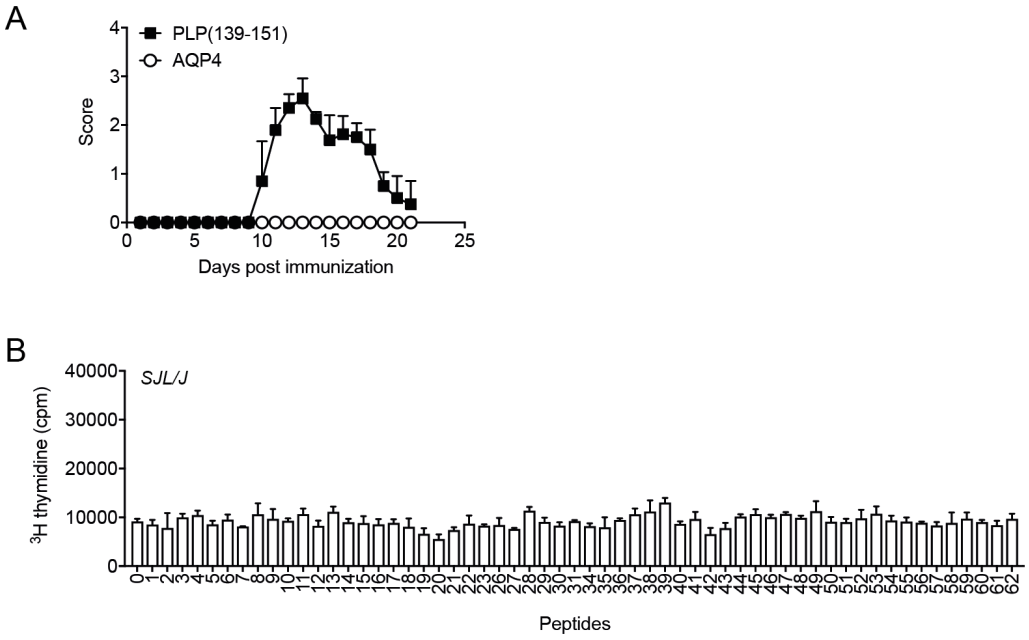

Figure 4.5: Searching for AQP4 T-cell epitopes on a different genetic background. SJL/J mice were immunized s.c. side-by-side with PLP(139-151) peptide and AQP4 full-length protein **(A)** or AQP4 full-length protein alone **(B)** emulsified in CFA. **(A)** Mice were monitored for symptoms of encephalomyelitis daily. Mean clinical scores ± SEM of immunized mice are shown (n = 5 per group). **(B)** Splenocytes and draining LN cells from AQP4 immunized SJL/J mice were tested for proliferation in response to single 20-mer peptides spanning the whole sequence of AQP4. Proliferation was measured by ^{3}[H]-thymidine incorporation. Mean values of triplicate cultures ± SD are shown. Data are representative of two independent experiments **(A, B)**.

4.2.2 Anti-AQP4 serum response in mice upon immunization with AQP4 full-length protein

Since NMO is believed to be an antibody-mediated disease of the CNS, it was of special interest to investigate whether mice could raise an AQP4-directed antibody response upon immunization with AQP4, particularly in regard to the development of an animal model exhibiting key features of the human disease. Thus, C57BL/6 WT and *Aqp4*$^{-/-}$ mice were immunized either with AQP4 full-length protein or AQP4(201-220) peptide emulsified in CFA. Sera were collected at different time points after immunization to be screened for anti-AQP4 antibodies. To detect those antibodies, a cell-based flow cytometric assay was used where sera of mice were incubated with LN18 cells transduced with AQP4 expressing lentivirus (Kalluri et al., 2010). As a control, mouse sera were also incubated with LN18 cells transduced with empty vector. To detect cell bound anti-AQP4 antibodies, anti-mouse IgG (H+L) (AlexaFluor488-labeled) was used. Samples were examined for anti-AQP4 antibodies by flow cytometry and ΔMFI was calculated as the ratio between MFIs of cells with and

without AQP4 expression (Figure Appendix.1). Upon immunization with full-length AQP4 protein, *Aqp4*$^{-/-}$ mice raised a robust anti-AQP4 serum response starting around day 19. In contrast, over a course of at least 45 days post immunization, there were at no time anti-AQP4 antibodies detectable in the sera of immunized WT mice (Figure 4.6 A).

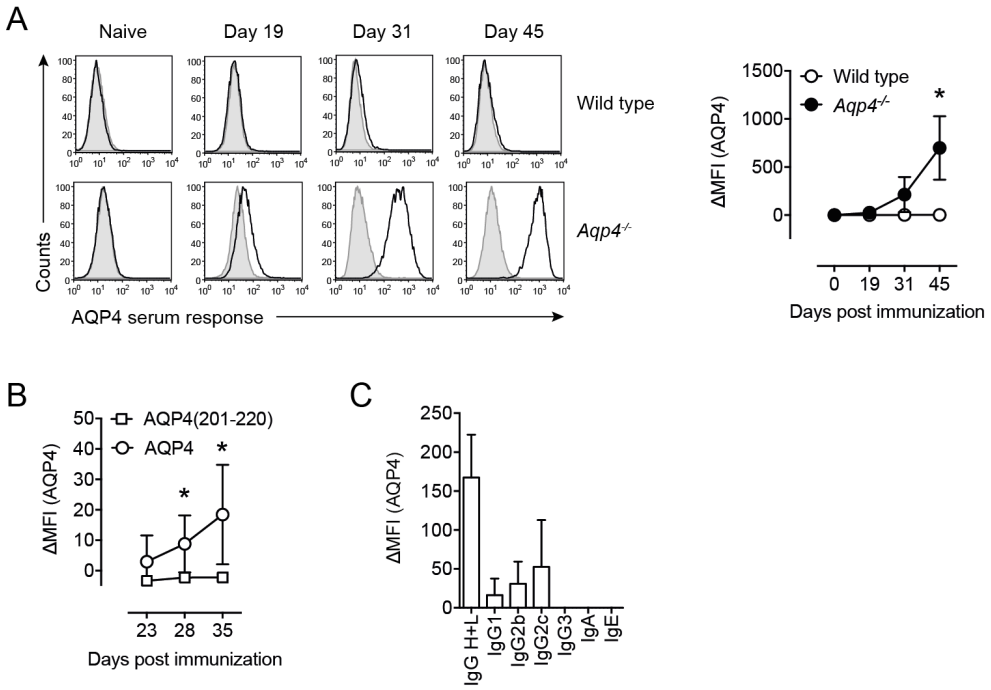

Figure 4.6: *Aqp4*$^{-/-}$ mice mount a robust antibody response to AQP4 upon immunization with full-length AQP4 protein. *Aqp4*$^{-/-}$ and C57BL/6 WT mice were immunized s.c. with either AQP4 full-length protein **(A, B, C)** or AQP4(201-220) peptide **(B)** emulsified in CFA. **(A)** Sera taken at different time points of naïve or AQP4-immunized mice were tested for anti-AQP4-specific antibodies in a cell-based flow cytometric assay with LN18 cells transduced with AQP4 expressing lentivirus. Anti-mouse total IgG H+L (AlexaFluor488-labeled) was used to detect anti-AQP4 antibodies (black line histograms). ΔMFI was calculated in relation to staining of LN18 cells transduced with empty vector (shaded histograms). Representative histograms (left) and plot of mean ΔMFI ± SD (right) are shown (n = 6 per group). **(B)** AQP4 serum response at different time points in *Aqp4*$^{-/-}$ mice immunized with AQP4 protein or AQP4(201-220) peptide. Mean ΔMFI ± SD (n = 6 per group). **(C)** To identify antibody classes and subclasses of AQP4-specific antibodies, fluorochrome-labeled anti-mouse Ig antibodies specific for IgG, IgA, IgE, IgG1, IgG2b, IgG2c and IgG3 were used. Mean ΔMFI ± SD (n = 6). *$p < 0.05$ (unpaired Student's t-test). Data are representative of three independent experiments **(A-C)**.

When *Aqp4*$^{-/-}$ mice were immunized side-by-side with either full-length AQP4 protein or the immunodominant T-cell epitope AQP4(201-220) peptide emulsified in CFA, conformational antibodies against AQP4 could only be detected in sera samples of protein-immunized mice (Figure 4.6 B). To check whether those anti-AQP4 antibodies were of potential pathologic relevance, antibody classes and subclasses were identified using anti-mouse Ig antibodies for IgG, IgA, IgE, IgG1, IgG2b, IgG2c and IgG3. Since anti-AQP4 antibodies were predominantly

of the IgG2c isotype they are complement fixing and thus likely able to contribute to immunopathology upon binding to their target antigen on the cell surface (Figure 4.6 C).

4.3 Tolerance mechanism to AQP4 in AQP4-sufficient mice

There are different mechanisms by which immunological tolerance to antigens is obtained. In regard to protective immunity provided by T cells, the ability to discriminate between foreign and self is crucial. That is why T cells undergo selection processes during their maturation in the thymus where cells that recognize self-antigens are either depleted from the repertoire (negative selection) or end up in the Foxp3$^+$ T regulatory (T_{reg}) cell lineage (Klein et al., 2014). The finding that AQP4-sufficient WT mice failed to raise a proliferative anti-AQP4 T-cell recall response upon immunization with AQP4 protein suggests a tight tolerance mechanism to this antigen, resulting in a very low precursor frequency of AQP4-specific conventional T cells in the physiologic repertoire. Alternatively, WT mice might harbor a high frequency of AQP4 specific T_{reg} cells. To better understand the mechanisms behind the induction of tolerance to AQP4, different approaches were chosen.

AQP4 is a tissue-restricted antigen and its expression during negative selection of thymocytes is AIRE-dependent (Anderson et al., 2002). In the thymus, AIRE-dependent genes are mostly expressed by medullary thymic epithelial cells (mTECs) but also hematopoietic APCs such as dendritic cells (DCs) can contribute to tolerance induction by cross-presentation of those antigens (Gallegos and Bevan, 2004) (Perry et al., 2014). In addition, a subset of B cells was reported of being able to express AIRE themselves, making them another player during negative selection of AQP4-specific thymocytes (Yamano et al., 2015). To narrow down which cells provide tolerance to AQP4 in the thymus, criss-cross bone marrow chimeras (BMCs) of C57BL/6 WT and *Aqp4*$^{-/-}$ mice were generated. If hematopoietic cells mediate central tolerance to AQP4 by presenting their intrinsic AQP4, transplantation of *Aqp4*$^{-/-}$ bone marrow into WT recipients should rescue AQP4-specific T-cell clones from deletion, resulting in a mature T-cell repertoire with AQP4-reactive clones. To test this, BMCs were immunized with AQP4 full-length protein emulsified in CFA. Some mice were sacrificed early to perform recall experiments as described before, others were monitored daily for signs of disease and tested for conformational antibodies in their sera. A robust anti-AQP4 antibody response was only

detectable over time in *Aqp4*$^{-/-}$ → *Aqp4*$^{-/-}$ controls whereas all other groups of mice, including *Aqp4*$^{-/-}$→ WT BMCs failed to generate an antigen-specific serum response (Figure 4.7 A).

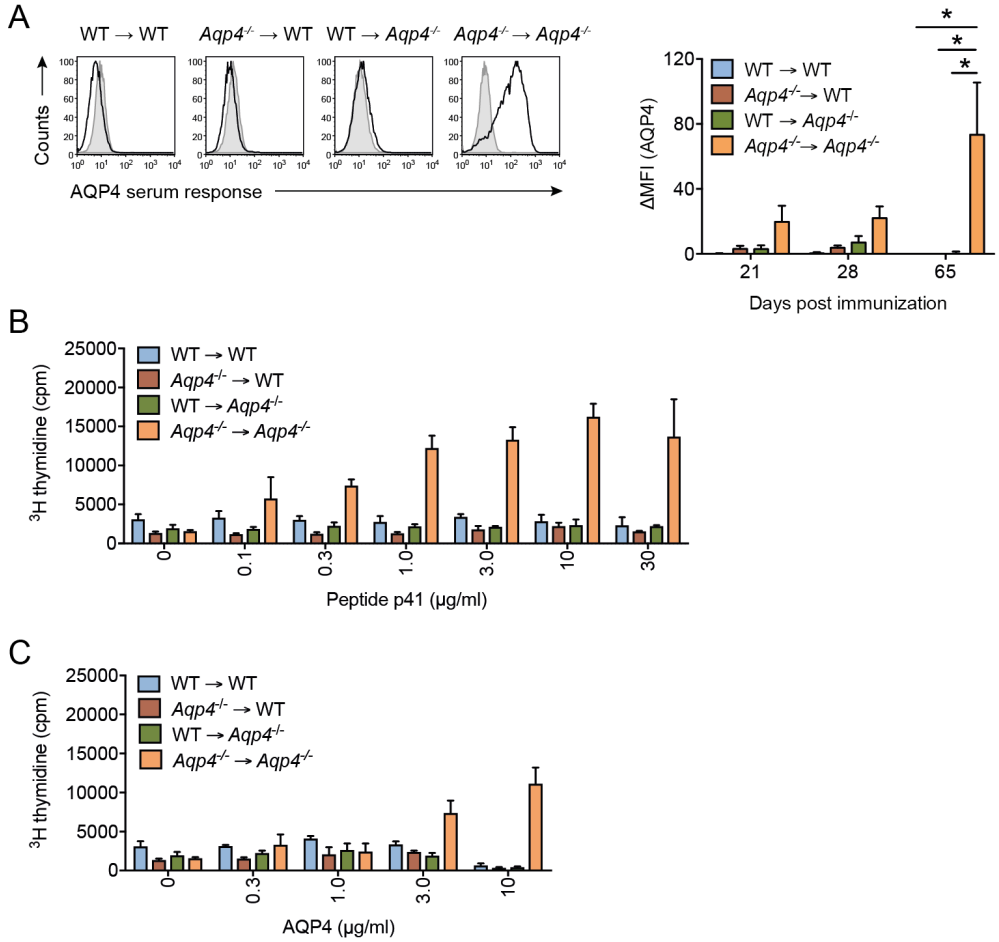

Figure 4.7: The naïve T-cell and B-cell repertoires of AQP4 sufficient mice are purged of AQP4-reactive clones. Criss-cross BMCs of C57BL/6 WT and *Aqp4*$^{-/-}$ mice were immunized with full-length AQP4 protein emulsified in CFA. **(A)** Sera of mice were collected at different time points after immunization and tested in a cell-based flow cytometric assay as described in Fig. 4.6. Anti-mouse IgG H+L (AlexaFluor488-labeled) was used to detect cell-bound AQP4 antibodies. Representative histograms for sera collected on day 65 after immunization (left) and mean ΔMFI ± SD (n = 6 per group) for AQP4-specific IgG (right) are shown. *$p < 0.05$ (ANOVA plus Sidak's post-test). Splenocytes and draining LN cells of AQP4-immunized BMCs were tested on day 14 for their proliferation to either AQP4(201-220) **(B)** or AQP4 protein **(C)** ex vivo. Proliferation was measured by ^{3}[H]-thymidine incorporation. Mean values of triplicate cultures ± SD are shown. Data are representative of three independent experiments **(A-C)**.

The same was true for AQP4-reactive T cells, which were only present in *Aqp4*$^{-/-}$ → *Aqp4*$^{-/-}$ controls. Here, T cells showed a profound proliferation in response to titrated AQP4(201-220) peptide (Figure 4.7 B) as well as full-length AQP4 protein (Figure 4.7 C).

The absence of AQP4-specifc T-cell and B-cell responses in *Aqp4*$^{-/-}$ → WT BMCs upon immunization with full-length AQP4 protein suggests, that tolerance to AQP4 is not

exclusively mediated by hematopoietic APCs (e.g. DCs or B cells) but rather depends on radiation-resistant thymic epithelial cells (TECs).

In addition to deletional tolerance, another fate of self-reactive T-cell clones during the thymic selection process is deviation into the Foxp3$^+$ T_{reg} lineage (Wirnsberger et al., 2011). To investigate whether the mature T-cell repertoire of WT mice contained exaggerated frequencies of AQP4 specific T_{reg} cells, C57BL/6 WT mice were treated with anti-CD25 neutralizing antibodies to deplete all T_{reg} cells prior to immunization with AQP4 full-length protein. This method is well established and has been used for breaking tolerance mediated by increased T_{reg}-cell frequencies (Korn et al., 2007). Prior to immunization with either AQP4 full-length protein or MOG(35-55) peptide, WT mice were injected with anti-CD25 antibody or IgG1 control antibody on days 3 and 5 before immunization. Only mice immunized with MOG(35-55) peptide according to the established EAE induction regimen developed symptoms of encephalomyelitis. Mice that were immunized with AQP4 protein did not get sick irrespective of whether or not they were depleted of peripheral T_{reg} cells upfront (Figure 4.8 A).

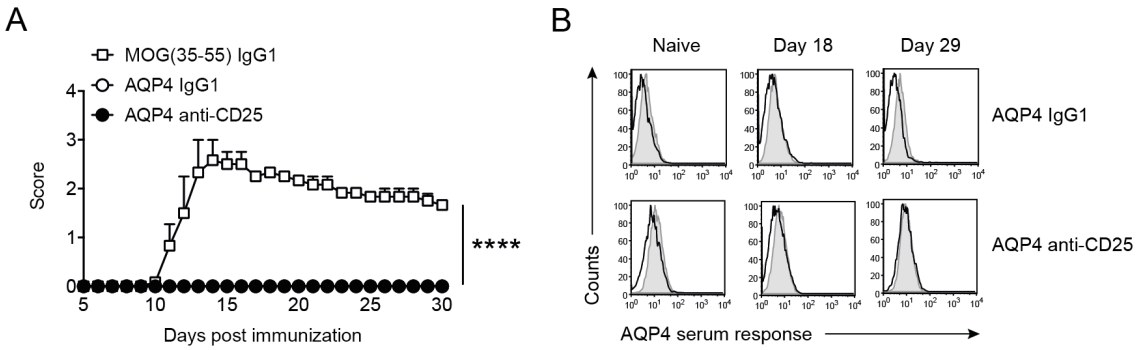

Figure 4.8: A tight central tolerance mechanism to AQP4 prevents an anti-AQP4 adaptive immune response in WT mice. C57BL/6 WT mice were immunized s.c. with full-length AQP4 protein or MOG(35-55) peptide emulsified in CFA as immunization control. On days -5 and -3 prior to immunization mice were injected with either control IgG1 or anti-CD25 antibodies to deplete T_{reg} cells. **(A)** Mean clinical scores ± SEM (n = 6 per group) are shown. ****$p < 0.0001$ (Mann-Whitney U test for nonparametric values). **(B)** Sera of mice were tested on days 18 and 29 after immunization for AQP4-specific antibodies using a cell-based assay described in Fig. 4.6. Representative histograms are shown. Data are representative of two independent experiment **(A, B)**.

Besides the clinical course, mice were also investigated for mounting an AQP4-specific antibody response upon immunization. Therefore, sera were collected on days 18 and 29 to compare antibody status with naïve sera taken before immunization. In line with missing clinical signs of encephalomyelitis none of the mice immunized with AQP4 protein raised an

anti-AQP4-specific serum response (Figure 4.8 B). Thus, depleting peripheral Foxp3$^+$ T_{reg} cells did not break the tolerance to AQP4 in WT mice.

Taken together, radiation-resistant TECs most likely play a role in mediating tolerance to AQP4 in the thymus by presenting the antigen during negative selection. Subsequently, AQP4-reactive T cells rather get depleted than deviated into the Foxp3$^+$ T_{reg} lineage, since dominant (T_{reg}-cell mediated) peripheral tolerance does not appear to play a major role in preventing AQP4-specific T-cell responses in WT mice.

Therefore, I focused on medullary thymic epithelial cells (mTECs) as potential source of AQP4 for negative selection in the thymus. I chose a loss-of-function approach to test the role of mTECs as expressers and presenters of AQP4. Conditional ablation of *Aqp4* in mTECs was achieved by crossing *Foxn1*^{Cre} mice with *Aqp4*$^{flox/flox}$ mice. In these *Foxn1*^{Cre} x *Aqp4*$^{flox/flox}$ mice expression of *Aqp4* is prevented only in Foxn1$^+$ mTECs while the antigen expression throughout the body remains unaltered. In a different system it could be shown, that preventing the AIRE-dependent expression of tissue-specific antigens in TECs resulted in an altered thymic output with self-reactive T cells no longer being eliminated (Khan et al., 2014). Thus, *Foxn1*^{Cre} x *Aqp4*$^{flox/flox}$ mice could serve as a model to test the mode of deletion of AQP4-specific T cells in the natural T-cell repertoire. However, when immunized with AQP4 full-length protein emulsified in CFA, *Foxn1*^{Cre} x *Aqp4*$^{flox/flox}$ mice did not develop clinical signs of encephalomyelitis (Figure 4.9 A). Accordingly, I did not observe a solid recall response to AQP4 peptides (Figure 4.9 B) or titrated AQP4 protein (Figure 4.9 C) in AQP4-immunized *Foxn1*^{Cre} x *Aqp4*$^{flox/flox}$ mice. Hence, it is likely that lack of AQP4 expression in mTECs is not sufficient to prevent negative selection of AQP4-specific T cells from the natural repertoire.

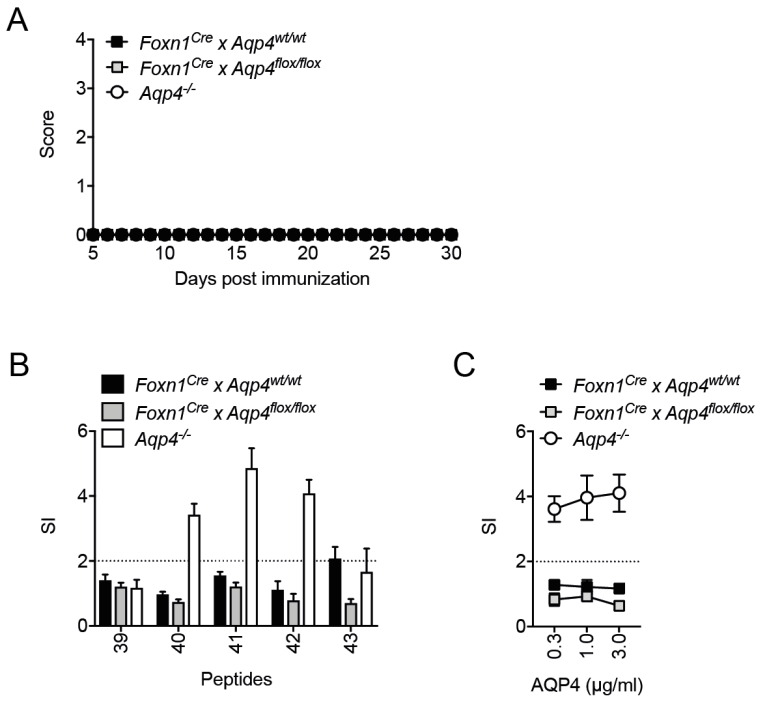

Figure 4.9: Conditional knockout of AQP4 in thymic epithelial cells does not break the tolerance to AQP4 in otherwise AQP4 sufficient mice. $Foxn1^{Cre}\,x\,Aqp4^{wt/wt}$, $Foxn1^{Cre}\,x\,Aqp4^{flox/flox}$ and $Aqp4^{-/-}$ mice were immunized with full-length AQP4 protein emulsified in CFA. **(A)** Mean clinical scores ± SEM (n = 6 per group) are shown. Splenocytes and draining LN cells were tested for their proliferative recall response to AQP4 peptides 39 – 43 **(B)** or AQP4 protein **(C)**. Proliferation was measured by ^{3}[H]-thymidine incorporation. Stimulation index means of triplicate cultures ± SD are shown. Data are representative of three independent experiments **(A-C)**.

4.4 Animal model for features of NMO disease

4.4.1 $Aqp4^{\Delta T}$ compound mice show clinical signs of disease upon immunization with AQP4 protein

In order to establish a preclinical model to investigate the immunopathology induced by a combination of AQP4-specific T cells and AQP4-specific antibodies, I constructed compound mice that expressed the target antigen, i.e. AQP4, in the CNS and peripheral tissues and whose natural T-cell repertoire still included AQP4-reactive clones. In a first approach $Tcra^{-/-}$ mice, that lack endogenous T cells but have an unaltered mature B-cell repertoire, were used as recipients for the mature and non-tolerized T-cell compartment of $Aqp4^{-/-}$ mice. Therefore, $CD4^{+}$ T cells from spleen and LNs of naïve $Aqp4^{-/-}$ mice were isolated by MACS and transferred i.p. into $Tcra^{-/-}$ mice. As a result of this reconstitution, these so-called

AQP4$^{\Delta T}$ *x Tcra*$^{-/-}$ mice now carried a T-cell repertoire with sufficiently high AQP4-specific T-cell precursor frequencies to mount productive anti-AQP4 effector T-cell responses upon immunization with AQP4. *AQP4*$^{\Delta T}$ *x Tcra*$^{-/-}$ mice were immunized with AQP4 protein or with an alternative CNS antigen MOG which is known to induce clinical signs of encephalomyelitis. In addition to antigen-specific T-cell responses, mice were also tested for the serum response to AQP4 or MOG, respectively, using a cell-based assay as described before. While *AQP4*$^{\Delta T}$ *x Tcra*$^{-/-}$ mice that were immunized with MOG raised a robust anti-MOG antibody response, none of the mice immunized with AQP4 protein tested positive for anti-AQP4 antibodies in the serum (Figure 4.10 C). Although AQP4-immunized mice failed to generate anti-AQP4 antibodies, they developed a neurologic syndrome that showed a similar course compared to the EAE observed in MOG-immunized mice (Figure 4.10 A). AQP4-immunized *AQP4*$^{\Delta T}$ *x Tcra*$^{-/-}$ mice developed paresis of the tail and the hind limbs around day 11. Moreover, *AQP4*$^{\Delta T}$ *x Tcra*$^{-/-}$ mice that were immunized with AQP4 protein showed an increased mortality as compared with MOG-immunized *AQP4*$^{\Delta T}$ *x Tcra*$^{-/-}$ mice (Figure 4.10 B). Due to the lack of an antibody response in AQP4-immunized mice, disease symptoms were most likely caused by AQP4-specific T cells. To examine and compare antigen-specific T-cell responses, mice from both groups were sacrificed at peak disease to be analyzed for infiltrating cells within the CNS by flow cytometry. The composition of the cellular infiltrate and cytokine profile of infiltrating T cells in mice immunized with AQP4 protein was similar to those of MOG-immunized mice (Figure Appendix.2). $CD4^+$ T cells, macrophages, dendritic cells and some neutrophils were detected in the immune cell infiltrates of the CNS and the total numbers and frequencies of these cells were comparable in AQP4- and MOG-immunized compound mice (Figure Appendix.2 A and Appendix.2 B). This was also true with regard to the cytokine profile of $CD4^+$ T cells both in brain and spinal cord. Whether mice were immunized with MOG or AQP4 protein, production of IFNγ and GM-CSF was predominant, only few $CD4^+$ T cells expressed IL-17 or IL-10 (Figure Appendix.2 C).

Since human NMO lesions in the CNS are characterized by perivascular loss of AQP4 immunoreactivity, mice were examined at peak disease for this feature by histological analysis. AQP4 staining of brain tissue was performed in both groups and did not reveal any kind of AQP4 loss near vessels that otherwise showed infiltration of immune cells, suggesting the necessity of anti-AQP4 antibodies being present to reproduce this feature of NMO lesions in mice (Figure 4.10 D).

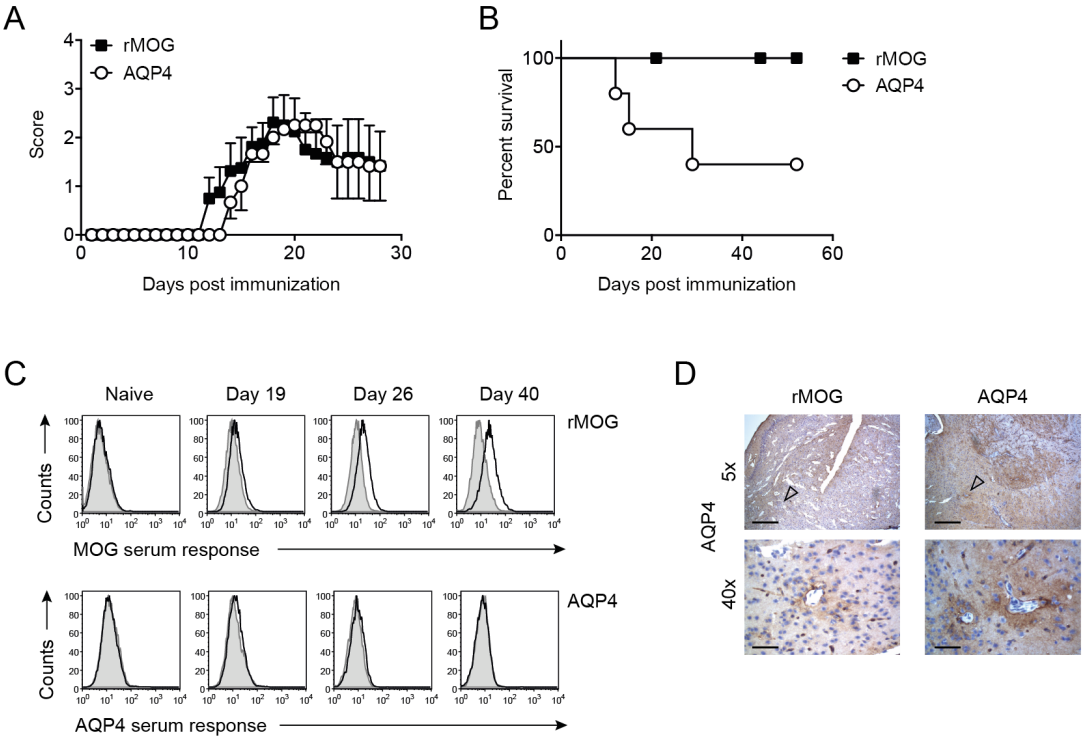

Figure 4.10: *AQP4*$^{\Delta T}$ compound mice develop clinical signs of disease upon immunization with AQP4 protein without raising an endogenous AQP4-specific serum response. *AQP4*$^{\Delta T}$ *x Tcra*$^{-/-}$ mice were generated by i.p. transfer of the mature T-cell compartment of *Aqp4*$^{-/-}$ mice into *Tcra*$^{-/-}$ mice. The mice were then immunized with full-length AQP4 protein or MOG protein emulsified in CFA. **(A)** Mean clinical scores ± SEM and **(B)** percent survival of immunized mice are shown (n = 6 per group). **(C)** Sera of mice were collected at several time points after immunization and tested for AQP4- or MOG-specific antibodies in a cell-based flow cytometric assay described in Fig. 4.6. Representative histogram plots illustrating the anti-MOG and anti-AQP4 serum responses are shown. **(D)** Some mice were sacrificed at day 20 after immunization to perform histological analysis. Representative AQP4 staining of the brain at 5x (scale bar 400 µm) and 40x magnification (scale bar 50 µm) is shown. Open arrows show vessels with infiltrating cells and without perivascular loss of AQP4 immunoreactivity. Data are representative of two independent experiments **(A-D)**.

The absence of an anti-AQP4-directed serum response in AQP4-immunized *AQP4*$^{\Delta T}$ *x Tcra*$^{-/-}$ mice raised the question whether not only the T-cell but also the B-cell compartment of AQP4-sufficient mice is depleted from AQP4-reactive clones. To address this question, I generated compound mice using *Rag1*$^{-/-}$ mice that lack both endogenous T cells and B cells as recipients. *Rag1*$^{-/-}$ mice were injected i.p. with whole splenocytes from *Aqp4*$^{-/-}$ donors, in order to not only transfer AQP4 reactive T cells but also B cells. As a control, some mice received splenocytes from WT donors. After immunization of these compound mice with either MOG or AQP4 protein emulsified in CFA, the animals were monitored for developing clinical signs of disease and more importantly for raising an antibody response against AQP4. Mice that were reconstituted with splenocytes from *Aqp4*$^{-/-}$ donors and immunized with AQP4 protein developed a disease that was characterized by weakness of the tail and the hind limbs, whereas

mice that received WT splenocytes and were immunized with AQP4 protein did not get sick (Figure 4.11 A).

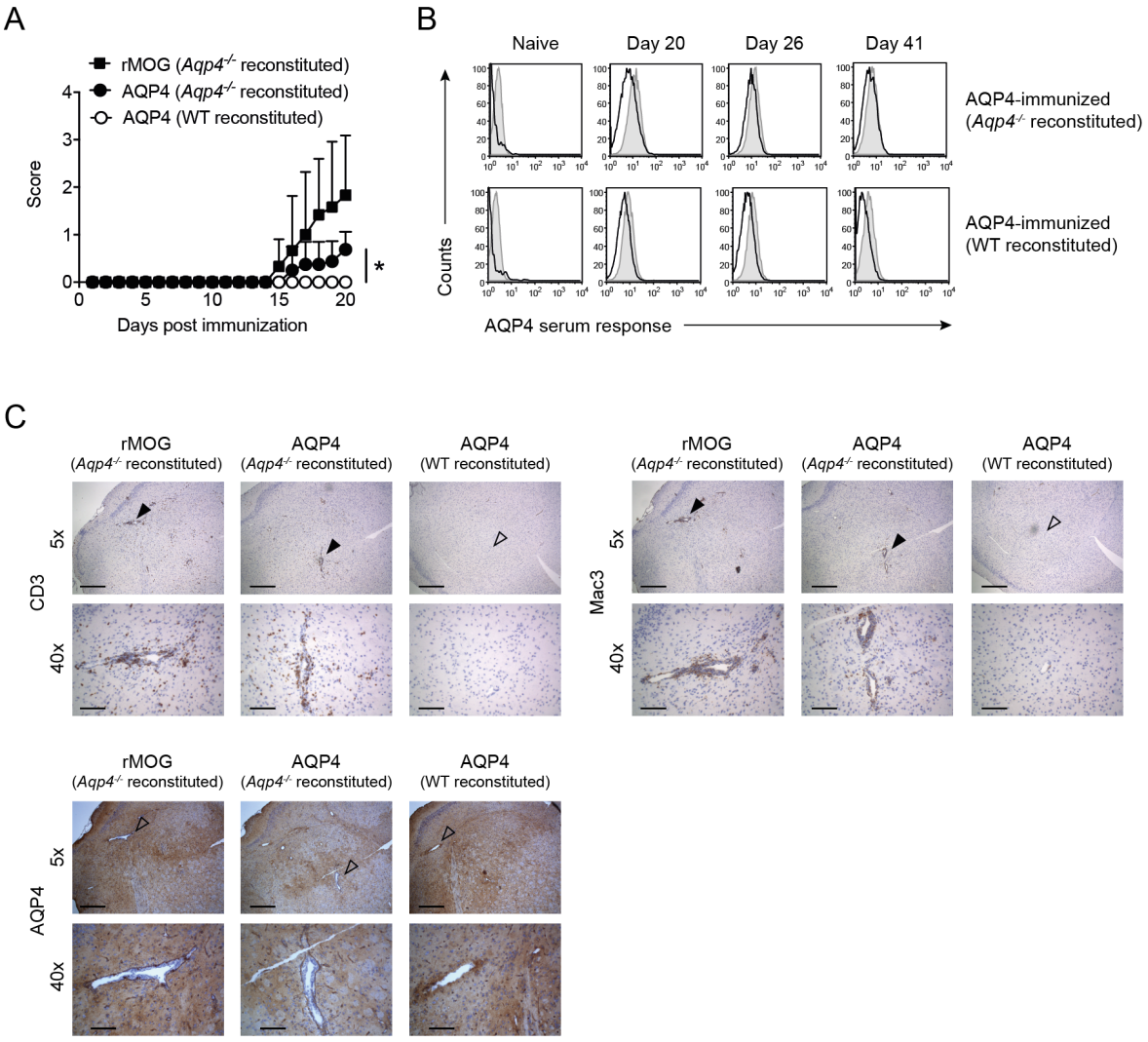

Figure 4.11: AQP4-reactive B-cell clones are depleted in the periphery of AQP4-sufficient mice upon transfer. *Rag1*$^{-/-}$ mice were reconstituted with whole spleen cells from *Aqp4*$^{-/-}$ mice harboring AQP4-reactive T cells and B cells. Some mice received whole spleen cells from C57BL/6 WT mice as control. Mice were immunized with either MOG protein or full-length AQP4 protein emulsified in CFA one day after i.p. cell transfer. **(A)** Mean clinical scores ± SEM are shown (n = 6 per group). **(B)** Sera of AQP4-immunized mice were tested for AQP4-specific antibodies using a cell-based flow cytometric assay as described. Representative histogram plots are shown. **(C)** Mice were sacrificed at day 25 after immunization for histological analysis of the brain. Representative CD3, Mac3 and AQP4 staining at 5x (scale bar 400 µm) and 40x magnification (scale bar 50 µm) is shown. In CD3 and Mac3 staining, open arrows show vessels without infiltrates, whereas closed arrows indicate vessels with infiltration of T cells and macrophages. Open arrows in AQP4 staining show vessels without perivascular loss of AQP4 immunoreactivity. Data are representative of two independent experiments **(A-C)**.

However, all AQP4-immunized mice failed to raise an anti-AQP4 antibody response even when they were reconstituted with splenocytes from *Aqp4*$^{-/-}$ donors (Figure 4.11 B). Accordingly, due to the absence of an anti-AQP4 antibody response in this model, there was no loss of AQP4 immunoreactivity detectable in the brain of AQP4-immunized mice (Figure 4.11 C). This finding suggested that AQP4-specific B cells present in the splenic B-cell repertoire of the *Aqp4*$^{-/-}$ donors were rapidly depleted as soon as they were transferred into *Rag1*$^{-/-}$ host mice with sufficient AQP4 expression in peripheral tissues.

4.4.2 Immunization with AQP4(201-220) epitope in addition with administration of anti-AQP4 antibody results in NMO-specific lesional patterns

To reproduce hallmark features of NMO disease in mice, the presence of AQP4-specific antibodies is a prerequisite (Zeka et al., 2015). As shown, raising an AQP4-directed serum response upon immunization with AQP4 protein was only successful in *Aqp4*$^{-/-}$ but neither in WT nor in *Aqp4*$^{\Delta T}$ compound mice even when they were reconstituted with AQP4-reactive B-cell clones in advance. Therefore, a different approach was chosen to combine AQP4-directed T-cell responses and AQP4-specific antibodies in AQP4-sufficient mice in order to develop a suitable model for NMO. Compound mice were again generated by transferring the mature CD4$^+$ T-cell repertoire of naïve *Aqp4*$^{-/-}$ mice into *Rag1*$^{-/-}$ recipients. These *Aqp4*$^{\Delta T}$ *x Rag1*$^{-/-}$ mice were then immunized with the immunodominant T-cell epitope AQP4(201-220) emulsified in CFA and injected i.v. with AQP4 immune serum generated in *Aqp4*$^{-/-}$ mice. *Aqp4*$^{\Delta T}$ *x Rag1*$^{-/-}$ mice that were immunized with AQP4(201-220) emulsified in CFA but only received naïve control serum showed minor signs of disease. In contrast, disease severity was significantly increased in those *Aqp4*$^{\Delta T}$ *x Rag1*$^{-/-}$ compound mice that were immunized with AQP4(201-220) peptide and in addition received immune serum containing anti-AQP4 antibodies (Figure 4.12 A). To ensure that only serum with high titers of anti-AQP4 antibodies was transferred, donor sera were analyzed in a cell-based flow cytometric assay prior to use (Figure 4.12 B).

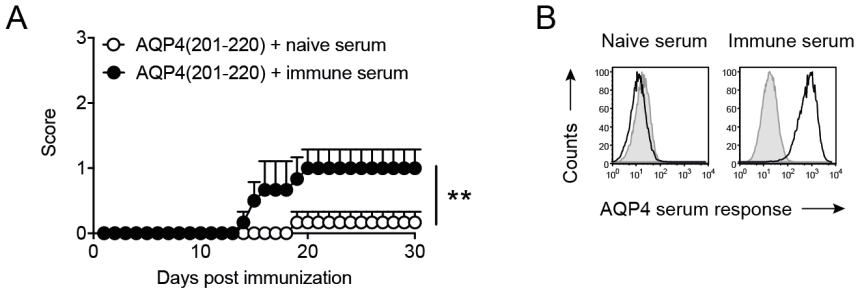

Figure 4.12: AQP4(201-220) is an encephalitogenic epitope. (A) To generate $Aqp4^{\Delta T}\,x\,Rag1^{-/-}$ compound mice, the mature T-cell compartment from $Aqp4^{-/-}$ mice was i.p. transferred into $Rag1^{-/-}$ mice. These $Aqp4^{\Delta T}$ compound mice were immunized with AQP4(201-220) peptide emulsified in CFA. On days 6 and 12 after immunization the mice i.v. received either one hundred microliters of naïve serum or immune serum with high titers of anti-AQP4 antibodies. Mean clinical scores ± SEM (n = 5 per group) are shown. $^{**}p < 0.01$ (Mann-Whitney U test for nonparametric values). **(B)** The transferred immune serum was harvested from AQP4-immunized $Aqp4^{-/-}$ mice and was tested in a cell-based flow cytometric assay as described to guarantee for high titers of anti-AQP4 antibodies prior to administration.

Similarly to i.v. administration of AQP4 immune serum, the disease phenotype of $Aqp4^{\Delta T}\,x\,Rag1^{-/-}$ mice immunized with AQP4(201-220) peptide was aggravated as compared to injection of an irrelevant monoclonal control antibody (IC-05) when I administered a monoclonal anti-AQP4 antibody (rAb-53) (Figure 4.13 A). In addition, compared to transfer of IC-05, administration of the murinized AQP4-specific antibody rAb-53 not only resulted in a more severe disease course but also a slightly increased mortality rate among immunized mice (Figure 4.13 B). Overall, the presence of AQP4-directed T-cell responses in combination with anti-AQP4 antibodies in AQP4-sufficient $Aqp4^{\Delta T}\,x\,Rag1^{-/-}$ mice resulted in a disease course that was similar in onset and overall severity to the EAE observed in mice immunized with MOG(35-55) peptide. However, when examined for NMO-like lesional patterns in the CNS by immunohistochemistry, only AQP4(201-220)-immunized $Aqp4^{\Delta T}\,x\,Rag1^{-/-}$ mice that additionally received anti-AQP4 antibodies showed perivascular loss of immunoreactivity against AQP4 in the CNS (Figure 4.13 C). Hence, the AQP4-specific humoral response is required to reproduce the typical NMO-like lesional pattern in the CNS of $Aqp4^{\Delta T}\,x\,Rag1^{-/-}$ mice.

In addition to clinical course and histopathology of the brain, $Aqp4^{\Delta T}$ compound mice were also analyzed for pathological changes of the retina upon immunization with AQP4(201-220) and antibody transfer by optical coherence tomography (OCT). Since Müller cells, which are located in the inner nuclear layer (INL) of the retina, express high amounts of AQP4, they have been shown to be a primary target of AQP4-directed T-cell responses as well as AQP4-specific antibodies (Zeka et al., 2016). To investigate potential changes of the retinal INL, in

which Müller cells are located, I used OCT to assess the retina of live $Aqp4^{\Delta T}$ compound mice prior to immunization (baseline) or after immunization with AQP4(201-220) or MOG(35-55) peptide and either control antibody treatment (IC-05) or treatment with anti-AQP4 monoclonal antibody (rAb53).

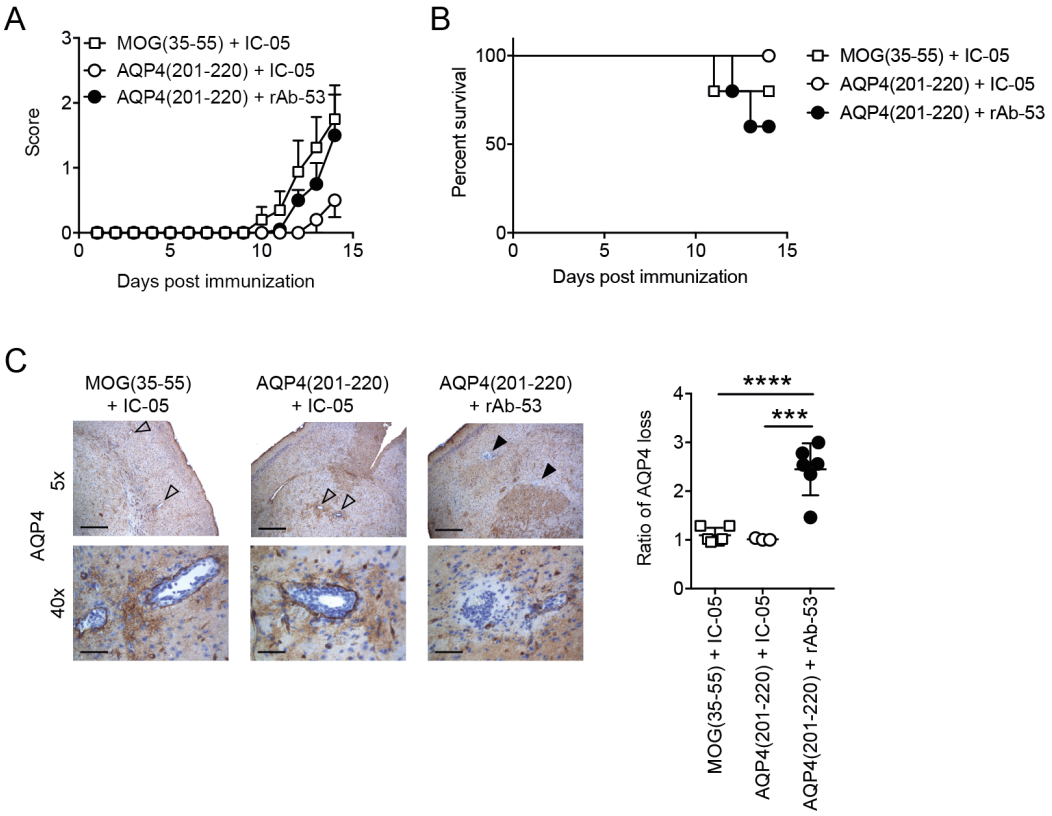

Figure 4.13: NMO-like lesions are only induced by AQP4(201-220)-specific T cells in additional presence of anti-AQP4 antibodies. $Aqp4^{\Delta T}\,x\,Rag1^{-/-}$ mice were immunized with either MOG(35-55) or AQP4(201-220) peptide emulsified in CFA. Some mice received i.v. the murinized monoclonal anti-AQP4 antibody rAb-53 on days 12 and 14 after immunization, others were injected i.v. with the control antibody IC-05. **(A)** Mean clinical scores ± SEM and **(B)** percent survival of immunized mice are shown (n = 6 per group). **(C)** Mice were sacrificed 4 h after the last antibody treatment on day 14 for histological analysis of the brain. Representative AQP4 staining of the brain at 5x (scale bar 400 µm) and 40x magnification (scale bar 50 µm) are shown on the left. Open arrows show vessels without perivascular loss of AQP4 immunoreactivity. Closed arrows indicate areas of AQP4 loss in vicinity of vessels. Quantification of AQP4 loss as ratio of the area with AQP4 signal loss divided by the area of the associated vessel lumen in the brain of the indicated treatment groups on the right (mean ± SD). ***$p < 0.001$, ****$p < 0.0001$ (ANOVA plus Sidak's post-test). Data are representative of two independent experiments **(A-C)**.

At the onset of clinical signs of disease, INL volumes of $Aqp4^{\Delta T}$ compound mice that received control antibody remained unchanged compared to baseline, regardless of whether the mice were immunized with MOG(35-55) or AQP4(201-220) peptide. In contrast, mice that were immunized with AQP4(201-220) peptide and were additionally treated with anti-AQP4

rAb-53 antibody showed a significant swelling of the INL at disease onset (Figure 4.14). Thus, although AQP4(201-220)-specific T cells alone induce a clinically manifest encephalomyelitis, for NMO-specific lesional patterns in the CNS with swelling of the INL in the retina the additional presence of anti-AQP4 antibodies is required.

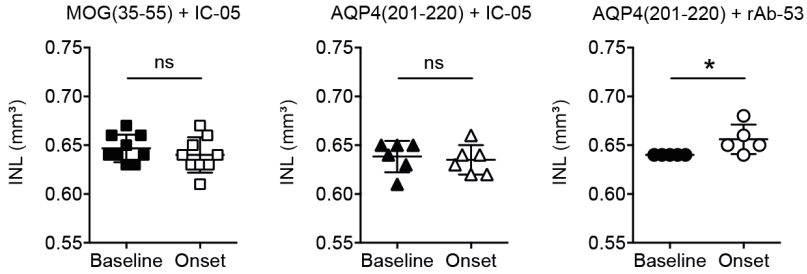

Figure 4.14: *Aqp4$^{\Delta T}$ x Rag1$^{-/-}$* mice immunized with AQP4(201-220) peptide plus i.v. injection of rAb-53 develop inner nuclear layer swelling in the retina at disease onset. *Aqp4$^{\Delta T}$ x Rag1$^{-/-}$* mice were immunized with either MOG(35-55) or AQP4(201-220) peptide emulsified in CFA. On day 12 after immunization the mice were injected i.v. with rAb-53 antibody or IC-05 control antibody. The retinae of the mice were analyzed using optical coherence tomography (OCT) once before immunization (baseline) and again on day 13 after immunization at onset of disease. Mean INL volumes of individual eyes ± SD are shown. *$p < 0.05$, ns = not significant (Student's t-test). One experiment with six mice per group is shown.

4.5 Tetramer staining of AQP4-specific T cells

T cells recognize and bind to complexes of major histocompatibility complex (MHC) and small peptides with their cognate T-cell receptors (TCRs). In order to detect and quantify antigen-specific CD4$^+$ T cells, soluble labeled ligands in the form of peptide-MHC (pMHC) class II multimers have emerged as a powerful tool (Lebowitz et al., 1999). Here, biotinylated pMHC are multimerized by streptavidin to assure an increase in avidity of pMHC tetramers towards TCRs that is high enough to allow for detection in flow cytometry. Thus, with the help of pMHC class II tetramers, that display an antigenic peptide in the class-II binding groove, CD4$^+$ T-cell responses can be analyzed for their specificity and phenotype.

To generate MHC class-II tetramers for detection of AQP4(201-220)-specific T cells, biotinylated monomers of both the IA^b beta chain with the covalently linked core epitope AQP4(205-215) and the IA^b alpha chain were produced in S2 cells in collaboration with the group of Prof. Klein, LMU. Incorporated Fos-Jun leucine zipper motifs forced dimerization of the co-expressed MHC class II chains and a BirA signal sequence on the alpha chain allowed for site specific biotinylation.

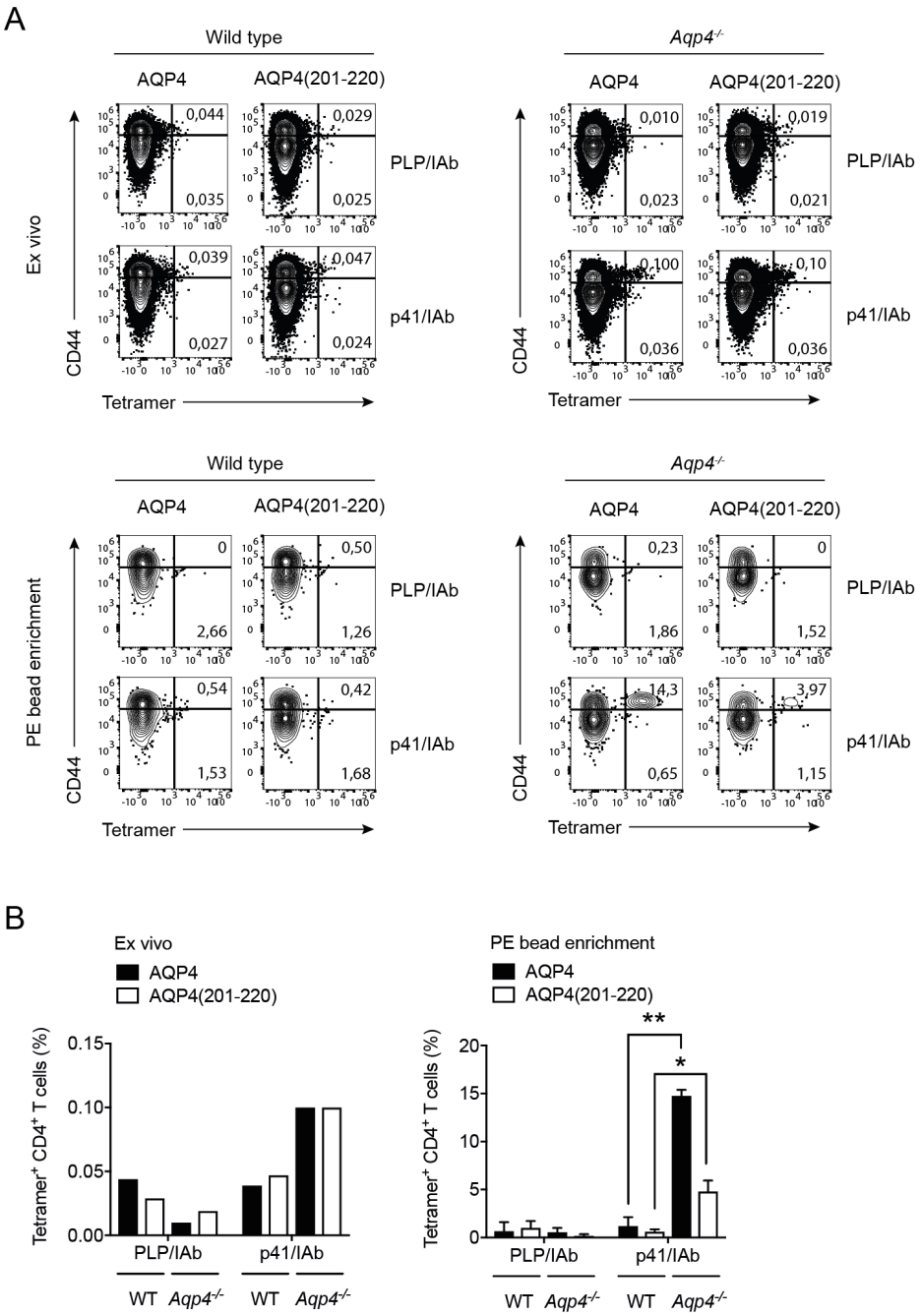

Figure 4.15: P41/IAb tetramer staining of AQP4-specific CD4$^+$ T cells in spleen and draining LNs of *Aqp4*$^{-/-}$ upon immunization with AQP4 protein or AQP4(201-220) peptide. C57BL/6 WT and *Aqp4*$^{-/-}$ mice were immunized with either full-length AQP4 protein or AQP4(201-220) peptide emulsified in CFA. On day 9 after immunization single cell suspension from spleen and draining LNs was generated. Cells were stained for FACS analysis with CD4 (BV510-labeled) and CD44 (FITC-labeled) antibodies as well as class-II tetramers for PLP (PLP/IAb) or AQP4 (p41/IAb) (both PE-labeled). An additional dumb channel was used including antibodies for B220, CD11c, CD11b and F4/80 (all PE-Cy7-labeled). Frequencies of tetramer$^+$ CD4$^+$ T cells were analyzed ex vivo as well as after PE-bead enrichment by MACS. **(A)** Representative dot plots of CD4$^+$ pre-gated splenocytes and draining LN cells from mice ex vivo (top) and after PE-bead enrichment (bottom). **(B)** Frequencies of tetramer$^+$ CD4$^+$ T cells in spleen and draining LNs of AQP4-immunized WT and *Aqp4*$^{-/-}$ mice ex vivo (left) or

after PE-bead enrichment (right). *$p < 0.05$, **$p < 0.01$ (Student's t-test). Data are representative of two independent experiments.

The biotinylated pMHC class II heterodimers were then tetramerized with PE-labeled streptavidin. In addition to the pMHC tetramer that displays AQP4(205-215) and is referred to as p41/IAb, a second irrelevant pMHC tetramer was generated containing a peptide sequence from PLP protein (PLP/IAb) (Hassler et al., 2019). Both tetramers were produced by Tobias Hassler in the laboratory of Prof. Klein, LMU.

To test whether the generated p41/IAb tetramer was suitable to detect AQP4-specific T cells, C57BL/6 WT and *Aqp4*$^{-/-}$ mice were immunized with either AQP4 full-length protein or AQP4(201-220) peptide emulsified in CFA. Cells from spleen and draining LNs were interrogated for AQP4-specific T-cell frequencies on day 9 after immunization by tetramer binding. Besides the PE-labeled soluble tetramers, p41/IAb and PLP/IAb (control staining), cells were incubated with antibodies to CD4 and CD44. To exclude irrelevant cells, an additional dump channel with antibodies to B220, CD11c, CD11b and F4/80 was used. By FACS analysis of single cell suspensions both ex vivo as well as after PE-bead enrichment by MACS, p41/IAb^{+} T cells were detected in sizeable fractions only in AQP4-immunized *Aqp4*$^{-/-}$ mice but not in WT mice (Figure 4.15 A), both after immunization of *Aqp4*$^{-/-}$ mice with full-length AQP4 and with AQP4(201-220) (p41) (Figure 5.15 B). With this tetramer, further analysis of the frequencies of AQP4-specific T cells will be possible in naïve and immunized repertoires and also within the T_{reg}-cell compartment that cannot usually be read out by antigen-specific proliferative responses.

5 Discussion

5.1 AQP4(201-220) is the major immunogenic T-cell epitope of AQP4 in C57BL/6 mice

Ever since AQP4 was discovered as the autoantigen in NMO (Lennon et al., 2004) (Lennon et al., 2005), great efforts have been made to understand the role of B cells and secreted autoantibodies as well as the contribution of T cells in the pathogenesis of this inflammatory autoimmune disease of the CNS. While AQP4-specific B-cell responses and the resulting antibody-mediated immunopathology are well characterized, only little is known about the role of AQP4-specific T cells. Yet, an underlying antigen specific T-cell response is necessary for the formation of AQP4-specific autoantibodies since in humans, they are predominantly IgG1, a T-cell-dependent subgroup of immunoglobulins (Snapper and Paul, 1987) (Toellner et al., 1998). Furthermore, activated T cells are able to mediate inflammation of the BBB, which might promote the entry of antibodies into the CNS (Bennett et al., 2009) (Bradl et al., 2009), and create an inflammatory milieu in the CNS that facilitates ADCC and CDC against astrocytic targets (Pohl et al., 2013) (Zeka et al., 2015).

To elucidate how AQP4-specific B cells and T cells collaborate to generate an AQP4-targeted adaptive immune response leading to CNS autoimmunity with clinical manifestation, various animal models have been created over the last couple of years. Besides administration of AQP4-IgG some of them involve the transfer of AQP4-specific T cells. While the effector phase of NMO was nicely recapitulated in some of these models, the events that trigger adaptive immune responses to AQP4 remain unknown. Recently, a *Clostridium perfringens* antigen has been reported to function as molecular mimic and potentially activate HLA-DR

restricted AQP4(61-80)-specific T cells in humans (Varrin-Doyer et al., 2012). The authors assume AQP4(61-80) to be a naturally processed epitope although it is unclear whether AQP4(61-80)-specific T cells contribute to antibody formation. There is a surprisingly large number of epitopes in humans (Matsuya et al., 2011) and a whole range of different T-cell epitopes in the sequence of AQP4 has been reported in Lewis rats (Pohl et al., 2011) (Zeka et al., 2015), C57BL/6 and SJL/J mice (Kalluri et al., 2011) (Nelson et al., 2010) (Jones et al., 2015) as well as humanized DRB1*0301 transgenic mice (Arellano et al., 2012). The latter express a MHC class II molecule that is associated with NMO according to HLA haplotype analysis of patients (Brum et al., 2010). Unfortunately, active immunization of animals with these epitopes failed to mount a T-cell driven immune response against AQP4 leading to NMO-like immunopathology. This raised the question of whether those epitopes are naturally processed at all. While B cells and secreted antibodies bind conformational determinants, T cells recognize peptides in association with MHC molecules on cell surfaces (Germain, 1994). APCs need to pick up and process appropriate antigens in order to present these as peptides in association with MHC molecules to T cells. $CD4^+$ T helper cells recognize peptides with a length of up to 24 amino acids that are presented in the open binding groove of MHC class II molecules.

To identify naturally processed T-cell epitopes of AQP4, in this study C57BL/6 mice were immunized with full-length murine AQP4 protein and screened for proliferative T-cell responses to single 20mer peptides overlapping by 15 amino acids each and spanning the whole sequence of AQP4. By using WT and *Aqp4*$^{-/-}$ mice, it was possible to screen for epitopes not only in a tolerized but also a non-tolerized T-cell repertoire. Here, AQP4(201-220) was identified as the major immunogenic T-cell epitope of AQP4 in the context of IA^b. Immunization with AQP4(201-220) resulted in a potent T-cell response against full-length AQP4 protein ex vivo, showing that it is a naturally processed epitope. Subsequent fine mapping of this region revealed AQP4(205-2015) as the core epitope.

However, AQP4(201-220)-specific T cells could only be identified in *Aqp4*$^{-/-}$ mice. Immunization of WT mice with AQP4 protein did not result in relevant AQP4 peptide specific T-cell responses, suggesting that AQP4-specific T cells might have an extremely low frequency in the normal immune repertoire since APCs process and present antigens regardless of whether they are foreign or endogenous (Lin and Stockinger, 1989). Indeed, the ability of APCs from WT and *Aqp4*$^{-/-}$ mice to process AQP4 protein for antigen presentation in recall

assays did not differ and therefore cannot account for the lack of an AQP4-specific T-cell response in AQP4-sufficient mice.

In addition to AQP4(201-220), AQP4(135-153) has been recently reported to be another AI^b-restricted immunogenic T-cell epitope of AQP4 (Jones et al., 2015) (Sagan et al., 2016). It was identified by using the immune epitope database (IEDB), an "in silico" approach to predict allele-specific binding affinities of peptides to MHC molecules. Hence, it was not confirmed to be a naturally processed epitope. In this study, this region did not turn up as a potential epitope candidate in any of the performed recall assays. Even when testing the non-tolerized T-cell repertoire of *Aqp4*$^{-/-}$ mice, only AQP4(201-220) triggered a proliferative AQP4-specific T-cell response.

5.2 Adaptive anti-AQP4 responses are efficiently tolerized in AQP4-sufficient mice

The immunization of *Aqp4*$^{-/-}$ mice with full-length AQP4 protein generated an AQP4(201-220)-specific T-cell response that was absent in WT mice. As shown by analysis of recall cultures and tetramer staining with p41/IAb, the T-cell repertoire of AQP4-sufficient mice was essentially devoid of TCRs specific for AQP4(201-220). Moreover, WT mice failed to generate an antibody response to AQP4, while *Aqp4*$^{-/-}$ mice raised a robust anti-AQP4 serum response upon immunization with the protein. Further analysis of these conformational anti-AQP4 antibodies revealed they were predominantly of the IgG2c isotype. Interaction between antigen-specific T cells and B cells is a prerequisite for B-cell maturation and Ig class-switch recombination to this subgroup of immunoglobulins (Lanzavecchia, 1985). Hence, when immunized with AQP4 protein, *Aqp4*$^{-/-}$ mice raised an adaptive immune response against AQP4 with productive collaboration between AQP4-specific T cells and B cells. In contrast, WT mice did not generate either AQP4-specific T-cell or B-cell responses after immunization with AQP4 protein, suggesting a strong deletional tolerance to this ubiquitously expressed self-antigen.

In order to prevent autoimmune responses, immature lymphocytes undergo negative selection processes during their development, resulting in mature T-cell and B-cell repertoires that are purged of self-reactive clones (Klein et al., 2014) (Klinman, 1996). This central tolerance to

self-antigens is accompanied by several peripheral tolerance mechanisms that include anergy, clonal deletion, diversion and suppression (Xing and Hogquist, 2012).

To elucidate the mode of tolerance induction to AQP4, several approaches were pursued, all of which concluded that the natural repertoire of T cells and B cells is indeed depleted of AQP4-reactive clones. In the case of T cells, tolerance to AQP4 most likely is mediated by deletional tolerance rather than by the action of T_{reg} cells in the periphery.

Tolerance induction and the fate of autoreactive thymocytes (i.e., clonal deletion or development into T_{reg} cells) in the thymus depend on the cell types expressing tissue-restricted antigens (TRAs) (Anderson et al., 2002) (Mouri et al., 2017). Here, mTECs and BM-derived cells such as B cells and DCs complement each other in the presentation of TRAs to cover a full spectrum of TRAs (Yamano et al., 2015). However, tolerance induction to AQP4 is not solely dependent on one of these cell types alone as demonstrated by evaluation of criss-cross BMCs of WT and *Aqp4*$^{-/-}$ mice as well as *Foxn1*^{Cre} *x Aqp4*$^{flox/flox}$ mice for their ability to mount AQP4-specific adaptive immune responses. In both experimental setups, central tolerance to AQP4 could not be broken and AQP4-specific adaptive immune responses could not be elicited in AQP4-sufficient mice. Regardless of whether hematopoietic cells (i.e., thymic B cells or DCs) or mTECs were prevented from expressing AQP4 in the thymus, AQP4-reactive T cells were efficiently removed from the repertoire. Here, deletion of self-reactive clones outweighs deviation of autoreactive T cells into the Foxp3^{+} T_{reg} lineage and peripheral mediated tolerance to AQP4 plays only a minor role. This could be shown in a functional approach where all T_{reg} cells in the peripheral immune compartment of WT mice were deleted using an antibody to CD25. Immunization of these T_{reg} depleted mice with AQP4 protein did not result in clinical signs of encephalomyelitis and anti-AQP4 antibodies could not be detected in the serum, indicating the absence of both AQP4-specific T-cell and B-cell responses due to deletional central tolerance.

Like T cells in the thymus, immature B cells are screened for autoreactive clones during their development in the bone marrow, with self-recognition leading to clonal deletion or clonal anergy (Shlomchik, 2008). In addition, autoreactive B cells can undergo receptor editing, and deletion often occurs only after the cell has exhausted its editing capacity and there are no more possibilities for further V gene rearrangements (Halverson et al., 2004).

This study provides indirect evidence, that similar to the T-cell repertoire, the B-cell repertoire of WT mice is devoid of AQP4-reactive clones. Here, the lack of an anti-AQP4 antibody response in AQP4-immunized WT mice is a result of a tolerized B-cell repertoire rather than

an insufficient antigen-specific T-cell help, because reconstitution of AQP4-reactive T cells cannot rescue an anti-AQP4 serum response in a WT B-cell repertoire. This was shown in *Aqp4*$^{\Delta T}$ *x Tcra*$^{-/-}$ compound mice that received the mature T-cell compartment of *Aqp4*$^{-/-}$ mice but still failed to raise an AQP4-specific serum response upon immunization with AQP4 protein. Even when *Rag1*$^{-/-}$ mice, lacking both endogenous T cells and B cells, were reconstituted with non-tolerized splenocytes from *Aqp4*$^{-/-}$ mice (containing T cells and B cells), they did not develop an anti-AQP4 serum response after immunization.

In general, mature B cells are not susceptible to tolerance induction with the exception of antigens that are presented on cell surfaces (Klinman, 1996). Several adoptive transfer experiments have demonstrated that mature peripheral B cells from conventional or transgenic donor mice can be tolerized to antigenic determinants on host cell surfaces upon transfer (Hamilton et al., 1974) (Russell et al., 1991). In fact, AQP4 is not only the most abundant water channel in the CNS but ubiquitously expressed as transmembrane protein throughout the body, in skeletal muscle, stomach, kidney and Müller cells of the retina. Hence, mature AQP4-reactive B-cell clones likely are depleted from the repertoire in an antigen-specific manner. Apoptotic AQP4-expressing cells might induce physical or functional purging of B-cells with AQP4-specific BCRs by anergy, receptor editing or activation-induced cell death, mechanisms that have been described to be important for induction of B-cell tolerance to other autoantigens (Shlomchik, 2008). In consequence, after transferring AQP4-reactive T cells and B cells, AQP4-immunized *Rag1*$^{-/-}$ mice raised an anti-AQP4 specific T-cell response that even resulted in an encephalomyelitic syndrome but still failed to mount an anti-AQP4 serum response. Hence, only when B cells are educated in the absence of AQP4 and antigen-specific peripheral tolerance induction is prevented, i.e. in *Aqp4*$^{-/-}$ mice, a robust anti-AQP4 antibody response is induced. Taken together, a tight deletional tolerance in WT mice results in B-cell and T-cell repertoires that are purged of AQP4-reactive clones suggesting that both thymic tolerance and B-cell tolerance need to fail in order to allow for antigen-specific NMO-like autoimmune pathology in the CNS.

Interestingly, although both conditions are rare, there is a coincidence of NMO and myasthenia gravis that is higher than expected by chance (Leite et al., 2012). Since myasthenia gravis is an autoimmune disease also mediated by autoantibodies, an underlying defect in B-cell tolerance might be the common basis for susceptibility to both diseases. In view of potential curative treatment options, further studies need to investigate how tolerance to AQP4 is broken in patients with NMO.

5.3 AQP4(201-220)-specific T-cells induce an encephalomyelitic syndrome

Besides their role in generating high-affinity pathogenic antibodies, the direct contribution of AQP4-specific T cells to the immunopathology in NMO is incompletely understood (Mitsdoerffer et al., 2013). In early experimental models of NMO, encephalomyelitic T cells of unrelated specificity (against myelin basic protein, MBP) were used to mediate inflammation at the BBB and therefore facilitate entry of i.v. transferred anti-AQP4 antibodies into the CNS (Bennett et al., 2009) (Bradl et al., 2009). Thus, in these models T-cell specificity was irrelevant as long as they allowed pathogenic anti-AQP4 antibodies to efficiently infiltrate the CNS, reach their target in astrocytic end feet and trigger complement-mediated tissue destruction. However, recent studies suggest a more complex role for AQP4-specific T cells in instigating the disease (Jones et al., 2015) and directing the inflammatory response deeper into the CNS parenchyma of the optic nerves, the brain and the spinal cord (Zeka et al., 2015). Moreover, there is strong evidence that the shared antigen specificity of B cells and T cells is critical for B cells to efficiently present antigens to T cells and undergo class-switch recombination to IgG1 (Bettelli et al., 2006). In one study an AQP4(268-285)-specific T-cell line was generated in Lewis rats by immunization with epitopes that were predicted to be good binders to the Lewis rat specific MHC class II complex (RT1.B^{L}). While immunization with these peptides alone did not result in a clinical manifestation, transfer of activated AQP4(268-285)-specific T cells into naïve recipient rats induced an encephalomyelitic syndrome. However, lesions were only reminiscent of NMO when additional heterologous human anti-AQP4 IgG was transferred (Zeka et al., 2015).

To test the encephalitogenic potential of AQP4(201-220)-specific T cells, $Aqp4^{\Delta T}$ compound mice that are AQP4-sufficient while harboring the non-tolerized mature T-cell repertoire of $Aqp4^{-/-}$ mice were actively immunized with either AQP4 protein or AQP4(201-220) peptide. As a result, the mice developed an encephalomyelitic syndrome that clinically resembled classic EAE with paresis of the tail and hind limbs and was caused by infiltrating T cells and macrophages. Due to clonal deletion of AQP4-reactive B cells in AQP4-sufficient mice, none of the AQP4-immunized $Aqp4^{\Delta T}$ compound mice raised an anti-AQP4-specific serum response. Additional transfer of either immune serum with high titers of anti-AQP4 antibodies generated in AQP4-immunized $Aqp4^{-/-}$ mice or the murinized monoclonal anti-AQP4 antibody

rAb-53 aggravated disease severity and resulted in NMO-like lesions with perivascular loss of AQP4-immunoreactivity. OCT-analysis of murine retinae revealed that swelling of the INL occurred only in the presence of both AQP4(201-220)-specific T cells and anti-AQP4-specific antibodies but not in T-cell mediated encephalomyelitis with either AQP4 or MOG as target antigens alone, suggesting a loss-of-function of Müller cells when AQP4, which is highly expressed in these cells, is targeted by a cellular and humoral immune response. Located in the INL, Müller glia cells express high amounts of AQP4 and play an important role in water and potassium homeostasis (Bringmann et al., 2006). This finding is in line with the Lewis rat model, in which retinal damage was shown to be a primary event and not secondary to optic neuritis (Zeka et al., 2016).

Thus, AQP4(201-220)-specific T cells alone induce encephalomyelitis, while NMO-specific lesions in the CNS with loss of AQP4-immunoreactivity and retinal disease with swelling of the INL only occurs in the presence of both, AQP4(201-220)-specific T cells and anti-AQP4 antibodies.

5.4 Tetramer staining of AQP4(201-220)-specific T cells is a tool for AQP4-specific TCR repertoire analysis and cloning

MHC tetramers are a powerful tool to characterize, quantify and sort antigen-specific T cells (Altman et al., 1996). While the first MHC class I tetramers were successfully used to study virus- and tumor-specific $CD8^+$ T cells, generation of MHC class II tetramers for the analysis of $CD4^+$ T cells turned out to be more challenging due to the low frequency of antigen-specific $CD4^+$ T cells, weak CD4-MHC interaction and technical difficulties in preparation of soluble pMHC class II complexes (Vollers and Stern, 2008). Most of these issues have been addressed (e.g. by stabilizing MHC molecules using leucine-zipper motifs (Scott et al., 1996), covalently linking the peptide to the beta chain (Kozono et al., 1994) and enriching $CD4^+$ T cells with magnetic beads) and pMHC class II tetramers are now commonly used to monitor the repertoire and the dynamics of T-cell responses. In particular, with respect to tolerance induction to specific autoantigens, pMHC class II tetramers are valuable for displaying T_{reg}-cell frequencies and investigating determinants involved in alternative cell fates of

autoreactive T cells (e.g. deletion or diversion into Foxp3$^+$ T_{reg} lineage) (Taniguchi et al., 2012) (Malhotra et al., 2016) (Hassler et al., 2019).

Here, the MHC class II tetramer p41/IAb was successfully used to detect AQP4(201-220)-specific T cells in sizeable fractions in the repertoire of AQP4-immunized *Aqp4*$^{-/-}$ mice but not WT mice, thus confirming the previous results from functional assays (i.e. peptide scans) that the normal immune repertoire is purged of AQP4-reactive clones. Since there are very few AQP4(201-220)-specific T cells in the tolerized T-cell repertoire of WT mice, central tolerance against AQP4 is mediated by deletion rather than diversion of autoreactive T cells. This is in line with a study suggesting, that widespread antigen expression is associated with deletion whereas more restricted antigens trigger the emergence of Foxp3$^+$ T_{reg} cells (Malhotra et al., 2016). It also corresponds well with the finding that AIRE-dependent expression of antigens in mTECs induces deletional tolerance, since the expression of AQP4 in the thymus is AIRE-dependent (Anderson et al., 2002).

The p41/IAb tetramer will be of central importance for further characterization of AQP4-specific T-cell responses and might help to shed light on cytokine phenotype, priming and migration of activated cells. In addition, a reliable read-out for AQP4(201-220)-specific Foxp3$^+$ T_{reg}-cell frequencies will be essential for potential future manipulations of central tolerance induction to AQP4 in WT mice. At last, by performing single cell sorting of p41/IAb tetramer$^+$ AQP4(201-220)-specific T cells from the non-tolerized repertoire of *Aqp4*$^{-/-}$ mice, analysis of TCR receptor genes will pave the way towards cloning of the TCR.

5.5 Conclusion and Outlook

In this study, a completely homologous model for human NMO was developed in *Aqp4*$^{\Delta T}$ compound mice involving induction of encephalitogenic AQP4(201-220)-specific T cells in combination with transfer of either mouse sera with high titers of anti-AQP4 antibodies or murinized monoclonal anti-AQP4 antibodies (rAb-53). Upon immunization and antibody transfer, the mice develop clinical signs of encephalomyelitis with NMO-like lesional patterns in the CNS and retina.

The basis for this experimental model that utilizes the correct autoantigen (i.e. AQP4) was laid by the recombinant production of full-length murine AQP4 and the identification of AQP4(201-220) as the major immunogenic IA^b-restricted T-cell epitope. It could be shown

that AQP4(201-220) is a naturally processed epitope and in principle elicits an encephalitogenic T-cell response. However, due to tight deletional tolerance against AQP4, there is no AQP4-directed panencephalitis upon sensitization with AQP4 in WT mice. Similar to the T-cell repertoire, the B-cell repertoire of WT mice is purged of AQP4-specific clones, which prevents the generation of anti-AQP4 antibodies in WT mice while *Aqp4*$^{-/-}$ mice mount a potent anti-AQP4 serum response upon immunization with AQP4 protein. Thus, in order to overcome deletional tolerance and allow for a novel murine model based on active immunization, *Aqp4*$^{\Delta T}$ compound mice had to be constructed by transferring the non-tolerized mature T-cell compartment of *Aqp4*$^{-/-}$ mice into AQP4-sufficient mice. However, induction of NMO-like lesions in these mice still depends on additional transfer of anti-AQP4 antibodies since AQP4(201-220)-specific T cells alone induce an encephalomyelitic syndrome that lacks landmark histologic features of human NMO unless anti-AQP4 antibodies are also present.

This work will now be the foundation for disentangling the immunologic basis of central tolerance against AQP4. E. g. which are the relevant APCs to purge the natural T-cell repertoire of AQP4-specific T cells during development. To improve a preclinical model of NMO, we need to deepen our understanding of the underlying mechanisms of central and peripheral tolerance breakdown also in the B-cell compartment in order to set the stage for modeling NMO-like immunopathology. Only a system where both endogenous AQP4-specific T cells and B cells are primed together upon sensitization is suitable to study the processes involved in early disease development. The newly generated MHC class II tetramer for detection of AQP4(201-220)-specific T cells will then serve as essential tool for further characterization, quantification and sorting of AQP4-specific CD4$^+$ T cells, ultimately leading to cloning of AQP4 specific TCRs that can then be interrogated as to their capacity to negatively select T cells, to divert them into the Foxp3$^+$ T_{reg} lineage, or to activate them for further differentiation into T follicular helper cells or effector T cells that induce immunopathology in the CNS.

Bibliography

Altman, J. D., Moss, P. A., Goulder, P. J., Barouch, D. H., McHeyzer-Williams, M. G., Bell, J. I., et al. (1996). Phenotypic analysis of antigen-specific T lymphocytes. *Science*, 274(5284), 94–96.

Anderson, A. C., Nicholson, L. B., Legge, K. L., Turchin, V., Zaghouani, H., & Kuchroo, V. K. (2000). High frequency of autoreactive myelin proteolipid protein-specific T cells in the periphery of naive mice: mechanisms of selection of the self-reactive repertoire. *The Journal of Experimental Medicine*, 191(5), 761–770.

Anderson, M. S., Venanzi, E. S., Klein, L., Chen, Z., Berzins, S. P., Turley, S. J., et al. (2002). Projection of an immunological self shadow within the thymus by the aire protein. *Science*, 298(5597), 1395–1401.

Arellano, B., Hussain, R., Zacharias, T., Yoon, J., David, C., Zein, S., et al. (2012). Human aquaporin 4281-300 is the immunodominant linear determinant in the context of HLA-DRB1*03:01: relevance for diagnosing and monitoring patients with neuromyelitis optica. *Archives of Neurology*, 69(9), 1125–1131.

Asavapanumas, N., Ratelade, J., & Verkman, A. S. (2014a). Unique neuromyelitis optica pathology produced in naïve rats by intracerebral administration of NMO-IgG. *Acta Neuropathologica*, 127(4), 539–551.

Asavapanumas, N., Ratelade, J., Papadopoulos, M. C., Bennett, J. L., Levin, M. H., & Verkman, A. S. (2014b). Experimental mouse model of optic neuritis with inflammatory demyelination produced by passive transfer of neuromyelitis optica-immunoglobulin G. *Journal of Neuroinflammation*, 11(1), 16–11.

Ben-Nun, A., Wekerle, H., & Cohen, I. R. (1981). The rapid isolation of clonable antigen-specific T lymphocyte lines capable of mediating autoimmune encephalomyelitis. *European Journal of Immunology*, 11(3), 195–199.

Bennett, J. L., Lam, C., Kalluri, S. R., Saikali, P., Bautista, K., Dupree, C., et al. (2009). Intrathecal pathogenic anti-aquaporin-4 antibodies in early neuromyelitis optica. *Annals of Neurology*, 66(5), 617–629.

Bettelli, E., Oukka, M., Carrier, Y., Gao, W., Korn, T., Strom, T. B., et al. (2006). Reciprocal developmental pathways for the generation of pathogenic effector TH17 and regulatory T cells. *Nature*, 441(7090), 235–238.

Bettelli, E., Pagany, M., Weiner, H. L., Linington, C., Sobel, R. A., & Kuchroo, V. K. (2003). Myelin oligodendrocyte glycoprotein-specific T cell receptor transgenic mice develop spontaneous autoimmune optic neuritis. *The Journal of Experimental Medicine*, 197(9), 1073–1081.

Bradl, M., Misu, T., Takahashi, T., Watanabe, M., Mader, S., Reindl, M., et al. (2009). Neuromyelitis optica: pathogenicity of patient immunoglobulin in vivo. *Annals of Neurology*, 66(5), 630–643.

Bringmann, A., Pannicke, T., Grosche, J., Francke, M., Wiedemann, P., Skatchkov, S. N., et al. (2006). Müller cells in the healthy and diseased retina. *Progress in Retinal and Eye Research*, 25(4), 397–424.

Brum, D. G., Barreira, A. A., Santos, dos, A. C., Kaimen-Maciel, D. R., Matiello, M., Costa, R. M., et al. (2010). HLA-DRB association in neuromyelitis optica is different from that observed in multiple sclerosis. *Multiple Sclerosis*, 16(1), 21–29.

Chen, W., Jin, W., Hardegen, N., Lei, K.-J., Li, L., Marinos, N., et al. (2003). Conversion of peripheral CD4+CD25- naive T cells to CD4+CD25+ regulatory T cells by TGF-beta induction of transcription factor Foxp3. *The Journal of Experimental Medicine*, 198(12), 1875–1886.

Crane, J. M., & Verkman, A. S. (2009). Determinants of aquaporin-4 assembly in orthogonal arrays revealed by live-cell single-molecule fluorescence imaging. *Journal of Cell Science*, 122(Pt 6), 813–821.

Crane, J. M., Lam, C., Rossi, A., Gupta, T., Bennett, J. L., & Verkman, A. S. (2011). Binding affinity and specificity of neuromyelitis optica autoantibodies to aquaporin-4 M1/M23 isoforms and orthogonal arrays. *The Journal of Biological Chemistry*, 286(18), 16516–16524.

Delarasse, C., Daubas, P., Mars, L. T., Vizler, C., Litzenburger, T., Iglesias, A., et al. (2003). Myelin/oligodendrocyte glycoprotein-deficient (MOG-deficient) mice reveal lack of immune tolerance to MOG in wild-type mice. *Journal of Clinical Investigation*, 112(4), 544–553.

Derbinski, J., Schulte, A., Kyewski, B., & Klein, L. (2001). Promiscuous gene expression in medullary thymic epithelial cells mirrors the peripheral self. *Nature Immunology*, 2(11), 1032–1039.

Duan, T., & Verkman, A. S. (2020). Experimental animal models of aquaporin-4-IgG-seropositive neuromyelitis optica spectrum disorders: progress and shortcomings. *Brain Pathology*, 30(1), 13–25.

Duan, T., Tradtrantip, L., Phuan, P.-W., Bennett, J. L., & Verkman, A. S. (2020). Affinity-matured "aquaporumab" anti-aquaporin-4 antibody for therapy of seropositive neuromyelitis optica spectrum disorders. *Neuropharmacology*, 162, 107827.

Fujinami, R. S., & Oldstone, M. B. (1985). Amino acid homology between the encephalitogenic site of myelin basic protein and virus: mechanism for autoimmunity. *Science*, 230(4729), 1043–1045.

Gallegos, A. M., & Bevan, M. J. (2004). Central tolerance to tissue-specific antigens mediated by direct and indirect antigen presentation. *The Journal of Experimental Medicine*, 200(8), 1039–1049.

Germain, R. N. (1994). MHC-dependent antigen processing and peptide presentation: providing ligands for T lymphocyte activation. *Cell*, 76(2), 287–299.

Haj-Yasein, N. N., Vindedal, G. F., Eilert-Olsen, M., Gundersen, G. A., Skare, Ø., Laake, P., et al. (2011). Glial-conditional deletion of aquaporin-4 (Aqp4) reduces blood-brain water uptake and confers barrier function on perivascular astrocyte endfeet. *PNAS*, 108(43), 17815–17820.

Halverson, R., Torres, R. M., & Pelanda, R. (2004). Receptor editing is the main mechanism of B cell tolerance toward membrane antigens. *Nature Immunology*, 5(6), 645–650.

Hamilton, J. A., Miller, J. F., & Kettman, J. (1974). Hapten-specific tolerance in mice. II. Adoptive transfer studies and evidence for unresponsiveness in the B cells. *European Journal of Immunology*, 4(4), 268–276.

Harkiolaki, M., Holmes, S. L., Svendsen, P., Gregersen, J. W., Jensen, L. T., McMahon, R., et al. (2009). T cell-mediated autoimmune disease due to low-affinity crossreactivity to common microbial peptides. *Immunity*, 30(3), 348–357.

Hassler, T., Urmann, E., Teschner, S., Federle, C., Dileepan, T., Schober, K., et al. (2019). Inventories of naive and tolerant mouse CD4 T cell repertoires reveal a hierarchy of deleted and diverted T cell receptors. *PNAS*, 116(37), 18537–18543.

Herwerth, M., Kalluri, S. R., Srivastava, R., Kleele, T., Kenet, S., Illes, Z., et al. (2016). In vivo imaging reveals rapid astrocyte depletion and axon damage in a model of neuromyelitis optica-related pathology. *Annals of Neurology*, 79(5), 794–805.

Hinson, S. R., Roemer, S. F., Lucchinetti, C. F., Fryer, J. P., Kryzer, T. J., Chamberlain, J. L., et al. (2008). Aquaporin-4-binding autoantibodies in patients with neuromyelitis optica impair glutamate transport by down-regulating EAAT2. *Journal of Experimental Medicine*, 205(11), 2473–2481.

Hinson, S. R., Romero, M. F., Popescu, B. F. G., Lucchinetti, C. F., Fryer, J. P., Wolburg, H., et al. (2012). Molecular outcomes of neuromyelitis optica (NMO)-IgG binding to aquaporin-4 in astrocytes. *PNAS*, 109(4), 1245–1250.

Hinterberger, M., Aichinger, M., Prazeres da Costa, O., Voehringer, D., Hoffmann, R., & Klein, L. (2010). Autonomous role of medullary thymic epithelial cells in central CD4(+) T cell tolerance. *Nature Immunology*, 11(6), 512–519.

Ho, J. D., Yeh, R., Sandstrom, A., Chorny, I., Harries, W. E. C., Robbins, R. A., et al. (2009). Crystal structure of human aquaporin 4 at 1.8 A and its mechanism of conductance. *PNAS*, 106(18), 7437–7442.

Jarius, S., Ruprecht, K., Wildemann, B., Kuempfel, T., Ringelstein, M., Geis, C., et al. (2012). Contrasting disease patterns in seropositive and seronegative neuromyelitis optica: A multicentre study of 175 patients. *Journal of Neuroinflammation*, 9(1), 14–17.

Jones, M. V., Huang, H., Calabresi, P. A., & Levy, M. (2015). Pathogenic aquaporin-4 reactive T cells are sufficient to induce mouse model of neuromyelitis optica. *Acta Neuropathologica Communications*, 3(1), 28–8.

Kalluri, S. R., Illes, Z., Srivastava, R., Cree, B., Menge, T., Bennett, J. L., et al. (2010). Quantification and functional characterization of antibodies to native aquaporin 4 in neuromyelitis optica. *Archives of Neurology*, 67(10), 1201–1208.

Kalluri, S. R., Rothhammer, V., Staszewski, O., Srivastava, R., Petermann, F., Prinz, M., et al. (2011). Functional characterization of aquaporin-4 specific T cells: towards a model for neuromyelitis optica. *PloS One*, 6(1), e16083.

Kawakami, N., Lassmann, S., Li, Z., Odoardi, F., Ritter, T., Ziemssen, T., et al. (2004). The activation status of neuroantigen-specific T cells in the target organ determines the

clinical outcome of autoimmune encephalomyelitis. *The Journal of Experimental Medicine*, 199(2), 185–197.

Khan, I. S., Mouchess, M. L., Zhu, M.-L., Conley, B., Fasano, K. J., Hou, Y., et al. (2014). Enhancement of an anti-tumor immune response by transient blockade of central T cell tolerance. *The Journal of Experimental Medicine*, 211(5), 761–768.

Klein, L., Kyewski, B., Allen, P. M., & Hogquist, K. A. (2014). Positive and negative selection of the T cell repertoire: what thymocytes see (and don't see). *Nature Reviews Immunology*, 14(6), 377–391.

Klinman, N. R. (1996). The "clonal selection hypothesis" and current concepts of B cell tolerance. *Immunity*, 5(3), 189–195.

Korn, T., Bettelli, E., Gao, W., Awasthi, A., Jäger, A., Strom, T. B., et al. (2007). IL-21 initiates an alternative pathway to induce proinflammatory T(H)17 cells. *Nature*, 448(7152), 484–487.

Kozono, H., White, J., Clements, J., Marrack, P., & Kappler, J. (1994). Production of soluble MHC class II proteins with covalently bound single peptides. *Nature*, 369(6476), 151–154.

Kuchroo, V. K., Anderson, A. C., Waldner, H., Munder, M., Bettelli, E., & Nicholson, L. B. (2002). T cell response in experimental autoimmune encephalomyelitis (EAE): role of self and cross-reactive antigens in shaping, tuning, and regulating the autopathogenic T cell repertoire. *Annual Review of Immunology*, 20, 101–123.

Kuchroo, V. K., Sobel, R. A., Yamamura, T., Greenfield, E., Dorf, M. E., & Lees, M. B. (1991). Induction of experimental allergic encephalomyelitis by myelin proteolipid-protein-specific T cell clones and synthetic peptides. *Pathobiology* 59(5), 305–312.

Kyewski, B., & Klein, L. (2006). A central role for central tolerance. *Annual Review of Immunology*, 24, 571–606.

Laemmli, U. K. (1970). Cleavage of structural proteins during the assembly of the head of bacteriophage T4. *Nature*, 227(5259), 680–685.

Lanzavecchia, A. (1985). Antigen-specific interaction between T and B cells. *Nature*, 314(6011), 537–539.

Lebowitz, M. S., O'Herrin, S. M., Hamad, A. R., Fahmy, T., Marguet, D., Barnes, N. C., et al. (1999). Soluble, high-affinity dimers of T-cell receptors and class II major histocompatibility complexes: biochemical probes for analysis and modulation of immune responses. *Cellular Immunology*, 192(2), 175–184.

Leite, M. I., Coutinho, E., Lana-Peixoto, M., Apostolos, S., Waters, P., Sato, D., et al. (2012). Myasthenia gravis and neuromyelitis optica spectrum disorder: a multicenter study of 16 patients. *Neurology*, 78(20), 1601–1607.

Lennon, V. A., Kryzer, T. J., Pittock, S. J., Verkman, A. S., & Hinson, S. R. (2005). IgG marker of optic-spinal multiple sclerosis binds to the aquaporin-4 water channel. *The Journal of Experimental Medicine*, 202(4), 473–477.

Lennon, V. A., Wingerchuk, D. M., Kryzer, T. J., Pittock, S. J., Lucchinetti, C. F., Fujihara, K., et al. (2004). A serum autoantibody marker of neuromyelitis optica: distinction from multiple sclerosis. *Lancet*, 364(9451), 2106–2112.

Lin, R. H., & Stockinger, B. (1989). T cell immunity or tolerance as a consequence of self antigen presentation. *European Journal of Immunology*, 19(1), 105–110.

Linington, C., Berger, T., Perry, L., Weerth, S., Hinze-Selch, D., Zhang, Y., et al. (1993). T cells specific for the myelin oligodendrocyte glycoprotein mediate an unusual autoimmune inflammatory response in the central nervous system. *European Journal of Immunology*, 23(6), 1364–1372.

Liu, Y., Harlow, D. E., Given, K. S., Owens, G. P., Macklin, W. B., & Bennett, J. L. (2016). Variable sensitivity to complement-dependent cytotoxicity in murine models of neuromyelitis optica. *Journal of Neuroinflammation*, 13(1), 301.

Lucchinetti, C. F., Mandler, R. N., McGavern, D., Brück, W., Gleich, G., Ransohoff, R. M., et al. (2002). A role for humoral mechanisms in the pathogenesis of Devic's neuromyelitis optica. *Brain*, 125(Pt 7), 1450–1461.

Ma, T., Yang, B., Gillespie, A., Carlson, E. J., Epstein, C. J., & Verkman, A. S. (1997). Generation and phenotype of a transgenic knockout mouse lacking the mercurial-insensitive water channel aquaporin-4. *Journal of Clinical Investigation*, 100(5), 957–962.

Malhotra, D., Linehan, J. L., Dileepan, T., Lee, Y. J., Purtha, W. E., Lu, J. V., et al. (2016). Tolerance is established in polyclonal CD4(+) T cells by distinct mechanisms, according to self-peptide expression patterns. *Nature Immunology*, 17(2), 187–195.

Manley, G. T., Fujimura, M., Ma, T., Noshita, N., Filiz, F., Bollen, A. W., et al. (2000). Aquaporin-4 deletion in mice reduces brain edema after acute water intoxication and ischemic stroke. *Nature Medicine*, 6(2), 159–163.

Matiello, M., Kim, H. J., Kim, W., Brum, D. G., Barreira, A. A., Kingsbury, D. J., et al. (2010). Familial neuromyelitis optica. *Neurology*, 75(4), 310–315.

Matsuya, N., Komori, M., Nomura, K., Nakane, S., Fukudome, T., Goto, H., et al. (2011). Increased T-cell immunity against aquaporin-4 and proteolipid protein in neuromyelitis optica. *International Immunology*, 23(9), 565–573.

Misu, T., Fujihara, K., Kakita, A., Konno, H., Nakamura, M., Watanabe, S., et al. (2007). Loss of aquaporin 4 in lesions of neuromyelitis optica: distinction from multiple sclerosis. *Brain*, 130(Pt 5), 1224–1234.

Mitsdoerffer, M., Kuchroo, V., & Korn, T. (2013). Immunology of neuromyelitis optica: a T cell-B cell collaboration. *Annals of the New York Academy of Sciences*, 1283, 57–66.

Mouri, Y., Ueda, Y., Yamano, T., Matsumoto, M., Tsuneyama, K., Kinashi, T., & Matsumoto, M. (2017). Mode of tolerance induction and requirement for aire are governed by the cell types that express self-antigen and those that present antigen. *Journal of Immunology*, 199(12), 3959–3971.

Mueller, D. L. (2010). Mechanisms maintaining peripheral tolerance. *Nature Immunology*, 11(1), 21–27.

Nelson, P. A., Khodadoust, M., Prodhomme, T., Spencer, C. M., Patarroyo, J. C., Varrin-Doyer, M., et al. (2010). Immunodominant T cell determinants of aquaporin-4, the autoantigen associated with neuromyelitis optica. *PloS One*, 5(11), e15050.

Pandit, L., Asgari, N., Apiwattanakul, M., Palace, J., Paul, F., Leite, M. I., et al. (2015). Demographic and clinical features of neuromyelitis optica: A review. *Multiple Sclerosis*, 21(7), 845–853.

Papadopoulos, M. C., & Verkman, A. S. (2012). Aquaporin 4 and neuromyelitis optica. *The Lancet Neurology*, 11(6), 535–544.

Papadopoulos, M. C., Bennett, J. L., & Verkman, A. S. (2014). Treatment of neuromyelitis optica: state-of-the-art and emerging therapies. *Nature Reviews. Neurology*, 10(9), 493–506.

Perry, J. S. A., Lio, C.-W. J., Kau, A. L., Nutsch, K., Yang, Z., Gordon, J. I., et al. (2014). Distinct contributions of Aire and antigen-presenting-cell subsets to the generation of self-tolerance in the thymus. *Immunity*, 41(3), 414–426.

Pohl, M., Fischer, M.-T., Mader, S., Schanda, K., Kitic, M., Sharma, R., et al. (2011). Pathogenic T cell responses against aquaporin 4. *Acta Neuropathologica*, 122(1), 21–34.

Pohl, M., Wekerle, H., Kawakami, N., Kitic, M., Bauer, J., Martins, R., et al. (2013). T cell-activation in neuromyelitis optica lesions plays a role in their formation. *Acta Neuropathologica Communications*, 1(1), 85.

Ratelade, J., Asavapanumas, N., Ritchie, A. M., Wemlinger, S., Bennett, J. L., & Verkman, A. S. (2013). Involvement of antibody-dependent cell-mediated cytotoxicity in inflammatory demyelination in a mouse model of neuromyelitis optica. *Acta Neuropathologica*, 126(5), 699–709.

Roemer, S. F., Parisi, J. E., Lennon, V. A., Benarroch, E. E., Lassmann, H., Brück, W., et al. (2007). Pattern-specific loss of aquaporin-4 immunoreactivity distinguishes neuromyelitis optica from multiple sclerosis. *Brain,* 130(Pt 5), 1194–1205.

Rossi, S. W., Jeker, L. T., Ueno, T., Kuse, S., Keller, M. P., Zuklys, S., et al. (2007). Keratinocyte growth factor (KGF) enhances postnatal T-cell development via enhancements in proliferation and function of thymic epithelial cells. *Blood*, 109(9), 3803–3811.

Russell, D. M., Dembić, Z., Morahan, G., Miller, J. F., Bürki, K., & Nemazee, D. (1991). Peripheral deletion of self-reactive B cells. *Nature*, 354(6351), 308–311.

Saadoun, S., & Papadopoulos, M. C. (2015). Role of membrane complement regulators in neuromyelitis optica. *Multiple Sclerosis*, 21(13), 1644–1654.

Saadoun, S., Waters, P., Bell, B. A., Vincent, A., Verkman, A. S., & Papadopoulos, M. C. (2010). Intra-cerebral injection of neuromyelitis optica immunoglobulin G and human complement produces neuromyelitis optica lesions in mice. *Brain*, 133(Pt 2), 349–361.

Sagan, S. A., Winger, R. C., Cruz-Herranz, A., Nelson, P. A., Hagberg, S., Miller, C. N., et al. (2016). Tolerance checkpoint bypass permits emergence of pathogenic T cells to neuromyelitis optica autoantigen aquaporin-4. *PNAS*, 113(51), 14781–14786.

Saini, H., Rifkin, R., Gorelik, M., Huang, H., Ferguson, Z., Jones, M. V., & Levy, M. (2013). Passively transferred human NMO-IgG exacerbates demyelination in mouse experimental autoimmune encephalomyelitis. *BMC Neurology*, 13(1), 104–9.

Scott, C. A., Garcia, K. C., Carbone, F. R., Wilson, I. A., & Teyton, L. (1996). Role of chain pairing for the production of functional soluble IA major histocompatibility complex class II molecules. *The Journal of Experimental Medicine*, 183(5), 2087–2095.

Shlomchik, M. J. (2008). Sites and stages of autoreactive B cell activation and regulation. *Immunity*, 28(1), 18–28.

Snapper, C. M., & Paul, W. E. (1987). Interferon-gamma and B cell stimulatory factor-1 reciprocally regulate Ig isotype production. *Science*, 236(4804), 944–947.

Sojka, D. K., Huang, Y.-H., & Fowell, D. J. (2008). Mechanisms of regulatory T-cell suppression - a diverse arsenal for a moving target. *Immunology*, 124(1), 13–22.

Sprent, J., & Kishimoto, H. (2002). The thymus and negative selection. *Immunological Reviews*, 185(1), 126–135.

Taniguchi, R. T., DeVoss, J. J., Moon, J. J., Sidney, J., Sette, A., Jenkins, M. K., & Anderson, M. S. (2012). Detection of an autoreactive T-cell population within the polyclonal repertoire that undergoes distinct autoimmune regulator (Aire)-mediated selection. *PNAS*, 109(20), 7847–7852.

Toellner, K. M., Luther, S. A., Sze, D. M., Choy, R. K., Taylor, D. R., MacLennan, I. C., & Acha-Orbea, H. (1998). T helper 1 (Th1) and Th2 characteristics start to develop during T cell priming and are associated with an immediate ability to induce immunoglobulin class switching. *The Journal of Experimental Medicine*, 187(8), 1193–1204.

Tradtrantip, L., Zhang, H., Anderson, M. O., Saadoun, S., Phuan, P.-W., Papadopoulos, M. C., et al. (2012a). Small-molecule inhibitors of NMO-IgG binding to aquaporin-4 reduce astrocyte cytotoxicity in neuromyelitis optica. *The FASEB Journal*, 26(5), 2197–2208.

Tradtrantip, L., Zhang, H., Saadoun, S., Phuan, P.-W., Lam, C., Papadopoulos, M. C., et al. (2012b). Anti-aquaporin-4 monoclonal antibody blocker therapy for neuromyelitis optica. *Annals of Neurology*, 71(3), 314–322.

Varrin-Doyer, M., Spencer, C. M., Schulze-Topphoff, U., Nelson, P. A., Stroud, R. M., Cree, B. A. C., & Zamvil, S. S. (2012). Aquaporin 4-specific T cells in neuromyelitis optica exhibit a Th17 bias and recognize Clostridium ABC transporter. *Annals of Neurology*, 72(1), 53–64.

Verkman, A. S. (2012). Aquaporins in clinical medicine. *Annual Review of Medicine*, 63, 303–316.

Vollers, S. S., & Stern, L. J. (2008). Class II major histocompatibility complex tetramer staining: progress, problems, and prospects. *Immunology*, 123(3), 305–313.

Weinshenker, B.G., & Wingerchuk, D. M. (2017). Neuromyelitis Spectrum Disorders. *Mayo Clinic Proceedings*, 92(4), 663-679.

Whittam, D., Wilson, M., Hamid, S., Keir, G., Bhojak, M., & Jacob, A. (2017). What's new in neuromyelitis optica? A short review for the clinical neurologist. *Journal of Neurology*, 264(11), 2330–2344.

Wingerchuk, D. M., Banwell, B., Bennett, J. L., Cabre, P., Carroll, W., Chitnis, T., et al. (2015). International consensus diagnostic criteria for neuromyelitis optica spectrum disorders. *Neurology*, 85, 177-189.

Wingerchuk, D. M., Lennon, V. A., Lucchinetti, C. F., Pittock, S. J., & Weinshenker, B. G. (2007). The spectrum of neuromyelitis optica. *The Lancet Neurology*, 6(9), 805–815.

Wirnsberger, G., Hinterberger, M., & Klein, L. (2011). Regulatory T-cell differentiation versus clonal deletion of autoreactive thymocytes. *Immunology and Cell Biology*, 89(1), 45–53.

Xing, Y., & Hogquist, K. A. (2012). T-cell tolerance: central and peripheral. *Cold Spring Harbor Perspectives in Biology*, *4*(6), a006957.

Yamano, T., Nedjic, J., Hinterberger, M., Steinert, M., Koser, S., Pinto, S., et al. (2015). Thymic B cells are licensed to present self antigens for central T cell tolerance induction. *Immunity*, 42(6), 1048–1061.

Zamvil, S. S., & Steinman, L. (1990). The T lymphocyte in experimental allergic encephalomyelitis. *Annual Review of Immunology*, 8, 579–621.

Zeka, B., Hastermann, M., Hochmeister, S., Kögl, N., Kaufmann, N., Schanda, K., et al. (2015). Highly encephalitogenic aquaporin 4-specific T cells and NMO-IgG jointly orchestrate lesion location and tissue damage in the CNS. *Acta Neuropathologica*, 130(6), 783–798.

Zeka, B., Hastermann, M., Kaufmann, N., Schanda, K., Pende, M., Misu, T., et al. (2016). Aquaporin 4-specific T cells and NMO-IgG cause primary retinal damage in experimental NMO/SD. *Acta Neuropathologica Communications*, 4(1), 82–10.

Zhang, H., & Verkman, A. S. (2014). Longitudinally extensive NMO spinal cord pathology produced by passive transfer of NMO-IgG in mice lacking complement inhibitor CD59. *Journal of Autoimmunity*, 53, 67–77.

Appendix

Supplementary figures

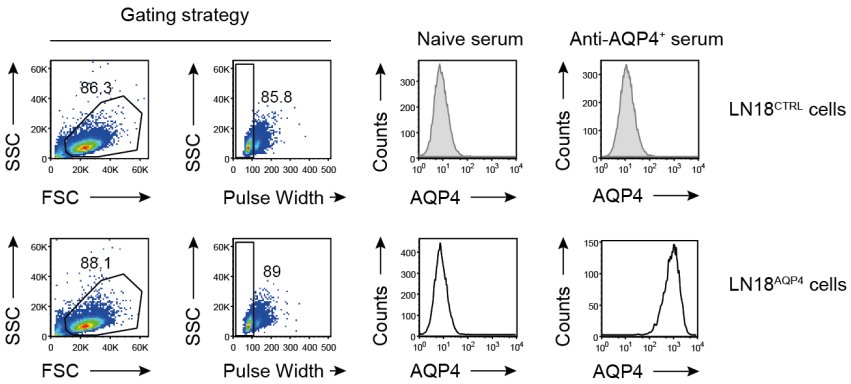

Figure Appendix.1: Cell-based flow cytometric assay to detect AQP4-specific antibodies in sera of mice. LN18 cells were transduced with AQP4-expressing lentivirus to ensure high expression of AQP4 in cell membrane. Sera of AQP4-immunized mice were diluted (1 : 50) in medium and then incubated with the cells. Anti-mouse total IgG H+L (AlexaFluor488-labeled) was used to detect anti-AQP4 antibodies (black line histograms). LN18 cells transduced with empty vector were used as control (shaded histograms).

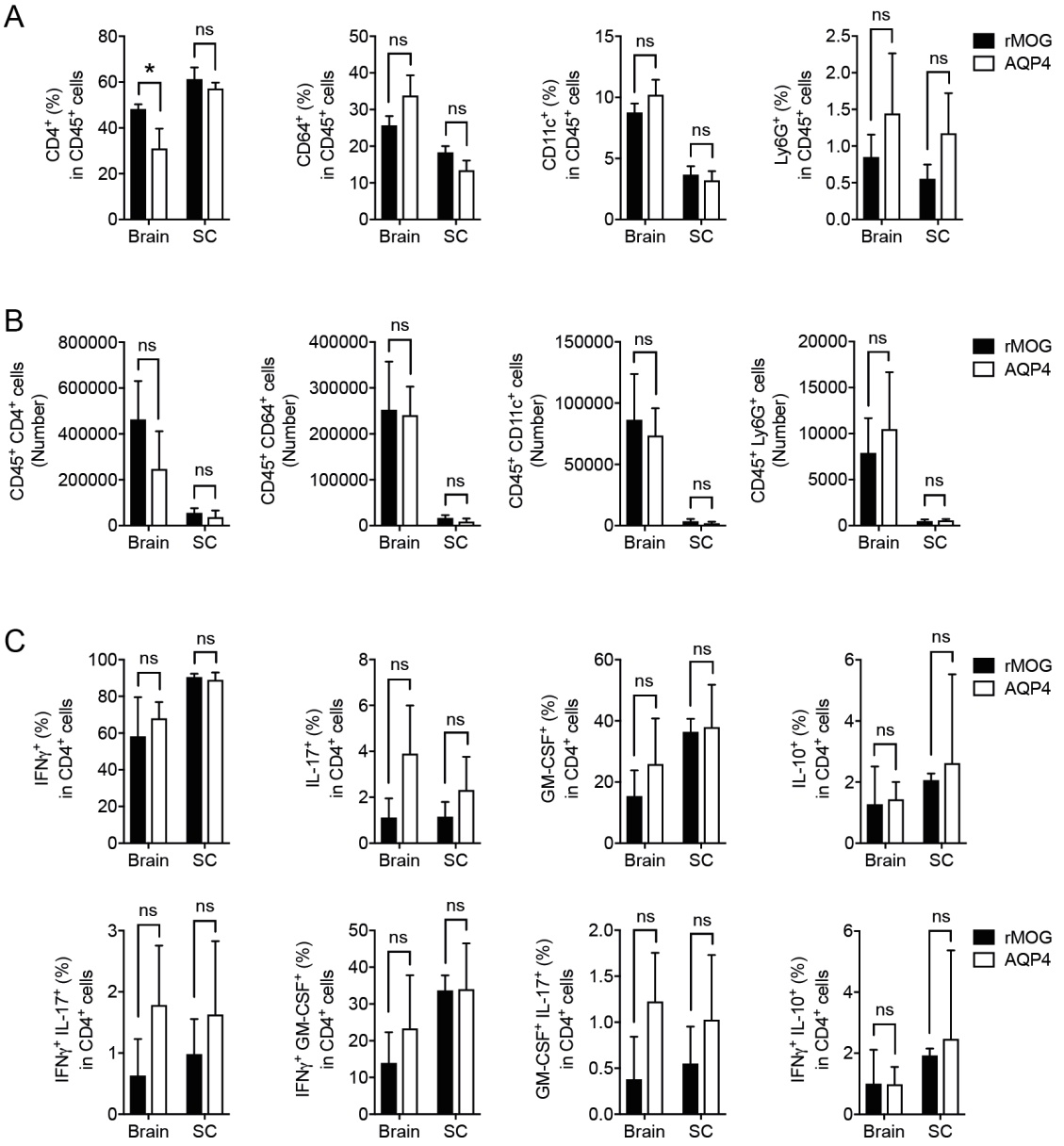

Figure Appendix.2: The inflammatory pattern with regard to infiltrating cells and cytokine production in brain and spinal cord of *AQP4$^{\Delta T}$* compound mice with encephalomyelitic syndrome as a result of immunization with AQP4 protein is similar to conventional EAE. *$AQP4^{\Delta T}$ x $Tcra^{-/-}$* mice were immunized s.c. with full-length AQP4 protein or MOG protein emulsified in CFA (see Fig. 4.10). Mononuclear cells from brain and spinal cord (SC) were prepared from mice with a clinical score of at least 2 for analysis by flow cytometry. Frequencies **(A)** and total numbers **(B)** of infiltrating CD4$^+$ T cells, CD64$^+$ macrophages, CD11c$^+$ dendritic cells and Ly6G$^+$ neutrophils within the CD45$^+$ cell population in brain and SC are shown. **(C)** After restimulation ex vivo with PMA and ionomycin for 2.5 hours, cells were also analyzed for cytokine production. Frequencies of IFNγ^+, IL-17$^+$, GM-CSF$^+$ and IL-10$^+$ producing cells as well as respective double producers within the CD4$^+$ T-cell gate in brain and SC are shown. Data is representative of two independent experiments **(A-C)**.

List of figures

Figure 1.1: The water channel protein AQP4. 12
Figure 1.2: Mechanisms of NMO pathogenesis. 13
Figure 3.1: Vector maps. 34
Figure 4.1: Expression and purification of mouse AQP4 protein. 46
Figure 4.2: AQP4(201-220) is the immunodominant IA^b-restricted epitope of AQP4. 48
Figure 4.3: Fine mapping of the immunodominant epitope AQP4(201-220). 49
Figure 4.4: Ability of WT and *Aqp4*$^{-/-}$ APCs to present processed AQP4 full-length protein and single AQP4 peptides to $CD4^+$ T cells. 50
Figure 4.5: Searching for AQP4 T-cell epitopes on a different genetic background. 51
Figure 4.6: *Aqp4*$^{-/-}$ mice mount a robust antibody response to AQP4 upon immunization with full-length AQP4 protein. 52
Figure 4.7: The naïve T-cell and B-cell repertoires of AQP4 sufficient mice are purged of AQP4-reactive clones. 54
Figure 4.8: A tight central tolerance mechanism to AQP4 prevents an anti-AQP4 adaptive immune response in WT mice. 55
Figure 4.9: Conditional knockout of AQP4 in thymic epithelial cells does not break the tolerance to AQP4 in otherwise AQP4 sufficient mice. 57
Figure 4.10: *AQP4*$^{\Delta T}$ compound mice develop clinical signs of disease upon immunization with AQP4 protein without raising an endogenous AQP4-specific serum response. 59
Figure 4.11: AQP4-reactive B-cell clones are depleted in the periphery of AQP4-sufficient mice upon transfer. 60
Figure 4.12: AQP4(201-220) is an encephalitogenic epitope. 62
Figure 4.13: NMO-like lesions are only induced by AQP4(201-220)-specific T cells in additional presence of anti-AQP4 antibodies. 63
Figure 4.14: *Aqp4*$^{\Delta T}$ *x Rag1*$^{-/-}$ mice immunized with AQP4(201-220) peptide plus i.v. injection of rAb-53 develop inner nuclear layer swelling in the retina at disease onset. 64
Figure 4.15: P41/IAb tetramer staining of AQP4-specific $CD4^+$ T cells in spleen and draining LNs of *Aqp4*$^{-/-}$ upon immunization with AQP4 protein or AQP4(201-220) peptide. 65

Figure Appendix.1: Cell-based flow cytometric assay to detect AQP4-specific antibodies in sera of mice. 86
Figure Appendix.2: The inflammatory pattern with regard to infiltrating cells and cytokine production in brain and spinal cord of $AQP4^{\Delta T}$ compound mice with encephalomyelitic syndrome as a result of immunization with AQP4 protein is similar to conventional EAE..... 87

List of tables

Table 3.1: Reagents used in the experiments. 19
Table 3.2: Plasmids used for cloning. 21
Table 3.3: Primers used for cloning. 21
Table 3.4: Primers used for genotyping. 21
Table 3.5: Enzymes used for cloning, genotyping or digestion of tissue. 22
Table 3.6: Kits used for cloning and protein biochemistry methods..... 22
Table 3.7: Composition of all media used in cell culture for primary cells and cell lines..... 23
Table 3.8: Composition of buffers and solutions. 24
Table 3.9: Antibodies used for FACS and western blot analysis as well as histology and application in cell cultures. 25
Table 3.10: Peptides used for immunization of mice and in cell culture for recall assays..... 27
Table 3.11: Mice used in the experiments. 29
Table 3.12: Cell lines used in cell-based flow cytometric assays or for production of mouse AQP4 protein. 29
Table 3.13: Magnetic beads used for purification of cell subsets. 29
Table 3.14: Cytokines used in cell culture. 30
Table 3.15: Equipment and consumables used for different experimental setups. 30
Table 3.16: Software used to collect and interpret data. 31
Table 3.17: Cycling program used for cDNA synthesis..... 32
Table 3.18: PCR mix to amplify *Aqp4* from cDNA. 33
Table 3.19: Cycling program for amplification of *Aqp4*. 33
Table 3.20: Cycling program for $Aqp4^{-/-}$. 42
Table 3.21: Cycling program for $Aqp4^{flox/flox}$ 42
Table 3.22: Cycling program for *Foxn1-cre*. 42

Attributions

The immunohistochemistry data shown in Figure 4.10 D, Figure 4.11 C and Figure 4.13 C were generated by Claudia Kemming in the lab of Tanja Kuhlmann (Institute for Neuropathology, UKM Münster, Germany).

The tetramers p41/IAb and PLP/IAb were generated by Tobias Hassler in the lab of Ludger Klein (Institute for Immunology, LMU Munich, Germany).

Abbreviations

ADCC	Antibody-dependent cell-mediated cytotoxicity
AIRE	Autoimmune regulator
APC	Antigen-presenting cell
AQP4	Aquaporin-4
BBB	Blood-brain-barrier
BCR	B-cell receptor
BM	Bone marrow
BMC	Bone marrow chimera
β-ME	Beta-Mercaptoethanol
β-OG	*n*-Octyl-β-D-glucopyranoside
BSA	Bovine serum albumin
CCR	Chemokine (C-C motif) receptor
CD	Cluster of differentiation
CDC	Complement-dependent cytotoxicity
CDCC	Complement-dependent cellular cytotoxicity
CFA	Complete Freund's adjuvant
CNS	Central nervous system
DAB	3,3'-Diaminobenzidine
DC	Dendritic cell
DMEM	Dulbecco's Modified Eagle Medium
DMSO	Dimethyl sulfoxide
DNA	Deoxyribonucleic acid
DNase	Deoxyribonuclease
dNTP	Nucleoside triphosphate
DTT	Dithiothreitol
EAAT2	Excitatory amino acid transporter 2
EAE	Experimental autoimmune encephalomyelitis
EDTA	Ethylenediaminetetraacetic acid
e.g.	For example *(exempli gratia)*
FACS	Fluorescence-activated cell sorting
Fc	Fragment crystallizable

FCS	Fetal calf serum
Foxp3	Forkhead box p3
GFAP	Glial fibrillary acidic protein
GM-CSF	Granulocyte macrophage colony-stimulating factor
His	Histidine
HLA	Human leukocyte antigen
HPLC	High-performance liquid chromatography
HRP	Horseradish peroxidase
i.p.	Intraperitoneal
i.v.	Intravenously
IEDB	Immune epitope database
IFN	Interferon
Ig	Immunoglobulin
IL	Interleukin
INL	Inner nuclear layer
LN	Lymph node
MACS	Magnetic-activated cell sorting
MBP	Myelin basic protein
MEM	Minimal essential medium
Met	Methionine
MFI	Mean fluorescence intensity
MHC	Major histocompatibility complex
MOG	Myelin oligodendrocyte glycoprotein
MS	Multiple sclerosis
mTEC	Medullary thymic epithelial cells
NCBI	National center for biotechnology information
NEAA	Non-essential amino acid
Ni-NTA	$Nickel^{2+}$ ion coupled to Nitrilotriacetic acid
NKT cells	Natural killer T cell
NMO	Neuromyelitis optica
NMOSD	Neuromyelitis optica spectrum disorder
OAP	Orthogonal array of particles
OCT	Optical coherence tomography

PBS	Phosphate-buffered saline
PCR	Polymerase chain reaction
PFA	Paraformaldehyde
PE	Phycoerythrin
PLP	Proteolipid protein
PMA	Phorbol myristate acetate
Rag	Recombination-activating gene
RNA	Ribonucleic acid
RPMI	Roswell Park Memorial Institute
s.c.	Subcutaneous
SC	Spinal cord
SD	Standard deviation
SDS-PAGE	Sodium dodecyl sulfate polyacrylamide gel electrophoresis
SEM	Standard Error of mean
SFCA	Surfactant-free cellulose acetate
SPF	Specific pathogen free
TAE	Tris-acetate-EDTA
TCR	T-cell receptor
TGF-β	Transforming growth factor β
T_H1 cell	T helper 1 cell
TNF	Tumor necrosis factor
TRA	Tissue-restricted antigen
T_{reg} cell	Regulatory T cell
WT	Wild type

Danksagung

Zum Abschluss meiner Dissertation möchte ich mich bei all jenen Menschen bedanken, die mich während der gesamten Promotionszeit begleitet und unterstützt haben. Mein besonderer Dank gilt:

Prof. Dr. Thomas Korn für das Vertrauen und die Chance an diesem Projekt zu arbeiten, seine Unterstützung über die gesamte Zeit meiner Promotion sowie für wertvolle Ratschläge und interessante Diskussionen. Ich habe viel gelernt.

Prof. Dr. Gabriele Multhoff für die Betreuung als Zweitgutachterin und für ihr Interesse und die Unterstützung bei den committee meetings der Graduiertenschule.

Prof. Dr. Achim Berthele für seine Bemühungen als mein Mentor.

Dr. Katja Lammens und Manuela Moldt für die Hilfe bei der Planung und Durchführung neuer Versuchsvorhaben. Durch eure Hilfe bei der Expression und Aufreinigung von AQP4 ist das Projekt erst so richtig in Fahrt gekommen.

Der gesamten Arbeitsgruppe Korn und den anderen Kolleg:innen aus dem Labor. Wir haben viel Zeit miteinander verbracht, uns fachliche Hilfestellung gegeben und oftmals auch darüber hinaus Erfahrungen und Erkenntnisse geteilt. Es sind schöne Freundschaften entstanden, die über die Zeit im Labor hinaus Bestand haben. Ich möchte mich vor allem bedanken bei Christopher, Sylvia, Christian, Ay-Lin, Vroni, Moni, Doro und Andi. Unsere lustigen Mittags- und Kaffeepausen waren eine willkommene Abwechslung zur konzentrierten Arbeit im Labor.

Meinen Eltern und Schwestern für ihre grenzenlose Unterstützung. Gerade auf der Zielgeraden habt ihr mit angepackt und mir Zeit geschenkt, sodass ich die Arbeit fertig schreiben konnte.

Meinem Freund für die Liebe und gemeinsame Kraftanstrengung, die es bedeutet zwei Kinder großzuziehen. Danke, dass du immer für mich da bist. Ich umarme dich.